ACHIEVING MARS SAMPLE RETURN ON A SINGLE ARES V LAUNCH

by

ASHLEY JONES

A THESIS

Submitted in partial fulfillment of the requirements
for the degree of Master of Science in Engineering
in
The Department of Mechanical and Aerospace Engineering
to
The School of Graduate Studies
of
The University of Alabama in Huntsville

HUNTSVILLE, ALABAMA

2010

In presenting this thesis in partial fulfillment of the requirements for a master's degree from The University of Alabama in Huntsville, I agree that the Library of this University shall make it freely available for inspection. I further agree that permission for extensive copying for scholarly purposes may be granted by my advisor or, in his/her absence, by the Chair of the Department or the Dean of the School of Graduate Studies. It is also understood that due recognition shall be given to me and to The University of Alabama in Huntsville in any scholarly use which may be made of any material in this thesis.

_____ _____

(student signature) (date)

THESIS APPROVAL FORM

Submitted by Ashley Jones in partial fulfillment of the requirements for the degree of Master of Science in Engineering and accepted on behalf of the Faculty of the School of Graduate Studies by the thesis committee.

We, the undersigned members of the Graduate Faculty of The University of Alabama in Huntsville, certify that we have advised and/or supervised the candidate on the work described in this thesis. We further certify that we have reviewed the thesis manuscript and approve it in partial fulfillment of the requirements for the degree of Master of Science in Engineering.

_____ Committee Chair
(Date)

_____

_____

_____ Department Chair

_____ College Dean

_____ Graduate Dean

ABSTRACT
The School of Graduate Studies
The University of Alabama in Huntsville

Degree Master of Science in Engineering_Engineering/Mechanical and Aerospace Engineering.

Name of Candidate Ashley Jones.
Title Achieving Mars Sample Return on a Single Ares V Launch.

To date, typical Mars Sample Return (MSR) architectures employ dual launches; however, MSR could be launched on a single Ares V—reducing cost, risk, and technology development. Ares V payload capability was modeled as a function of Earth launch energy. Four architectures were developed, all utilizing a common outbound strategy but unique return strategies, where predicted masses were compared to Ares V capabilities. In the feasibility study, the direct ascent (DA) architectures exceeded Ares V capability. However, the Mars orbit rendezvous (MOR) architectures yielded sufficient mass margin. In the sensitivity study, key parameters were varied, and the results showed the parameters of significance to be those associated with the Mars Ascent Vehicle (MAV). The MSR mission should employ MOR, utilizing a two-stage MAV with a solid first stage component. With MOR, system parameters (e.g., payload masses, mass growth allowances, propellants) can be adjusted to maximize mission objectives.

Abstract Approval: Committee Chair _____

Department Chair _____

Graduate Dean _____

ACKNOWLEDGMENTS

I would like to thank Drs. Michael P.J. Benfield and Matthew W. Turner for their guidance in orbital mechanics as well as document formatting. I owe special thanks to Dr. Benfield for sharing this research topic with me.

I would like to thank my parents, grandparents, friends, and colleagues whose support and encouragement were invaluable to me while pursuing this advanced degree.

TABLE OF CONTENTS

LIST OF FIGURES

LIST OF TABLES

Table Page

LIST OF SYMBOLS

a_x	semi-major axis g_o
CaLV	Cargo Launch Vehicle
CEV	Crew Exploration Vehicle
ConOps	Concept Operations
C_3	energy of a launch vehicle required to escape orbit
$(C_3)_{dep}$	energy of a spacecraft required for planetary departure
DA	Direct Ascent
DA-SS	Direct Ascent using a Single-stage MAV
DA-2S	Direct Ascent using a Two-stage MAV
DRM	Design Reference Mission
EDL	Entry, Landing, and Descent
EDS	Earth Departure Stage
EEC	Earth Entry Capsule
EELV	Evolved Expendable Launch Vehicle
ERV	Earth Return Vehicle
FOM	Figure of Merit
GLOW	Gross Lift-Off Weight
g_o	acceleration due to gravity; referenced to Earth
h_a	apoapsis altitude
h_p	periapsis altitude

iMARS	International Mars Architecture for the Return of Samples
I_{sp}	specific impulse
ISS	International Space Station
LEO	Low Earth Orbit
LLO	Low Lunar Orbit
LMO	Low Mars Orbit
MAV	Mars Ascent Vehicle
MEPAG	Mars Exploration Program Analysis Group
MER	Mars Exploration Rover
MGA	Mass Growth Allowance
MGS	Mars Global Surveyor
MM	Mass Margin
MOI	Mars Orbit Insertion
MOR	Mars Orbit Rendezvous
MOR-SS	Mars Orbit Rendezvous using a Single-Stage MAV
MOR-2S	Mars Orbit Rendezvous using a Two-Stage MAV
MSL	Mars Science Laboratory
MSR	Mars Sample Return
NASA	National Aeronautics and Space Administration
OS	Orbiting Sample
PBAN	Polybutadiene Acrylonitrile
PMER	Preliminary Mass Estimating Relationship
PMF	Propellant Mass Fraction

r_a	radius of apoapsis
R_o	planetary central body radius
r_p	radius of periapsis
RSRB	Reusable Solid Rocket Booster
SC	Sample Canister
TEI	Trans-Earth Injection
TLI	Trans-Lunar Injection
TMI	Trans-Mars Injection
U.S.	United States
V_{HE}	hyperbolic excess velocity
V_p	velocity at periapsis on approach hyperbola
$V_p^{'}$	velocity at periapsis on desired orbit
ZBO	Zero Boil-off
ΔV	change in velocity required for a spacecraft to perform a given orbital maneuver
ΔV_{Ascent}	ΔV required for Mars ascent
$\Delta V_{Descent}$	ΔV required for Mars descent
ΔV_{MOI}	ΔV required to perform Mars orbit insertion
ΔV_{TEI}	ΔV required to perform trans-Earth injection
μ	

CHAPTER 1

INTRODUCTION

1.1 History of Exploration

Exploration is human nature. Historically, man has gone to great lengths to explore the world. Leaders and conquerors have stepped beyond their boundaries in search of riches, civilizations, passageways, and territories. Exploration has been driven primarily by necessity and is often further inspired by curiosity. In earlier centuries, man was unable to explore beyond certain geographical boundaries. Now, with the vast advancements in science and technology, man has begun venturing beyond his own planet in search of the answers to the questions about the solar system's origins.

Exploration is often a response to necessity. Early European explorers sought spices and other goods from Asia by way of sea. This led to the accidental discovery of the Americas by Christopher Columbus on his 1492 voyage to the West [1]. In the 1600s, religious and political differences drove the English Pilgrims to settle in the Americas. Within two centuries, the United States of America was formed [1]. Upon purchasing the Louisiana Territory, President Thomas Jefferson sent Meriwether Lewis and William Clark to find a water route to the Pacific Ocean. Along the way, they found new Native American tribes, plant and animal species, and geological landmarks [2].

1.2 History of Space Exploration

After World War II, rising tensions between the United States (U.S.) and the Soviet Union became a major military concern. During the late 1940s, the United States War Department (later renamed the Department of Defense) strived to stay ahead of the Soviet Union in rocketry and upper atmospheric technology. When the U.S. announced plans to launch its first orbiting satellite to gain scientific information about Earth, the Soviet Union responded immediately by planning a similar mission. The Soviets launched the first Earth orbiting satellite, Sputnik, in October 1957, which inspired the U.S. to launch Explorer in January 1958, and plan more ambitious missions for the near future. The launch of Sputnik and increasing tensions between the superpowers drove the U.S. to establish the National Aeronautics and Space Administration (NASA) in October 1958 [3].

The Mercury and Gemini projects gave birth to the first American manned spaceflights, which prepared the U.S. for the upcoming aggressive requirements of the lunar program, Project Apollo. The Apollo era contributed heavily to planetary exploration technology and science. Among these technological contributions was the Saturn V rocket, which surpassed the lift capability of the existing fleet of launch vehicles [3].

The success of previous interplanetary missions has provided a wealth of knowledge about atmospheric conditions, solar and magnetic activity, and surface topography of various planets in the solar system. In the 1970s, the Pioneer missions journeyed the depths of the solar system and returned information on surface topography and magnetic fields of various planets, including Venus and Saturn. The deep space

Pioneer probes also collected data on solar activity throughout the course of their journeys [4]. The Magellan orbiter, launched in May 1989, returned images of the polar regions of Venus [5]. The Cassini missions sent spacecraft to orbit Saturn and observe its moons. Water expulsion was found on the southern region of Saturn's moon Enceladus [6]. The knowledge gained from these deep space missions, as well as many others, have contributed dramatically to the science community, as these discoveries are critical to understanding the origins of the solar system.

In order to develop a clearer understanding of the origins of the solar system, it is necessary to explore beyond Earth. Although a number of successful piloted lunar missions have been performed, and have returned a wealth of knowledge about the moon's composition and evolution, planetary science would benefit from further exploration. Mars is the planetary body closest to the Earth and moon, and its physical conditions make it the most similar planet to Earth in the solar system. Successful pursuit of Mars exploration would advance Earth and planetary science to new levels [7, 8].

Exploration of Mars has included a number of successful flybys, orbiting missions, and surface landings. The 1976 Viking mission found evidence of a drastic change from a once warmer and wetter climate. Additionally, it is almost certain that liquid water once flowed on Mars' surface [9]. Orbiting missions in the 1990s by Mars Global Surveyor (MGS) and Mars Observer led to the development of higher fidelity models of the Martian gravity field. MGS and Mars Odyssey returned thermospheric wind data, which is essential for structural design of spacecraft entering the Martian atmosphere [10, 11]. Surface landings by the Mars Exploration Rovers (MERs), Spirit and Opportunity, showed that habitable environments likely existed near, and possibly at,

the surface [9]. The Phoenix lander landed on Mars in May 2008 in the northern polar region where the Mars Odyssey orbiter had detected solidified water in a previous mission. Phoenix currently resides on the surface of Mars, where it continues its task of characterizing the chemistry of the local surface, subsurface, and atmospheric materials [12]. With each robotic Martian mission, more information is gathered about the Mars' current and ancient planetary characteristics, which brings the scientific community closer to understanding the origins and formation of the Earth, and thus the solar system.

1.3 The Future in Space Exploration

President George W. Bush announced on January 14, 2004 the Vision for Space Exploration, currently known as the Space Exploration Initiative. This plan entails returning man to the moon, and later landing a human on Mars. These goals will be completed by discontinuing the Space Shuttle and International Space Station (ISS) program and replacing them with Project Constellation. Constellation will seek to explore beyond low Earth orbit by sending robotic missions, and eventually manned missions, to the moon, and then to Mars [13]. To achieve the goals of Project Constellation, a new fleet of launch vehicles and spacecraft are being developed. To enable the upcoming lunar manned missions, a crew exploration vehicle (CEV), Orion, is required for transporting the three-man crew into low Earth orbit (LEO). The CEV will be launched on the Ares I rocket, one of two new launch vehicles in development for the Constellation program. Ares V, the heavy lift launch vehicle of the new fleet, will launch the Earth departure stage (EDS) into LEO, carrying the Altair lunar lander. In LEO, the CEV will dock with EDS, which will then carry the integrated vehicle to the moon [14].

The launch capability of Ares V will enable robust space missions, thus furthering the interplanetary exploration sought by the Space Exploration Initiative.

In addition to lunar landings, the Space Exploration Initiative seeks to land humans on Mars, and later travel on to other planets. However, before a manned Mars mission is possible, extensive robotic exploration and environmental characterization is necessary.

1.4 Future Exploration of Mars

The success of previous Mars missions suggests that the scientific community awaits the next step in exploration—human Mars missions. To safely land humans on the surface of Mars, it is imperative that scientists understand the nature of the surface and atmosphere so that engineers can develop the components (i.e. lander, ascent vehicle, rover, etc.) appropriate for Martian conditions. Additionally, it is necessary to produce the support systems required for sustaining human life and carrying out the scientific surface operations associated with these manned missions. While science has experienced a tremendous increase in knowledge about Mars' surface and atmosphere from previous robotic Mars missions, a tangible sample of the planet has yet to be returned to Earth. A surface sample would reveal a wealth of knowledge about the nature and evolution of Mars' core, crust, surface, and atmosphere. This new knowledge will bridge the gap between the U.S. desire to send humans to Mars and the technology to achieve successful manned missions [8].

In order to plan for a series of Mars sample return (MSR) missions, NASA created the Mars Exploration Program Analysis Group (MEPAG). MEPAG is tasked with planning and prioritizing the major goals sought by Mars scientists [15]. Based on

input from scientists, MEPAG has established four major goals for Mars sample return, commonly known as *Life*, *Climate*, *Geology*, and *Preparation for Human Exploration*. These goals, while not yet prioritized, each have their own objectives, which are listed in the order in which they must be accomplished for each particular goal. Associated with each of these objectives are the necessary investigations to be conducted in order to achieve Mars sample return and, eventually, human Mars exploration [8]. MEPAG goals and objectives are summarized in Table 1.1.

Table 1.1: MEPAG goals and objectives.

Objectives	**Goal I: Life**
	1. Habitability
	2. Carbon Cycling
	3. Life Forms
	Goal II: Climate
	1. Mars' Atmosphere Under Current Orbital Configuration
	2. Mars' Atmosphere Under Previous Orbital Configurations
	3. Ancient Martian Climate and Climate Processes
	Goal III: Geology
	1. Martian Crust
	2. Martian Interior
	3. Phobos and Deimos
	Goal IV: Preparation for Human Exploration
	1. Surface Assessment
	2. Risk and Cost Reduction
	3. Effect of Martian Atmosphere on Spacecraft

A robotic Mars sample return mission, equipped with the proper science instruments can help scientists to achieve these goals by returning a tangible sample of Mars' surface. A more robust architecture would provide a higher landed mass capability, thus allowing more science payload to be carried to Mars' surface. With an

increase in the amount of science equipment that can be utilized on the surface, more goals and objectives can be achieved on a single mission.

1.5 Summary

Exploration has led humans to encounter things they never expected to find. Columbus set sail in 1492 seeking an alternate route to Asia and instead found the Americas. Similarly, President Jefferson sent Louis and Clark on a westward voyage to explore the Louisiana territory in search of a cross-continental water route; additionally, they found numerous animals, several Native American tribes, and the Rocky Mountains. In later years, the founding of NASA led to great technological advancements and discoveries about the solar system. History has shown that by exploring beyond physical boundaries, man finds things he never dreamed of discovering. Thus the importance of further exploration is not only finding what is sought after, but what unintentional discoveries may be made along the journey. Currently, very little is known about Mars, and the success of a single sample return mission would contribute vast amounts of information about the Earth and solar system to the scientific community.

Mars sample return is the next step in planetary exploration. The new generation of launch vehicles (i.e., Ares I and Ares V) is currently in development. With the improvements in launch capability to come with Ares V, revolutionary space missions can be achieved, thus enhancing the current understanding of the Earth and solar system. The goals and objectives sought by scientists have been established, and MEPAG continues to plan and prioritize the investigations for Mars exploration. In the decades since the Apollo era, numerous studies have been performed to assess the technological requirements of performing Mars sample return. Researchers have performed a number

of trade studies on mission scenarios, trajectories, vehicle designs, and propulsion systems for Mars sample return strategies. These studies are summarized in the literature review presented in Chapter 2.

CHAPTER 2

LITERATURE REVIEW

2.1 Introduction

It has been a goal from the early days of mankind to find the answers to the questions about Earth's origins. There is very little information about the formation of Earth, and it is believed that some of the answers to Earth's history lie on and under the surface of Mars [7]. Additionally, Mars is the planet most similar to Earth in this solar system, as it is the most inhabitable non-terrestrial of the planets. Numerous spacecraft have been sent to Mars to obtain information about the planet's geological composition. Although information from satellites, landers, and rovers about Mars' surface and atmosphere has been returned, no tangible sample of the planet has been acquired. A successful Mars sample return mission could achieve a number of scientific objectives. The MEPAG goals of *Life*, *Climate*, *Geology*, and *Preparation for Human Exploration* cannot be fulfilled until a series MSR missions completes the required investigations [8].

The search for past or present life forms on Mars is a major issue for the scientific community. The composition and evolution of the planet's three major layers and atmosphere are of particular interest to MEPAG, as this could conclude a great deal of

information about life on Mars. Scientists are also interested in the ages and histories of select geological bodies, as well as the reasons for variations in regolith from different regions of the planet. Ultimately, the human exploration of Mars is a major goal of the Space Exploration Initiative. In order to enable manned missions to Mars, risks associated with human exploration and feasibility of in-situ propellant utilization must be assessed. Martian samples are needed to achieve all these goals, and it is believed that a Mars sample return mission would have the greatest scientific impact on finding the answers to Earth's evolution [14].

2.2 Mars Sample Return Missions

Various sources for Mars sample return missions were studied. These twenty-eight sources include proposals, trade studies, and sensitivity analyses on outbound and inbound strategies, vehicle designs, and propulsion systems. This section categorizes the architectures proposed in fifteen of the sources studied. Each architecture is comprised of required orbital maneuvers, among which are trans-Mars injection (TMI), Mars orbit insertion (MOI), descent, ascent, and trans-Earth injection (TEI). The components required to achieve these orbital maneuvers include an orbiter, Earth return vehicle (ERV), lander, and Mars ascent vehicle (MAV).

2.2.1 Architectures

This section provides an overview of the MSR studies that have been completed to date. Fifteen of the studies gathered could be categorized into three major architectures: Mars orbit rendezvous (MOR), orbiting sample (OS), and direct ascent (DA). Each architecture is comprised of a set of orbital maneuvers, and these maneuvers require specific components to achieve the given mission. Additionally, this section

briefly discusses the performance advantages and the respective risks associated each of these architectures.

2.2.1.1 Mars Orbit Rendezvous Architectures

Several studies [16-19] propose a sample transfer via Mars orbit rendezvous (MOR) and docking prior to Earth return. An orbiter inserts the integrated vehicle into the desired low Mars orbit (LMO), otherwise known as the parking orbit. A lander, carrying a rover and ascent vehicle, separates from the orbiter and lowers the payload to Mars' surface. Upon completion of landing operations, the lander deploys the rover to begin surface operations. After surface operations (e.g., sample retrieval), the Mars ascent vehicle ascends to the parking orbit where it docks with the orbiter. The sample canister (SC) is transferred into the orbiter, or into a return stage within the orbiter. Once the SC is secured, the return vehicle separates and departs toward Earth on a hyperbolic escape trajectory. Utilizing an additional vehicle for Earth return increases mission complexity, as does rendezvous and docking in Mars orbit. Increasing the number of orbital maneuvers, and thus mission components, decreases the system mass, as less propellant is required.

2.2.1.2 Orbiting Sample Architectures

Much like MOR, numerous studies [20-27] propose an orbiting sample (OS) transfer in Mars orbit. An orbiter inserts the integrated vehicle into the desired parking orbit. A lander, carrying a rover and ascent vehicle, separates from the orbiter and lowers the payload to Mars' surface. Upon completion of landing operations, the lander deploys the rover to begin surface operations. After surface operations sample retrieval, the MAV ascends to the parking orbit. However, rather than docking with the MAV (as in MOR), the orbiter detects the MAV in orbit. Once the proximity of the MAV is

appropriate, the MAV propels the SC toward the orbiter. The orbiter detects and captures the OS. The orbiter, or a return stage aboard the orbiter, separates and departs on a hyperbolic return trajectory. As in the MOR architectures, sample transfer in Mars orbit increases mission complexity; however, the increased number of orbital maneuvers would require more and thus less robust components. Additionally, the technology for this orbiting sample concept has yet to be developed.

2.2.1.3 Direct Ascent Architectures

Few studies [28-30] propose a direct Earth return, as this would require a far more robust ascent vehicle. Rather than braking into Mars orbit to transfer the sample to a return vehicle, the MAV would simply burn beyond Mars orbit directly onto a hyperbolic escape trajectory. Although the ΔV (velocity change required for a spacecraft to perform a given orbital maneuver [31], detailed further in Section 4.4.3, required for this combined maneuver would be lower, the mass of the ascent vehicle would be much greater than that for the MOR and OS architectures. The direct ascent architecture is a simpler and lower risk concept than the MOR and OS architectures because less maneuvers and components are needed. However, the propellant mass required to power the combined Mars ascent and Earth return maneuvers would require an increase in propellant mass for the lander, as the MAV is a payload of the lander. Similarly, because the lander is a payload of the orbiter, the orbiter's mass would increase due to mass growth of the lander.

2.2.2 Components

This section provides an overview of the components required for the Mars sample return sources studied. Each component (i.e., orbiter, Earth return vehicle, lander, Mars ascent vehicle, Earth entry capsule, and sample canister) is associated with a

specific orbital maneuver required for a mission. The reader will note that the need for certain components may be negated depending on the given architecture.

2.2.2.1 Orbiter

In all architectures, an orbiter is required to brake the integrated vehicle from trans-Mars injection (TMI) into Mars orbit. The orbiter must maintain the desired parking orbit for communications throughout landing, surface operations, and ascent. In the direct ascent architectures, the orbiter is no longer required after ascent. In the case of Mars orbit rendezvous, the orbiter maintains a parking orbit throughout the duration of surface operations and ascent. The orbiter will not be expended until after docking with the MAV for sample transfer. The orbiter will either depart on a hyperbolic escape trajectory carrying the SC, or it will deploy a return vehicle (i.e., ERV) to return the SC to Earth.

2.2.2.2 Earth Return Vehicle

For the direct ascent architectures, the MAV performs a combined ascent-return maneuver, thus negating the need for a separate return vehicle. In the case of Mars orbit rendezvous, a separate return vehicle (i.e., ERV) is required to return the surface samples to Earth. The ERV remains attached to the orbiter throughout surface operations and ascent. Upon docking with the MAV, the SC is transferred into an Earth entry capsule (EEC) aboard the ERV. Once the SC is secured, the ERV separates from the orbiter and departs on a hyperbolic escape trajectory. Upon approaching Earth, the ERV deploys the EEC (which will land in the surface of an uninhabited region) into Earth's atmosphere while diverting away from the Earth via a non-return trajectory.

2.2.2.3 Lander

In all reviewed architectures, a lander is required to lower the MAV and science payloads to Mars' surface. Once the orbiter has achieved the desired Mars orbit, the lander separates from the orbiter and begins the descent phase. The MAV and rover are considered payloads to the lander during the descent maneuver. Upon completion of landing operations, the lander deploys the rover to begin surface operations. After surface operations and sample retrieval are complete, the MAV launches off the lander platform. The lander is used for communication during the ascent phase, after which it is no longer required.

2.2.2.4 Mars Ascent Vehicle

In all reviewed architectures, an ascent vehicle (i.e., MAV) is required to perform one of two primary functions: launch the SC (filled with surface samples) into Mars orbit, where it rendezvouses and docks with the orbiter for sample transfer; or launch the SC directly onto a direct Earth return trajectory. For the Mars orbit rendezvous architectures, the MAV (containing the SC) launches into LMO to rendezvous and dock with the orbiter. The MAV is no longer required after sample transfer is complete. In the case of direct ascent, the MAV launches from Mars' surface, carrying the SC, which is secured within the EEC. Rather than braking into Mars orbit to rendezvous with the orbiter/ERV, the MAV's propulsion system provides enough thrust beyond Mars orbit onto an Earth return trajectory. Upon Earth approach, the MAV deploys the EEC into Earth's atmosphere while diverting onto a non-return trajectory.

2.2.2.5 Sample Canister

A containment device (i.e., sample canister) is required to house the surface samples. This container must be airtight and encapsulate the samples such as to prevent

mixing or crushing during sample retrieval and Earth return [7]. Table 2.1 gives a summary of the sample and SC masses used in several sources. Note that the common assumption for sample mass is 0.5 kg, and the SC masses do not exceed 5 kg.

Table 2.1: Source comparison for sample mass.

Sample Mass (kg)	**SC Mass (kg)**	**Source**
0.5	N/A	Baker [32]
>0.5	N/A	Beaty [7]
0.3	2.7	Desai [16]
0.5	4.6	Jordan [20]
>0.5	N/A	Mattingly [21]
N/A	*3.6	Mitcheltree [33]
0.5	**4.6	Oberto [25]
N/A	***3.6	Price [24]
N/A	5	Whitehead [34]
0.5	*5	Willenberg [35]
*architecture uses two sample canisters		
**includes mass of sample		
***rendezvouses with Space Shuttle or ISS for sample retrieval		

2.2.2.6 Earth Entry Capsule

An Earth entry capsule is required to house and secure the SC en route to Earth. For direct ascent, the EEC is carried by the MAV from Mars' surface directly to Earth. For rendezvous in Mars orbit, the EEC is carried by the return vehicle from LMO to Earth. In all architectures, the return vehicle deploys the EEC into Earth's atmosphere, and the EEC will make a surface landing in an uninhabited location. The EEC must protect the SC during Earth return, reentry, and landing, such that the surface samples do not experience any form of alteration or contamination [7]. Table 2.2 gives a summary of the Earth entry capsule masses used in several sources. Note that the EEC mass varies over a range between 20 and 150 kg.

Table 2.2: Source comparison for Earth entry capsule mass.

EEC Mass (kg)	Source
80	Baker [32]
80	Cook [29]
27	Desai [16]
150	Donahue [17]
*44	Jordan [20]
42	Mitcheltree [33]
42.9	Mitcheltree [36]
**24.2	Price [24]
80	Valentian [37]
20	Wercinkski [38]
*NASA Langley Research Center concept	
**architecture uses two EECs	

2.2.3 Maneuvers

This section provides an overview of the orbital maneuvers required in the Mars sample return studies. Each of these maneuvers is achieved using a specific component. The reader will note that the need for certain maneuvers is negated depending on the given architecture.

2.2.3.1 Trans-Mars Injection

Trans-Mars injection (TMI) is an orbital maneuver, performed by the launch vehicle's upper stage, which propels a spacecraft toward Mars from Earth. In this study, the integrated vehicle will be carried to Mars via TMI by the Ares V upper stage. An Ares V performance plot is provided in Sumrall [39], and is shown in Figure 2.1. The plot gives the allowable Ares V payload mass as a function of launch energy (C_3) for two upper stage configurations, EDS and Centaur V2. Tables 9 through 16 [40] list the C_3 and ΔV_{TMI} of the various launch opportunities from 2009 to 2024.

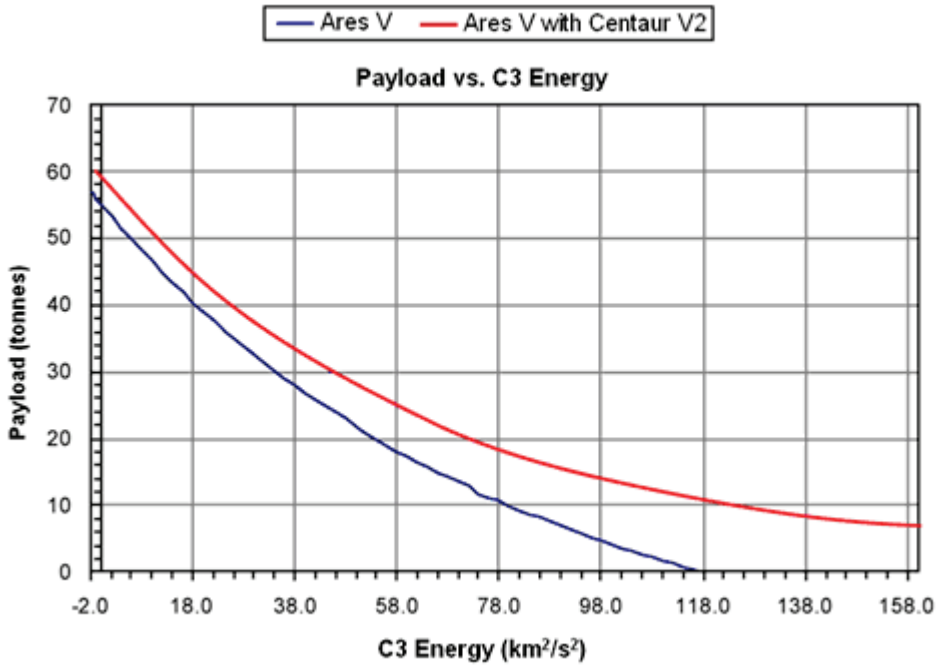

Figure 2.1: Ares V Escape Performance.

2.2.3.2 Mars Orbit Insertion

Mars orbit insertion (MOI) is an orbital maneuver, performed by the orbiter, which captures into a planet's orbit. Once the desired orbit is achieved, the lander can separate and begin descent operations while the orbiter remains as a communication asset. Table 2.3 lists the Mars arrival and parking orbits used in various studies, as well as the corresponding ΔV values required for MOI (ΔV_{MOI}). Note that the most common choice is a 500 km circular orbit. Only one source lists an elliptical orbit, and the others consist of circular orbits with altitudes less than 600 km.

Table 2.3: Source comparison for ΔV_{MOI}.

Periapsis (km)	Apoapsis (km)	ΔV_{MOI} (km/s)	Source
500	500	0.750 – 0.800	Baker [32]
500	500	N/G	Beaty [7]
556	556	N/G	Benton [41]
500	500	N/G	Cervone [42]
300	300	4.170	Desai [43]
400	400	2.261	Donahue [17]
250	33,793	N/G	George [40]
500	500	N/G	Jordan [20]
300	450	1.361*	Matousek [19]
240	35,000	N/G	Mattingly [21]
	75,000	N/G	
500	500	1.106	Oberto [25]
500	500	N/G	Walberg [44]
250	250	N/G	Wercinski [38]
500	500	N/G	Whitehead [45]

2.2.3.3 Mars Descent

Mars descent is the maneuver, performed by a descent stage, which lowers the science payloads to Mars' surface. The descent phase is a series of maneuvers, propulsive and non-propulsive, designed to accurately land the system in the site of interest with minimal propellant required.

The Mars Phoenix entry, descent, and landing (EDL) sequence began with atmospheric entry of an aeroshell. Entry was followed by jettison of the aeroshell's frontal heat shield and deployment of parachutes. Finally, the Phoenix lander was deployed and used propulsive descent until touchdown on the Mars surface [46].

The EDL sequence of the Mars Pathfinder spacecraft, which landed on the Martian surface July 4, 1997, took a similar approach to that of the Mars Phoenix. As in the Phoenix EDL scenario, Pathfinder's aeroshell performed atmospheric entry, followed

by parachute deployment and jettison of the heat shield. The lander separated from the aeroshell and deployed a system of tether-like cables, or bridles, to lower the rover. Airbags inflated on the rover, and propulsive descent continued to lower the vehicle to the surface. The bridles released the rover to be dropped to the surface, where it tumbled until it reached equilibrium. The flyaway controller diverted the lander away from the rover, allowing surface operations to commence [47].

As in the Phoenix EDL approach, the Mars Science Laboratory (MSL), expected to land on Mars in 2010, will perform atmospheric entry via aeroshell, followed by parachute deployment. The aeroshell will be jettisoned, and a propulsive descent phase will lower the system to approximately 100 m above the surface. The MSL rover will then separate from the lander. The rover will be suspended via Sky Crane, a system of tether-like cables, known as triple bridles, used to safely lower the surface payloads to the ground. After touchdown on the Mars surface, the triple bridles will release the rover, and the flyaway controller will divert the lander, or descent stage, away from the rover so that surface operations may commence [48-50].

In all of the scenarios discussed above, some propulsive descent is required to land the science payload on the surface. Zubrin [18] gives a descent ΔV of 350 m/s. This value is based on the assumptions of descent from a 500 km circular orbit and the use of parachutes as a non-propulsive means of braking. The amount of propulsion required for the lander is reduced by employing alternate landing strategies. At least seven other studies [21, 38, 48, 49, 51-53] have thus employed parachutes as a means of non-propulsive braking.

2.2.3.4 Mars Ascent

Mars ascent is a maneuver, performed by the MAV, which launches the SC (filled with surface samples) off the Martian surface for Earth return. For rendezvous in Mars orbit, the MAV launches off the surface and achieves LMO, where it will rendezvous with the orbiter/ERV for sample transfer. For direct ascent, the MAV launches off the surface directly onto a TEI escape trajectory. Table 2.4 lists the ΔV values required for Mars ascent (ΔV_{Ascent}), along with their respective orbits and MAV configurations, from various sources. Note that the majority of the architectures listed are for two-stage MAVs which launch to a 500 km circular Mars orbit and require a ΔV between 3,000 and 5,000 m/s. Note that, among the studies reviewed, there is a common interest for MAVs propelled by solid rocket motors [54] or liquid bipropellant engines [54]. Additionally, the staged MAV configurations have a nearly equal split of ΔV between the two stages. Note that in Whitehead [30], the ΔV is split equally between the two stages of the MAV.

Table 2.4: Source comparison for ΔV_{Ascent}.

ΔV_{Ascent} (m/s)	Mars Orbit (km)	MAV Configuration	Source
3,800	500	2-stage	Baker [32]
4,650	500		Cervone [42]
3,000		Stage 1	Cook [29]
3,050		Stage 2	
		2-stage	Desai [16]
6,500	400	direct ascent	Donahue [28]
4,900	300		Matousek [19]
	500	2-stage, solid	Mattingly [21]
	400		MEPAG [55]
		2-stage, solid	Price [24]
3,000		Stage 1	Valentian [37]
3,050		Stage 2	
4,371	500	Solid	Whitehead [45]
4,157		Liquid	
		3-stage, solid	Whitehead [56]
6,500		1-stage, direct ascent	Whitehead [30]
3,250		Stage 1, direct ascent	
3,250		Stage 2, direct ascent	
4,333		1-stage	
2,000	500 +/- 100	Stage 1: STAR 17A	Willenberg [35]
2,468		Stage 2: STAR 13A	
2,000	500 +/- 100	Stage 1: STAR 17	
2,468		Stage 2: MON-25/MMH	
	500 +/- 100	1-stage	

2.2.3.5 Trans-Earth Injection

Trans-Earth injection (TEI) is an orbital maneuver, performed by a return vehicle, which propels a spacecraft toward Earth. For rendezvous in Mars orbit, the ERV separates from the orbiter after sample transfer and departs onto a TEI escape trajectory. For direct ascent, the MAV performs a combined ascent-to-TEI maneuver directly from the Mars surface. Donahue [28] gives a range of ΔV_{TEI} between 1.0 and 1.5 km/s, where the exact value varies by launch opportunity.

2.2.3.6 Reentry

Reentry into Earth's atmosphere is performed by an Earth entry capsule, or EEC, at the end of the TEI phase. The ERV (or MAV) releases the EEC (containing the surface samples) into Earth's atmosphere via a non-return trajectory. The EEC lands in the surface of Earth at an uninhabited location [7].

Another concept for returning the surface samples to Earth is through rendezvous and docking with the Space Shuttle or ISS. Exposing the biochemical materials on Earth could prove to be hazardous to the surroundings, so some studies have considered introducing these samples onboard the shuttle or ISS before bringing them to the ground.

2.3 Ares V

Propulsive capability of the launch vehicle limits the level of scientific gain that can be achieved on an interplanetary mission. This section provides an overview of the Ares V launch vehicle. Ares V is a concept in development for the Constellation program which will be used for heavy-lift purposes. The following sections describe Ares V in terms of its intended purposes, vehicle profile, performance parameters such as specific impulse [54] and propellant mass fraction [54] (defined in Chapter 4), and propulsive capability for interplanetary missions.

2.3.1 Intended Purposes

The Constellation program for human space exploration will begin with the return to lunar exploration. The launch vehicles for lunar and interplanetary exploration are currently in development. Ares V will be used as a heavy-lift vehicle in conjunction with the crewed launch vehicle, Ares I [57]. Ares V has the highest payload capability of any other launch vehicle concept to date. Sumrall provides a lift comparison between the

retired Apollo era launch vehicle, Saturn V, and Ares V. Saturn V provided a trans-Lunar injection (TLI) payload capability of 44.9 metric tons (mT), or 99,000 lb_m, whereas Ares V will provide a TLI capability of 62.8 mT (138,500 lb_m) [39]. With this increase in launch mass capability from Ares V, Constellation can power more robust missions that can be completed in a shorter timeframe [28].

The current Constellation concept of operations (ConOps) is as follows. Ares V will launch into low Earth orbit. The EDS will rendezvous and dock with the CEV, launched into a low Earth orbit LEO of 185.2 km [57] by Ares I. EDS will then propel the combined vehicle to low Lunar orbit (LLO) via TLI [28]. Figure 2.2, from Sumrall [14], illustrates the lunar mission scenario using Ares V as the cargo launch vehicle (CaLV).

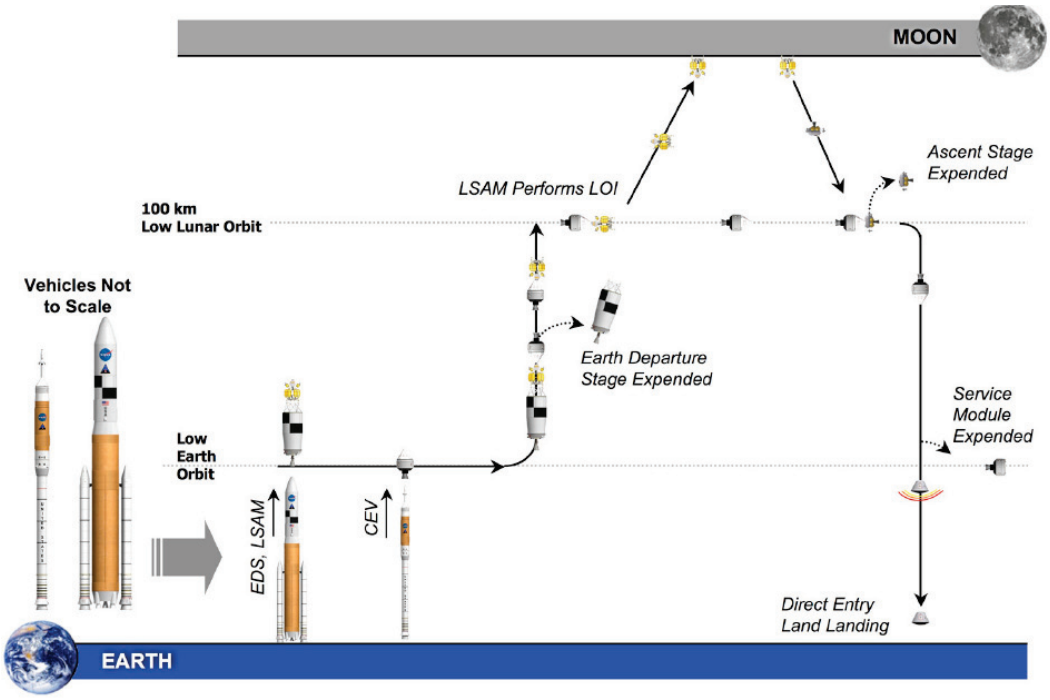

Figure 2.2: AresV ConOps.

2.3.2 Vehicle Profile

The launch vehicle is a major contributor when determining the overall system mass of a planetary mission. The amount of science payload, or the number of science instruments, that can be carried on a mission is directly related to the amount of mass that can be carried by the launch vehicle. This section provides an overview of the Ares V vehicle profile.

The Ares V vehicle configuration 51.00.39 stands 360.5 ft (116.2 m) tall and has a core diameter of 33 ft (10 m). The Ares V gross liftoff weight (GLOW) of 7,440,326 lb_f (3,374.875 mT). The Ares V platform consists of three major sections: a core stage, two solid boosters, and the Earth Departure Stage. Sumrall [58] provides a detailed description of the vehicle stages.

The core stage consists of five RS-68 engines which uses the propellant combination LOx/LH_2. The core stage has a propellant mass fraction (PMF) of 0.9052, at a vacuum specific impulse (I_{sp}) of 414.2 s. Each of the two five-segment Reusable Solid Rocket Boosters (RSRBs) uses a PBAN (polybutadiene acrylonitrile) grain with a PMF of 0.8628 and a vacuum I_{sp} of 272.8 s. The upper stage, EDS, is powered by a single J-2X, a Saturn V derived engine fueled by LOx/LH_2. The EDS liftoff PMF is 0.8808, and the vacuum I_{sp} is 449 s [58].

2.3.3 Performance

For the Ares V configuration 51.00.39, Sumrall [39] provides the vehicle performance curve for payload mass as a function of C_3 energy. From Sumrall's Ares V performance plot (Figure 2.1), Ares V has a marginally higher lift capability for the Centaur V2 upper stage than for the Earth departure stage. When the C_3 for Earth escape

is designated, the performance plot can be used to find the allowable Ares V payload mass that can be launched into a circular low Earth orbit of 185 km. Later configurations of Ares V are expected to have more optimal performances [39].

While the Centaur upper stage has been developed and used over the years, it was designed for other purposes, including the launching of the Cassini spacecraft on a Titan IV-B booster in October 1997 [6]. A Centaur upper stage would have to be modified to fit the Ares V platform, whereas EDS is specifically being designed as the Ares V upper stage.

2.4 Summary

The information presented in this chapter describes the proposed architectures, orbital maneuvers, and necessary components for the Mars sample return mission concepts studied. The predicted Ares V performance, presented in Section 2.2.3.1, surpasses that of any existing launch vehicle. The information presented in this chapter is later used to develop a feasibility study and a sensitivity study for Mars sample return. The following chapter describes the scientific importance of Mars sample return and the contribution of this research to the scientific community.

CHAPTER 3

RESEARCH STATEMENT

3.1 Objective

Many factors will play into the development of a Mars sample return mission. Three primary figures of merit—risk, cost, and performance—must be considered and weighted differently depending on current constraints. Numerous trade studies should be performed to determine the amount of technology development needed, the desired cost, and the amount of science to be returned. All of these figures will be directly affected by factors such as the particular mission scenario, system mass, and complexity of mission components. It is important to identify the effects that individual components' sizes and performances have on overall system mass. To be able to determine the effects that each parameter has on a given return strategy is key to developing both a mass and cost efficient Mars sample return mission.

Given the current fleet of Evolved Expendable Launch Vehicles (EELVs), the common architecture for Mars sample return uses a dual launch [7, 26, 27, 32]. The International Mars Architecture for the Return of Samples (iMARS) working group has developed five architectures for a dual-launch Mars sample return mission [7] A heavy-lift launch vehicle, usually an Ariane 5, will launch an orbiter composite, which carries

the orbiter, Earth Return Vehicle, and Earth Entry Capsule. A second heavy-lift class rocket will launch a lander composite, which will carry the Mars lander, Mars ascent vehicle, rover, and sample canister. The orbiter will achieve the desired parking orbit, and the lander will descend to Mars' surface directly from a hyperbolic trajectory. After surface operations are complete, the MAV, containing the sample container, will launch into the aforementioned parking orbit, where it will rendezvous with the orbiter/ERV. After the SC is transferred to the ERV, the MAV and orbiter will be expended, and the ERV will depart toward Earth. Some architectures may involve a simple direct Earth return, or direct ascent, rather than braking into Mars orbit to rendezvous with the orbiter [7].

Each of the three iMARS architectures uses a dual launch scenario. An Altas V 551 class would suffice for the launch of either composite (lander or orbiter) and would allow direct transfers to Mars. An Ariane V would only be capable of launching the orbiter composite, and would still need additional launch capability from Earth swing-bys. None of the iMARS architectures propose an entire MSR mission on a single launch [7]. Should one of the two launches fail in any given architecture, the entire mission would be lost. The risk associated with a mission involving multiple launches is therefore higher than a mission involving only one launch, particularly if the two composites are launched at different opportunities [7].

3.2 Feasibility

The first goal of this study is to determine the feasibility of performing a Mars sample return mission using a single Ares V launch, given the performance of Ares V. Four architectures have been developed, each demonstrating a unique method for

returning a sample of Martian soil to Earth. Each of these architectures is modeled using mass estimating relationships and a mass margin for a baseline set of mission and engine parameters. A positive mass margin infers that a given mission is possible on a single Ares V launch, whereas a negative margin precludes the possibility that the architecture can be accomplished using state-of-the-art technology.

3.3 Sensitivity

The second goal of this study is to determine the effects that varying parameters associated with the mission have on the individual component masses, as well as on the overall predicted system mass. With the first goal of this study answered, one needs to understand the limitations of the viability of each candidate mission architecture. Understanding the sensitivities of the mission variables to the overall predicted system mass will allow future mission planners to focus on the key parameters that must be calculated in greater detail.

Mission parameters (ΔV , I_{sp} , dry mass, mass growth allowance, etc.) are varied for the four architectures. The limits of these parameters are obtained from the data in the literature review. The output variables of interest include the calculated propellant mass, the calculated individual component mass, the overall predicted system mass, and the mass margin. The calculated propellant mass is the amount of propellant required for each defined maneuver for a given architecture. The individual component mass is the calculated value for each major architecture component (orbiter, lander, MAV, etc.). The mass margin for an architecture at any given launch opportunity is driven by Ares V capability and overall predicted system mass, which is the sum of the individual

component masses. This study will identify the variables which have the most significant impact on the predicted system mass and the associated mass margin.

3.4 Contribution of Research

Several major goals are sought by the scientific community for a Mars sample return mission. The search for past and present life forms on Mars is of great interest. Scientists are highly interested in studying the nature and development of the Martian surface, mantle, and core. In order to enable a successful manned mission, it is first necessary to assess the requirements for establishing and sustaining a human presence on Mars. Once this human presence is established on Mars, this could ultimately pave the way for further planetary exploration. These milestones depend heavily on the success of the Mars sample return mission [55].

A dual launch introduces risk with each of the two launch vehicles. In the case that one launch fails, the entire mission is lost. However, should the baseline mission for a given architecture be feasible on a single Ares V launch, this additional risk associated with a second launch would be eliminated. Depending on mission strategy, the amount of payload that Ares V can launch could eliminate the need for the Earth swing-bys required in the iMARS architectures. Additionally, Ares V could enable a greater sample mass to be returned.

Optimizing a mission for Mars sample return requires that mission planners determine the variables which have the greatest impact on system mass. The figures of merit (FOMs) which must be considered when planning an MSR mission include cost, risk, and performance. Mission planners can design a mission which provides the desired balance of the FOMs.

Developing a mission that can be achieved on a single Ares V launch would enable the U.S. to return a sample of Martian soil to Earth. From this small sample, a wealth of knowledge can be learned about the nature and evolution of Mars' geology, climate, and life forms. This new knowledge will pave the way for manned Mars missions, enabling the establishment of a permanent human presence on Mars. Additionally, further planetary exploration may then be possible, from which even more artifacts and knowledge about the evolution of the Earth and solar system can be uncovered [55].

CHAPTER 4

METHODOLOGY

4.1 Introduction

This study determines the feasibility of a robotic Mars sample return mission using a single Ares V launch. This chapter outlines the process by which the results of the feasibility analysis were obtained. The MSR mission scenario, presented in the following sections, describes the necessary orbital maneuvers associated with the mission and the components required to achieve these maneuvers. The mission scenario was chosen based on the data presented in the literature review. This chapter also describes the process by which the overall system mass and mass margin are calculated for each of the candidate architectures.

4.2 Design Reference Mission

This section describes the design reference mission (DRM) used in the four architectures. The orbital maneuvers required in the DRM are defined, as well as the corresponding components required to achieve these maneuvers.

4.2.1 Mission Scenario

Mars sample return mission is a purely robotic mission. A single Ares V launch carries the integrated vehicle to low earth orbit, from which point it uses the Earth

Departure Stage or a modified Centaur upper stage to escape Earth's gravity and place it on a hyperbolic trajectory toward Mars. No additional stage is required for trans-Mars Injection. Upon Mars approach, the Ares V upper stage deploys the orbiter, carrying all other mission components, and is expended. The orbiter brakes into the desired LMO and then deploys the lander to perform descent operations. The lander carries the MAV and rover to Mars' surface; once secured on the surface, the lander deploys the rover, and the rover begins retrieving surface samples. Once the samples are loaded into the SC (onboard the MAV), the MAV launches off the surface and into Mars orbit, where it will rendezvous and dock with the orbiter for sample transfer. Upon completion of sample transfer, the Earth return vehicle separates from the orbiter and carries the SC (secured within the Earth entry capsule) onto a hyperbolic TEI trajectory. Upon Earth approach, the ERV releases the EEC into Earth's atmosphere and diverts away from the Earth on a non-return trajectory. Note that for direct ascent, the MAV (carrying the SC within the EEC) launches directly off the Martian surface onto a TEI trajectory. Upon Earth approach, the MAV diverts away from the Earth on a non-return trajectory just after releasing the EEC into Earth's atmosphere. Figure 4.1 illustrates the mission scenario for this study.

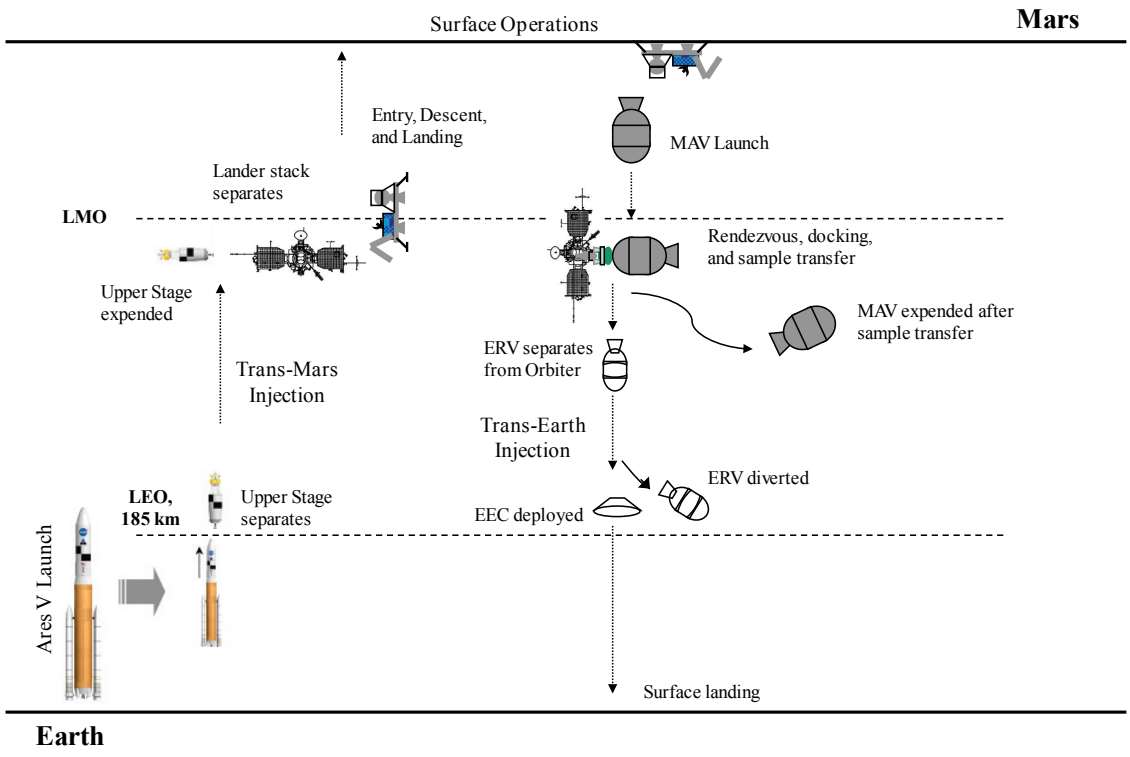

Figure 4.1: Mission scenario.

For any given mission scenario, it is necessary to define both the required orbital maneuvers as well as the required vehicle components for said maneuvers. Four architectures have been modeled to provide comparisons between the required system architecture mass for a given mission and the maximum architecture system mass allowed by Ares V for a given launch opportunity. The outbound strategies modeled in this study include direct ascent and Mars orbit rendezvous. The orbiting sample strategy was not considered on the basis of the increased risk and lack of current technology associated with the mid-orbit SC trajectory. For both the direct ascent and Mars orbit rendezvous strategies, the ascent vehicle was varied between single-stage and two-stage.

Each architecture contains four primary components and five major maneuvers which are described in the sections below.

4.2.2 Mission Components

This section describes the mission components required for the DRM. Each of these components is tasked with specific functions, including the orbital maneuver that each component is expected to perform.

4.2.2.1 Orbiter

An orbiter provides the necessary support systems (thermal, communication, structure, etc.) for the integrated vehicle during interplanetary transfer from Earth to Mars. Once at Mars, the primary function of the orbiter is to achieve LMO via its liquid propulsion system. The orbiter maintains the desired orbit during surface operations to serve as the communications link between the Martian surface and Earth. In the case of direct ascent, the orbiter's primary mission ends with the MAV launch. In the case of Mars orbit rendezvous, an ERV stays attached to the orbiter in LMO throughout descent, surface, and ascent operations of the surface components. The orbiter docks with the MAV in LMO, receives the sample from the MAV, and transfers it into the ERV. After the ERV separates and departs on a hyperbolic return trajectory, the orbiter is no longer required, and is thus expended.

4.2.2.2 Lander

The primary function of the lander is to support and protect the MAV, rover, and other secure payloads, while descending to the surface of Mars. The lander uses both propulsive and non-propulsive means to adequately slow the platform before reaching the surface. Based on the success of previous Mars landings, this study assumes the use of parachutes to reduce the propellant mass required to slow the platform [46, 59, 60].

Upon completion of landing operations, the lander deploys the rover to begin sample collection, while the MAV remains a dormant package onboard the lander. The lander itself may conduct some form of science operations and may be equipped with the capability for collection of core samples [7]. Time spent on the Martian surface varies between 500 and 700 Earth days, depending on Earth launch date [40]. After surface samples have been gathered and placed within the MAV, the MAV launches off the lander platform to begin ascent. The lander is left only to communicate with the orbiter during MAV ascent.

4.2.2.3 Mars Ascent Vehicle

The primary function of the MAV is to launch the SC (filled with surface samples) either into Mars orbit, where it rendezvouses and docks with the orbiter for sample transfer; or directly onto a TEI trajectory. In the case of direct ascent, the MAV deploys the EEC into Earth's atmosphere as it diverts away from the Earth on a non-return trajectory. In the case of MOR, the MAV is no longer needed once sample transfer to the ERV is complete.

4.2.2.4 Earth Return Vehicle

For the Mars orbit rendezvous architecture, an ERV is required to return the sample to Earth. The ERV remains attached to the orbiter throughout lander and rover surface operations and MAV ascent. Upon docking with the MAV, the SC will be transferred into the EEC (aboard the ERV). After the SC is transferred, the ERV separates from the orbiter and departs on a TEI trajectory. The ERV deploys the EEC into Earth's atmosphere as it diverts away from the Earth onto a non-return trajectory. For direct ascent, the MAV performs the same function as the ERV. Instead of docking with the orbiter for sample transfer, the MAV, already loaded with the EEC and SC,

simply launches off the Martian surface directly onto a hyperbolic TEI trajectory. Upon Earth approach, the MAV deploys the EEC (containing the SC) into Earth's atmosphere while diverting away onto a non-return trajectory.

4.2.3 Required Orbital Maneuvers

This section describes the necessary orbital maneuvers for the DRM. Each of these maneuvers has a specific purpose, as well as a corresponding component required to achieve the maneuver.

4.2.3.1 Trans-Mars Injection

Trans-Mars Injection is an orbital maneuver, performed by the Ares V upper stage, which propels a spacecraft toward Mars. In this study, the Ares V upper stage (EDS or Centaur V2) will propel the system on a TMI trajectory from a low Earth orbit of 185.2 km [39]. The total outbound flight time varies between 100 and 400 days, depending on Earth launch date [40]. For this study, the analysis is two-dimensional, thus no plane changes or inclination angles are considered. Additionally, midcourse corrections are not considered in this study because the ΔV required for these maneuvers is orders of magnitudes smaller than the ΔV for any other maneuver.

4.2.3.2 Mars Orbit Insertion

Mars orbit insertion is an orbital maneuver, performed by the orbiter, which allows the integrated vehicle to achieve the necessary Mars orbit. In this study, the orbiter will insert into the desired parking orbit from a TMI trajectory via a liquid bipropellant system. The orbiter slows the system to the correct velocity required to inject onto the desired periapsis. In order for the lander to transport the science payloads to the surface, it is imperative that the orbiter first achieve the correct orbit. Because

ΔV_{MOI} is dependent upon the particular Mars orbit, the periapsis altitude (h_p) is varied in the sensitivity study, so that the effect on system mass can be studied. Because the ΔV required for rendezvous and docking, maintaining parking orbit, and stage separation is orders of magnitude smaller than ΔV_{MOI}, the additional ΔV for these maneuvers is neglected.

4.2.3.3 Mars Descent

Mars descent is a maneuver, performed by the lander, which lowers the science payloads to the Martian surface. The lander performs a combination of propulsive and aerodynamic methods (Sky Crane [49, 50], parachutes, etc.) to lower the supported payloads (MAV and rover) to the surface. It is essential that the lander provide adequate braking such that the supported payloads are not damaged or altered in any way when the lander impacts the Martian surface. To reduce the amount of propellant mass associated with propulsive braking, this study assumes the use of parachutes as a non-propulsive means of braking [50, 59]. Once the descent phase is complete, the surface operations (i.e. sample collection) can begin. Additionally, the descent ΔV ($\Delta V_{Descent}$) is varied in the sensitivity study such that the effect on system mass can be studied.

4.2.3.4 Mars Ascent

Mars ascent is a maneuver, performed by the MAV, which launches the surface samples (secured within the SC) for Earth return. The MAV either brakes into orbit to rendezvous and dock with the orbiter for sample transfer, or directly onto a TEI trajectory to deploy the EEC (containing the SC) into Earth's atmosphere. For the direct ascent architectures, the additional ΔV associated with midcourse corrections is neglected, as these maneuvers require ΔV of orders of magnitude smaller than the ΔV for direct

ascent. For all architectures, the ΔV required for Mars ascent is varied in the sensitivity study such that the effect on system mass can be studied.

4.2.3.5 Trans-Earth Injection

Trans-Earth injection is an orbital maneuver, performed by the return vehicle, which provides the necessary change in velocity to propel a spacecraft toward Earth from Mars via a hyperbolic trajectory. TEI is performed either directly by the MAV from Mars' surface, or by the ERV from Mars orbit. In either case, the returning vehicle carries the surface samples back to Earth. The total inbound flight time varies between 150 and 200 days, depending on Earth launch date [40]. Additional ΔV required for midcourse corrections is not considered, as the ΔV required with these maneuvers is orders of magnitude smaller than ΔV_{TEI}. For all architectures, ΔV_{TEI} is varied in the sensitivity study such that the effect on system mass can be studied.

4.3 Summary of Architectures

This section provides an overview of the architectures developed. The outbound strategy, surface operations, return strategies, and reentry method are introduced in this section. The architectures developed were direct ascent using a single-stage MAV (DA-SS), Mars orbit rendezvous using a single-stage MAV (MOR-SS), direct ascent using a two-stage MAV (DA-2S), and Mars orbit rendezvous using a two-stage MAV (MOR-2S).

4.3.1 Overview of Architectures

Four architectures were developed using the above components and maneuvers to assess how the overall required system mass is affected by such trades as staging, return strategies, variations in orbit altitude, and engine parameters including I_{sp} and payload

masses. Because each architecture has a distinct combination of orbital maneuvers, it requires its own set of spacecraft components. Each of these components has very specific functions as a result of the chosen mission scenario. Table 4.1 presents the required outbound and return maneuvers and their respective components for each of the four architectures. Note that for the DA-2S and MOR-2S architectures, the MAV consists of two stages, each of which is a separate component.

Table 4.1: Maneuvers and components for MSR mission scenario.

Strategy	Maneuver	DA-SS	MOR-SS	DA-2S	MOR-2S
Outbound	TMI	Ares V	Ares V	Ares V	Ares V
	MOI	Orbiter	Orbiter	Orbiter	Orbiter
	Descent	Lander	Lander	Lander	Lander
Return	Ascent	MAV	MAV	MAV	MAV
	TEI		ERV		ERV

4.3.2 Outbound Strategy

All four architectures use the same outbound strategy, i.e. TMI from a low Earth orbit of 185 km via EDS or Centaur V2 [39]; followed by a Mars orbit insertion into the desired LMO altitude; and finally, descent to Mars' surface via propulsive braking and parachutes. Once the orbiter has achieved the desired Mars orbit, the lander system separates and begins its descent to the Mars surface. For direct ascent, the orbiter is no longer carrying any critical payload and remains in orbit only for the purposes of communications during descent, surface operations, and ascent. For Mars orbit rendezvous, an ERV remains attached to the orbiter during descent, surface operations, and ascent. The lander carries the science payload (including the rover and MAV), as well as the necessary equipment required for surface operations for 500 to 700 days [40],

to the surface using both propulsive means (i.e. rocket engines) and parachutes to slow the system to acceptable landing loads.

4.3.3 Surface Operations

Upon touchdown, the lander deploys the rover to begin collecting surface samples. Meanwhile, the lander may perform sample collection in the form of drilling or some other stationary means. Upon completion of sample collection, the rover returns the surface samples to the sample canister (onboard the lander), and the lander places the canister inside the MAV (also onboard the lander) [7].

The rover is intended to be a mobile vehicle which collects surface samples from a 2.5 km range on the Martian surface [7]. There is no requirement for further technology development in the aspect of surface range mobility, as the Mars Exploration Rovers (MERs), Spirit and Opportunity, have each driven more than 6 km under various geological and weather conditions [61].

4.3.4 Return Strategies

Once loaded with surface samples, the MAV launches off the surface to return them to Earth. Each architecture demonstrates a unique strategy for Earth return. For the direct ascent architectures, the MAV launches from Mars' surface directly onto a hyperbolic escape trajectory. For the Mars orbit rendezvous architectures, the MAV launches into Mars orbit to rendezvous and dock with the orbiter. The sample canister is transferred into the EEC onboard the ERV. The ERV then separates from the orbiter and departs on a hyperbolic return trajectory.

4.3.5 Reentry

In all four architectures, the returning vehicle will deploy the EEC into Earth's atmosphere while diverting away from the Earth via a non-return trajectory. The EEC

(similar to the ones used in the Stardust and Genesis missions), containing the SC, reenters Earth's atmosphere and impacts the surface in an uninhabited location. Reentry and surface landing are performed without mixing, contaminating, or altering the Martian surface samples in any way [7].

4.4 Development of Architectures

This section describes each architecture, including the orbital maneuvers required and the corresponding components employed for these maneuvers. The process for calculating the overall system mass and mass margin for each architecture is defined. Additionally, an individual flow diagram is presented for each architecture to illustrate the process for calculating system mass and mass margin.

4.4.1 Overview

Four architectures were modeled to determine, based on a given set of engine parameters (discussed in Chapter 5), whether a Mars sample return mission is feasible on a single Ares V launch, and the effect that each parameter has on system mass. In the direct ascent architectures, the MAV acts as both an ascent vehicle and a return vehicle. For Mars orbit rendezvous, the MAV and the ERV are two separate vehicles with distinct functions. For the two major Mars sample return strategies in this study, the feasibility of mission and the sensitivities of overall system mass are observed over two MAV configurations: single-stage and two-stage.

Each architecture compares the predicted system mass to the payload mass allowance of Ares V, and the difference between the two is expressed as percent mass margin (MM). In addition, a sensitivity analysis was performed using ModelCenter® to determine the parameters which have the greatest influence on system mass.

4.4.2 Assumptions

The single-stage MAV architectures assume a chemical propulsion system for the ascent vehicle. The two-stage MAV models assume a solid first stage motor and a chemical bipropellant system for the upper stage. All other components were assigned a chemical bipropellant system. Given the data presented in Table 2.1, the mass of the sample canister is assumed to be ten times the mass of the surface sample. All components in each architecture are assumed to have complete burnout of propellant. Additionally, this study assumes zero boil-off (ZBO) of all cryogenic bipropellant systems, and the additional mass for storage of cryogenic propellants is not considered. The nomenclature used in the process for calculating the predicted system mass ($m_{o,pre}$) and mass margin for each architecture is shown in Table 4.2.

Table 4.2: Nomenclature for mass estimation.

m_{dry}	dry, or structural mass; does not include propellant or payload
m_f	final mass of component, after propellant burnout; includes structure and payload
m_{pay}	payload, or inert, mass
m_{prop}	propellant mass
m_o	gross mass, or mass at launch; includes structure, propellant, and payload
m_{wet}	wet mass; includes the mass of the entire component without payload
$m_{o,given}$	the payload mass that Ares V is capable of carrying to LEO; given by Sumrall's Ares V performance plot for two Ares V upper stage configurations [39]
$m_{o,pre}$	predicted system mass; the mass that Ares V must carry to LEO; calculated in architectures
m_{EEC}	mass of Earth entry capsule before being loaded with SC
m_{ERV}	mass of Earth return vehicle; does not include payload
m_{Land}	mass of lander component; does not include payload
m_{MAV}	mass of Mars ascent vehicle component; does not include payload
m_{Orb}	mass of orbiter component; does not include payload
m_{Rover}	mass of rover
m_{Sample}	mass of surface sample
m_{SC}	mass of sample canister
MM	mass margin; percent difference between Ares V capability and predicted system mass (Section 4.4.8)

4.4.3 ΔV for Mars Orbit Insertion

The ΔV required for Mars orbit insertion must be calculated based on the orbital mechanics relationships defined in Brown [31]. Table 4.3 defines the orbital mechanics terms used in this section.

Table 4.3: Orbital mechanics terms.

Term	Units	Description
a_x	km	Semi-major axis of an orbit (Figure 4.2)
C_3	km^2/s^2	Energy required for a launch vehicle to escape a planet's orbit
h_a	km	Apoapsis altitude (Figure 4.2)
h_p	km	Periapsis altitude (Figure 4.2)
r_a	km	Radius of apoapsis (Figure 4.2)
r_p	km	Radius of periapsis (Figure 4.2)
R_o	km	Planetary central body radius (Figure 4.2)
V_{HE}	km/s	Hyperbolic excess velocity; velocity required for a spacecraft to escape a planet's orbit
V_p	km/s	Velocity at periapsis of an orbit
ΔV	km/s	Velocity change required for a spacecraft to perform a given orbital maneuver
μ	km^3/s^2	Planetary gravity constant

The calculation begins with designating the Earth launch opportunity. Hyperbolic excess velocity (V_{HE}) is defined as the velocity required for a spacecraft to escape a planet's orbit. There is a distinct V_{HE} associated with any given launch date. For that launch date, there is a corresponding V_{HE} associated with Mars arrival. These velocities for departure and arrival shall be known as $(V_{HE})_{dep}$ and $(V_{HE})_{arv}$, respectively.

The energy associated with hyperbolic excess velocity is defined as C_3 [31], or the square of the corresponding V_{HE}. This is expressed as

$$C_3 = (V_{HE})^2, \tag{0.1}$$

where the units of C_3 and V_{HE} are km^2/s^2 and km/s, respectively.

Certain planetary constants, namely the gravitational parameter (μ) and equatorial radius (R_o), are given in Brown [31] as 42,828.3 km^3/s^2 and 3,397 km, respectively for Mars.

The desired LMO altitude will determine the energy required for braking into Mars orbit. The periapsis can be defined as the point of a spacecraft's orbit closest to a planet's central radius. The periapsis altitude (h_p) is expressed in units of km. Similarly, the apoapsis can be defined as the point of a spacecraft's orbit furthest from a planet's central radius. The apoapsis altitude (h_a) is expressed in units of km. The radius of periapsis (r_p) is defined as the sum of the periapsis altitude and the planet's central body radius. Similarly, the radius of apoapsis (r_a) is defined as the sum of the apoapsis altitude and the planet's central body radius. The apoapsis and periapsis radii are expressed in km as

$$r_a = h_a + R_o \tag{0.2}$$

and

$$r_p = h_p + R_o . \tag{0.3}$$

An orbit's semi-major axis (a_x) can be defined as one half the linear distance from the center of the orbit to the orbit's outermost point. Quantitatively, this is expressed as

$$a_x = \frac{r_a + r_p}{2} . \tag{0.4}$$

Figure 4.2 illustrates the relationships between the periapsis, apoapsis, and semi-major axis of a planet's orbit.

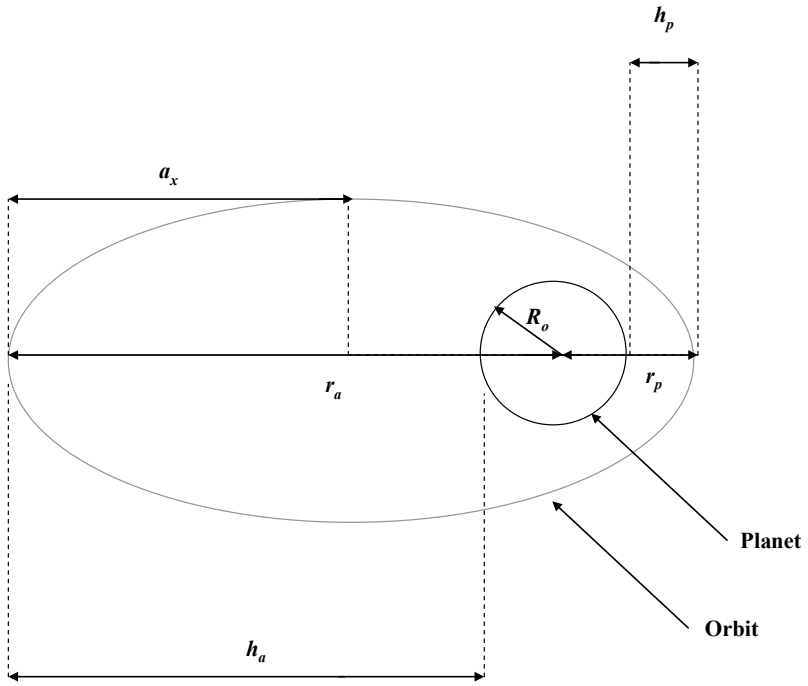

Figure 4.2: Orbital relationships.

To find the velocity change required to achieve a Mars orbit from a TMI approachhyperbola, it is necessary to find the periapsis velocities of both the approach hyperbola and the desired orbit. The velocity at periapsis of the approach hyperbola (V_p) is expressed in km/s as

$$V_p = \sqrt{\left(V_{HE}\right)_{arv}^2 + \frac{2\mu}{r_p}}, \qquad 0.5$$

and the periapsis velocity on the desired Mars orbit ($V_p^{'}$) is

$$V_p^{'} = \sqrt{\frac{2\mu}{r_p} - \frac{\mu}{a_x}}, \qquad 0.6$$

also having units of km/s.

The ΔV for Mars orbit insertion is the positive difference between the two periapsis velocities, expressed as

$$\Delta V = \left| V_p - V_p^{'} \right|. \qquad 0.7$$

This ΔV associated with Mars arrival is a required input for sizing the orbiter in each architecture.

4.4.4 Direct Ascent Using a Single-Stage MAV

This section defines the necessary procedure for determining the predicted system mass ($m_{o,pre}$) and mass margin (MM) associated with direct ascent using a single-stage MAV. Figure 4.3 illustrates the procedure for calculating $m_{o,pre}$ and MM.

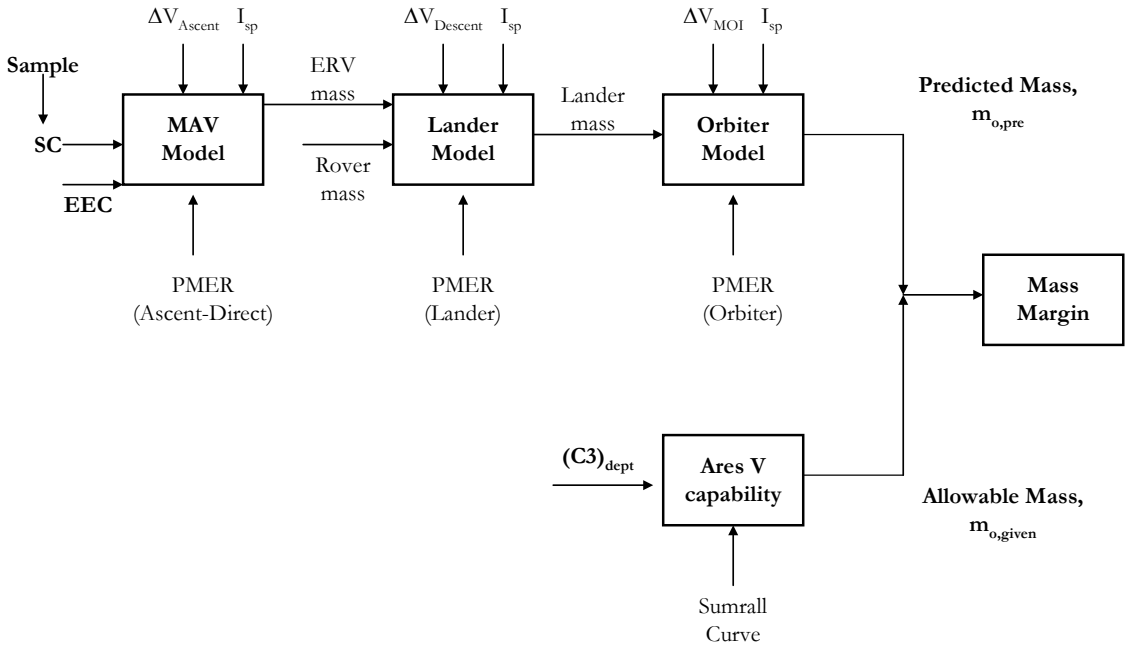

Figure 4.3: Model flow diagram, DA-SS.

4.4.4.1 MAV

The MAV model requires the input of certain system parameters. The (I_{sp}) of the MAV's propulsion system, the mass growth allowance (MGA), the payload, and the ΔV required for direct ascent must all be designated. The reader may refer to Figure 4.3 for an illustrative concept of the procedure for calculating the MAV gross mass.

The payload mass of the MAV, m_{pay}, consists of the surface sample, the SC, and the EEC masses, or m_{Sample}, m_{SC}, and m_{EEC}, respectively. All of these masses are expressed in units of kg. The payload mass of the MAV for direct ascent is

$$m_{pay} = m_{Sample} + m_{SC} + m_{EEC}\,. \tag{0.8}$$

The user inputs an arbitrary value for m_{prop}. This value will later be iterated until it converges to its actual value. Once m_{prop} is guessed, the model calculates the propellant mass fraction (PMF) using Thomas's [62] Preliminary Mass Estimating Relationship (PMER) and applying the coefficients a, b, and c corresponding to direct ascent [62]. Note that these coefficients were obtained by applying curve fits to various mass relationships. This gives an equation for PMF of the MAV, expressed as

$$PMF = \frac{a}{1 + \frac{b}{\left(m_{prop}\right)^{c}}}\,. \tag{0.9}$$

When PMF is known, the dry mass (m_{dry}) can be calculated knowing the relationships

$$m_{wet} = m_{dry} + m_{prop} \tag{0.10}$$

and

$$PMF = \frac{m_{prop}}{m_{wet}}\,. \tag{0.11}$$

Note that the wet mass (m_{wet}) does not include payload. Rearranging the two equations,

$$m_{dry} = m_{wet} - m_{prop} \tag{0.12}$$

and

$$m_{wet} = \frac{m_{prop}}{PMF}\,. \tag{0.13}$$

The two equations can be solved simultaneously to obtain the dry and wet masses. Substituting 4.13 into 4.12, the dry mass is derived as

$$m_{dry} = m_{prop}\left(\frac{1}{PMF} - 1\right), \tag{0.14}$$

and wet mass is obtained using Equation 4.10.

The final mass, m_f, consists of the entire component, including payload, after propellant burnout. Note that a mass growth allowance (MGA) must be applied to account for increases in structural mass. Final mass is thus

$$m_f = (MGA)\, m_{dry} + m_{pay}. \tag{0.15}$$

The actual propellant mass can be calculated from Tsiolkowski's equation. Note that g_o is the acceleration due to gravity on Earth (g_o = 9.81 m/s^2). Specific impulse (I_{sp}) is a performance parameter which can be thought of as the fuel efficiency of a propulsion system [54]. Propellant mass is calculated in the form

$$m_{prop} = m_f\left[\exp\left(\frac{\Delta V}{g_o I_{sp}}\right) - 1\right]. \tag{0.16}$$

A circular reference is created when calculating m_{prop}; therefore the model iterates until m_{prop} and m_f converge to their actual values.

Finally, the gross mass, m_o, is simply the sum of the propellant and final masses, and is given as

$$m_o = m_f + m_{prop}. \tag{0.17}$$

It is essential to obtain the MAV's gross mass, $(m_o)_{MAV}$, because the MAV is one of the lander's payloads. To find the mass of the MAV component, the payload is subtracted from the gross mass and is expressed as

$$m_{MAV} = (m_o)_{MAV} - (m_{pay})_{MAV}. \quad 0.18$$

4.4.4.2 Lander

The lander model requires the input of certain system parameters. The I_{sp} of the lander's propulsion system, the mass growth allowance, the payload, and the ΔV required for descent must all be designated. The reader may refer to the flow diagram in Figure 4.3 for an illustrative concept of the procedure for calculating the gross mass of the lander.

The payload of the lander, m_{pay}, consists of the MAV's mass (before sample collection) and the rover's mass (m_{Rover}). The payload mass, in kg, is simply

$$m_{pay} = (m_o)_{MAV} + m_{Rover} - m_{Sample}. \quad 0.19$$

Note that the sample mass is included in $(m_o)_{MAV}$ and must therefore be subtracted, as the lander does not carry the surface samples as part of its payload.

As with the MAV, the lander's propellant mass must be given an initial guess. The PMER, Equation 4.9, is then used to calculate PMF, using the coefficients a, b, and c corresponding to a lander. Equations 4.14 and 4.10 are then applied to obtain m_{dry} and m_{wet}, respectively. Equation 4.15 is applied to obtain m_f, and the actual propellant mass is calculated by applying Equation 4.16. Gross mass of the lander is obtained from Equation 4.17. It is essential to obtain the lander's gross mass, $(m_o)_{Land}$, because the

lander is the orbiter's payload. To find the mass of the lander component, the payload is subtracted from the gross mass and is expressed as

$$m_{Land} = \left(m_o\right)_{Land} - \left(m_{pay}\right)_{Land}. \qquad 0.20$$

4.4.4.3 Orbiter

The orbiter model requires the input of certain system parameters. The I_{sp} of the orbiter's propulsion system, the mass growth allowance, and the payload must all be designated. ΔV_{MOI} was obtained using the procedure defined in section 4.4.3. The reader may refer to the flow diagram in Figure 4.3 for an illustrative concept of the procedure for calculating the gross mass of the orbiter.

The payload of the orbiter consists of only the lander. The payload mass, in kg, is simply

$$\left(m_{pay}\right)_{Orb} = \left(m_o\right)_{Land}. \qquad 0.21$$

As with the lander, the orbiter's propellant mass must be given an initial guess. The PMER, Equation 4.9 is then used to calculate PMF, using the coefficients a, b, and c corresponding to an orbiter. Equations 4.14 and 4.10 are then applied to obtain m_{dry} and m_{wet}, respectively. Equation 4.15 is applied to obtain m_f, and the actual propellant mass is calculated by applying Equation 4.16. Gross mass of the orbiter is obtained from Equation 4.17. The orbiter's gross mass, in kg, is the overall predicted system mass and is referred to as $m_{o,pre}$ in mT. This is the payload mass required for direct ascent using a single-stage MAV (DA-SS). Ares V must have an equal or greater payload capability to power this particular mission. To find the mass of the orbiter component, the payload is subtracted from the gross mass and is expressed as

$$m_{Orb} = \left(m_o\right)_{Orb} - \left(m_{pay}\right)_{Orb} \quad 0.22$$

4.4.5 Mars Orbit Rendezvous Using a Single-Stage MAV

This section defines the necessary procedure for determining the predicted system mass and mass margin associated with Mars orbit rendezvous using a single-stage MAV. Figure 4.4 below illustrates the procedure for calculating $m_{o,pre}$ and MM. Note that for MOR, there is a separate vehicle (ERV) required for the TEI maneuver. Because MOR requires that the ascent and TEI maneuvers be performed by two separate vehicles, the procedure for calculating $m_{o,pre}$ and MM is slightly different from that of the DA-SS architecture.

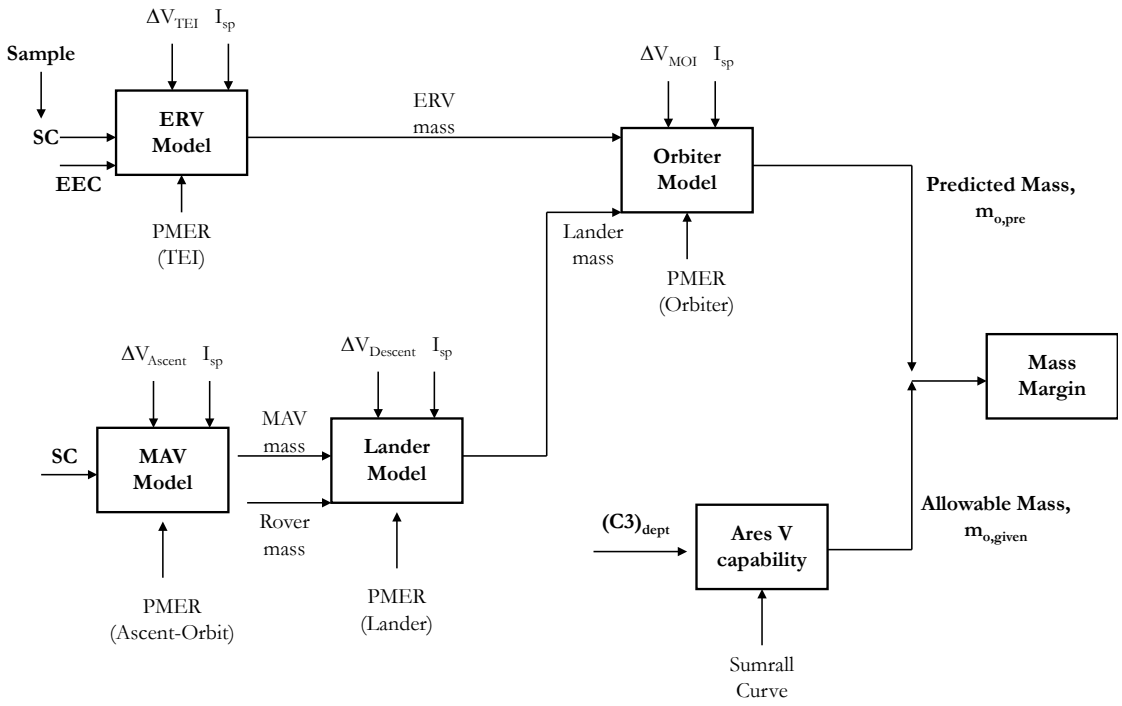

Figure 4.4: Model flow diagram, MOR-SS.

For MOR-SS, the payload of the MAV consists of only the surface sample and the SC. The EEC is not carried on the MAV, as Earth return is performed by another vehicle. The payload of the MAV is therefore

$$m_{pay} = m_{Sample} + m_{SC} . \tag{0.23}$$

Additionally, the orbiter carries a second payload, the ERV, which remains attached to the orbiter until completion of sample transfer from the MAV. The ERV carries the EEC (containing the SC filled with surface samples) back to Earth via TEI. The payload of the ERV is therefore

$$m_{pay} = m_{Sample} + m_{SC} + m_{EEC} . \tag{0.24}$$

The orbiter's payload mass must be adjusted such that it includes the mass of the ERV. This is expressed as

$$m_{pay} = m_{Land} + m_{ERV} . \tag{0.25}$$

4.4.6 Direct Ascent Using a Two-Stage MAV

This section defines the necessary procedure for determining the predicted system mass and mass margin associated with direct ascent using a two-stage MAV. Figure 4.5 illustrates the procedure for calculating $m_{o,pre}$ and MM. Note that for DA-2S, the MAV component is staged, and must therefore be treated as two separate components.

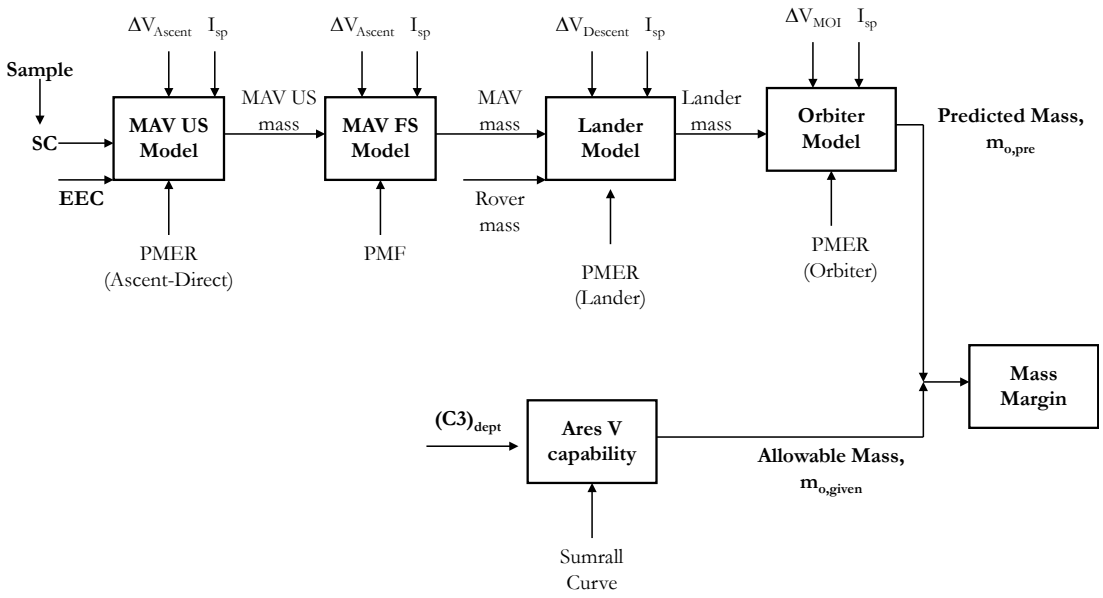

Figure 4.5: Model flow diagram, DA-2S.

For DA-2S, the same procedure defined in Section 4.4.3 is applied, but the MAV now consists of two stages. The payload for the upper stage component consists of the surface sample, SC, and EEC (see Equation 4.8). The only payload of the first stage component is the upper stage component. Quantitatively, this is expressed as

$$\left(m_{pay}\right)_{MAV,FS} = \left(m_o\right)_{MAV,US}. \qquad 0.26$$

The reader will also note that in the case of a staged MAV, the first stage component is assumed to be a solid rocket motor, and is assigned a PMF, rather than applying the PMER.

4.4.7 Mars Orbit Rendezvous Using a Two-Stage MAV

This section defines the necessary procedure for determining the predicted system mass and mass margin associated with Mars orbit rendezvous using a two-stage MAV. Figure 4.6 illustrates the procedure for calculating $m_{o,pre}$ and MM. Note that for MOR, an ERV is required for the TEI maneuver. Additionally, the MAV is staged and must therefore be treated as two separate components.

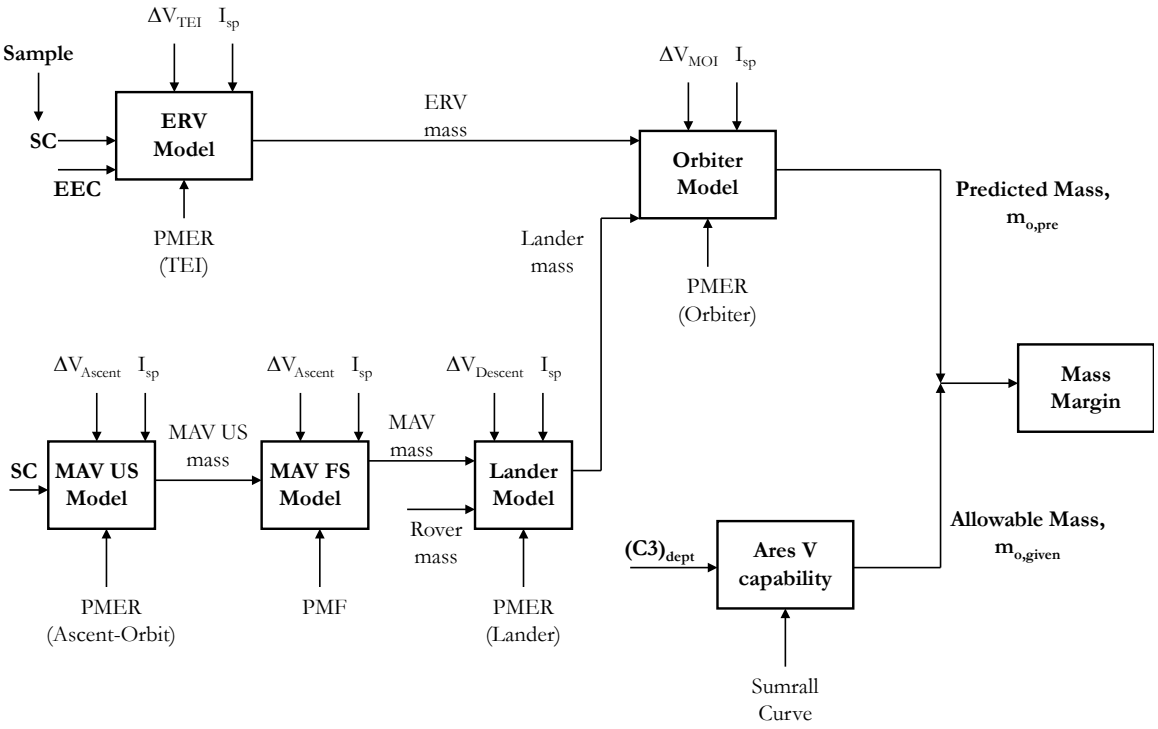

Figure 4.6: Model flow diagram, MOR-2S.

For MOR-2S, the payload of the MAV consists of only the surface sample and the SC (Equation 4.23). The EEC is not carried on the MAV, as Earth return is performed by

another vehicle. As in the DA-2S architecture, the MAV is staged and must therefore be treated as two separate components. The upper stage component carries only the surface samples and SC, while the first stage component carries the entire upper stage. The payload mass for the upper stage is expressed as Equation 4.23, and the payload mass for the first stage is expressed as Equation 4.26.

The ERV carries the EEC (containing the SC filled with surface samples) back to Earth via TEI. The payload of the ERV is given by Equation 4.24. Additionally, the orbiter's payload mass must be adjusted such that it includes the mass of the ERV. This is given by Equation 4.25.

Because the MAV is staged, the first stage component is assigned a value, rather than applying the PMER.

4.4.8 Mass Margin

Mass margin (MM) is defined as the percent difference between the allowable mass (provided by Ares V) and the predicted system mass (calculated in the architectures). In order to find the mass margin, the Ares V payload capability must be determined. Section 4.4.8.1 describes the procedure used for obtaining Ares V payload capability, and Section 4.4.8.2 defines the process used to calculate mass margin.

4.4.8.1 Allowable System Mass

To find the mass that Ares V is capable of sending to Mars from low Earth orbit (185 km, per Sumrall [39]), an equation was developed from the Ares V Performance plot in Sumrall's presentation, *Ares V Overview* [39]. The plot gives Ares V payload capability as a function of C_3 energy for both the EDS and Centaur V2 upper stages. C_3 refers to the departure energy, $(C_3)_{dept}$. The plot was replicated to obtain equations for

the two curves; numerous points along each curve were recorded and tabulated in Microsoft Excel®, and a second-order polynomial was fit to each of the two curves. To increase fidelity, each of the curves was split into two separate curves, and an equation was fit to each segment. The equation obtained from Sumrall's plot for EDS was found to be

$$m_{o,given} = 0.006C_3^2 - 0.9082C_3 + 59.222, \quad 0.27$$

with an R^2 value of 0.9997. The equation obtained for the Centaur upper stage was found to be

$$m_{o,given} = 0.0041C_3^2 - 0.871C_3 + 54.872, \quad 0.28$$

with an R^2 value of 0.9999. The C_3 ranges from -1.65 to 66.08 km^2/s^2 for EDS, and from -0.90 to 31.15 km^2/s^2 for Centaur. The C_3 range of interest, for Earth departure, is from 7.74 to 13.79 km^2/s^2 per George [40]. Note that this range falls within the lower and upper bounds of the equations for both upper stage configurations. The reader will also note that the above masses have units of metric tons (mT). These masses are named $m_{o,given}$ because they are extrapolated from the Sumrall curves and represent the maximum payload that Ares V can carry to LEO for a given C_3 value. This mass must be greater than the predicted system mass calculated in the architectures in order to power a given mission.

4.4.8.2 Mass Margin Calculation

The mass margin (MM) is the percent difference between $m_{o,given}$ and $m_{o,pre}$. This is expressed as follows:

$$MM = \frac{m_{o,given} - m_{o,pre}}{m_{o,given}}. \qquad 0.29$$

Each of the four architectures computes an individual mass margin, and the results of each are documented in Chapter 5.

4.5 Sensitivity Analysis

In addition to determining what mission strategy (i.e. direct ascent, Mars orbit rendezvous, etc.) yields the best mass margin, future MSR mission planners should also consider which system parameters have the most significant effect on system mass. Identifying these parameters and their effects on system mass will enable the most cost efficient and mass efficient MSR mission conceivable. Increasing the mass margin could possibly return more scientific data about the Martian surface to scientists. If a larger rover, or multiple rovers, could be landed on the surface, then a larger sample could be gathered, and a broader range of the Martian surface could be studied.

The engine parameters of interest in this study include I_{sp}, MGA, PMF, and payloads (sample, EEC, and rover masses) associated with each component. The orbital parameters of interest in this study include $\left(V_{HE}\right)_{dept}$ and $\left(V_{HE}\right)_{arv}$ (used when varying launch opportunity), h_p, and the ΔV associated with each maneuver. Each of the four architectures is studied separately, and the outputs of each are compared at the end. Each parameter is varied over an appropriate range based on the data presented in Chapter 2. The outputs of the sensitivity study include the change in predicted system mass and mass margin. The results of the sensitivity study are presented in Chapter 5.

4.6 Summary

Four architectures were modeled to determine, based on a given set of baseline values, the predicted system mass and mass margin. Each of these architectures has a unique return strategy. The effect of the return strategy on system mass is critical to developing a mass and cost efficient Mars sample return mission. Furthermore, a sensitivity analysis was performed so that the effect of certain mission parameters could be studied. Knowing the effect of these parameters, as well as orbital maneuvers and staging trades, would allow future mission planners to build an architecture with the desired balance of cost, risk, and performance.

CHAPTER 5

RESULTS

5.1 Introduction

This section provides explanation and graphical representations of the analyses performed. For the first part of the study, a design reference mission (DRM) was developed based on commonly used values of certain engine and orbital parameters. The feasibility of this DRM on a single Ares V launch was determined for each of the four architectures. This feasibility is based on the Ares V payload capacity given in Sumrall [39], for two upper stage configurations, i.e., EDS and Centaur V2. Feasibility is expressed quantitatively as mass margin (MM). A positive mass margin implies that a given architecture is possible on a single Ares V launch. A negative mass margin implies that the predicted mass of a given architecture exceeds the launch capability of Ares V, thus precluding the feasibility of the mission on a single Ares V launch. For the second part of this study, a sensitivity analysis was performed to determine the effect of each parameter on system mass. These parameters were all assigned appropriate ranges of variation, based on the information presented in the literature review, and were varied individually to study the effects on overall system mass. Key to developing a mass and cost efficient Mars sample return mission is for mission planners to be able to determine

the magnitude of effect that each variable has on system mass. Section 5.2 describes the baseline values and parameter variations used in this study, and Section 5.3 provides the results given by the architectures modeled in Microsoft Excel® and Phoenix Integration Model Center®.

5.2 Baseline Values and Variations

The baseline values were chosen based on the information presented in the literature review. The parameters of interest were given appropriate ranges of variation, also based on the information in the literature review, and the effects of each variation on overall system mass and mass margin are presented in Section 5.3. Table 5.1 gives the baseline parameter values used in the feasibility study, with their respective units, for each of the four architectures. Tables 5.2, 5.3, 5.4, and 5.5 give the parameter baseline values, ranges of variation, and units for the DA-SS, MOR-SS, DA-2S, and MOR-2S architectures, respectively.

Table 5.1: Baseline parameter values.

	DA-SS		MOR-SS		DA-2S		MOR-2S	
$(V_{HE})_{arv}$	4.418	km/s	4.418	km/s	4.418	km/s	4.418	km/s
h_p	500	km	500	km	500	km	500	km
ΔV								
Descent	0.35	km/s	0.35	km/s	0.35	km/s	0.35	km/s
Ascent, FS	-----	km/s	-----	km/s	3.25	km/s	2.5	km/s
Ascent, US	6.5	km/s	5.0	km/s	3.25	km/s	2.5	km/s
TEI	-----	km/s	1.5	km/s	-----	km/s	1.5	km/s
I_{sp}								
ERV	-----		320.1	sec	-----		320.1	sec
MAV US	320.1	sec	320.1	sec	320.1	sec	320.1	sec
MAV FS	-----		-----		285	sec	285	sec
Lander	320.1	sec	320.1	sec	320.1	sec	320.1	sec
Orbiter	320.1	sec	320.1	sec	320.1	sec	320.1	sec
MGA	1.3		1.3		1.3		1.3	
PMF								
MAV FS	-----		-----		0.9		0.9	
Payloads								
m_{Sample}	0.5	kg	0.5	kg	0.5	kg	0.5	kg
m_{Rover}	900	kg	900	kg	900	kg	900	kg
m_{EEC}	40	kg	40	kg	40	kg	40	kg

Table 5.2: Parameter variations for DA-SS.

Parameter	Baseline		Lower Bound		Upper Bound		Increment Size	
$(V_{HE})_{arv}$	4.418	km/s	2.4	km/s	5.5	km/s	varies by launch date	
h_p	500	km	250	km	600	km	50	km
ΔV								
Descent	0.35	km/s	0.25	km/s	0.50	km/s	0.01	km/s
Ascent	6.5	km/s	6.0	km/s	6.5	km/s	0.1	km/s
I_{sp}								
MAV	320.1	s	313.6	s	446.3	s	varies by propellant	
Lander	320.1	s	313.6	s	446.3	s	varies by propellant	
Orbiter	320.1	s	313.6	s	446.3	s	varies by propellant	
MGA	1.3		1.15		1.3		0.01	
Payloads								
m_{Sample}	0.5	kg	0.5	kg	3.0	kg	0.1	kg
m_{EEC}	40	kg	20	kg	150	kg	10	kg
m_{Rover}	900	kg	500	kg	2,000	kg	100	kg

Table 5.3: Parameter variations for MOR-SS.

Parameter	Baseline		Lower Bound		Upper Bound		Increment Size	
$(V_{HE})_{arv}$	4.418	km/s	2.4	km/s	5.5	km/s	varies by launch date	
h_p	500	km	250	km	600	km	50	km
ΔV								
Descent	0.35	km/s	0.25	km/s	0.50	km/s	0.01	km/s
Ascent	6.5	km/s	6.0	km/s	6.5	km/s	0.1	km/s
TEI	1.5	km/s	1	km/s	2	km/s	0.1	km/s
I_{sp}								
ERV	320.1	s	313.6	s	446.3	s	varies by propellant	
MAV	320.1	s	313.6	s	446.3	s	varies by propellant	
Lander	320.1	s	313.6	s	446.3	s	varies by propellant	
Orbiter	320.1	s	313.6	s	446.3	s	varies by propellant	
MGA	1.3		1.15		1.3		0.01	
Payloads								
m_{Sample}	0.5	kg	0.5	kg	3.0	kg	0.1	kg
m_{EEC}	40	kg	20	kg	150	kg	10	kg
m_{Rover}	900	kg	500	kg	2,000	kg	100	kg

Table 5.4: Parameter variations for DA-2S.

Parameter	Baseline		Lower Bound		Upper Bound		Increment Size	
$(V_{HE})_{arv}$	4.418	km/s	2.4	km/s	5.5	km/s	varies by launch date	
h_p	500	km	250	km	600	km	50	km
ΔV								
Descent	0.35	km/s	0.25	km/s	0.50	km/s	0.01	km/s
Ascent, FS	3.25	km/s	3.0	km/s	3.25	km/s	0.05	km/s
Ascent, US	3.25	km/s	3.0	km/s	3.25	km/s	0.05	km/s
I_{sp}								
MAV US	320.1	s	313.6	s	446.3	s	varies by propellant	
MAV FS	285	s	260	s	300	s	5	s
Lander	320.1	s	313.6	s	446.3	s	varies by propellant	
Orbiter	320.1	s	313.6	s	446.3	s	varies by propellant	
MGA	1.3		1.15		1.3		0.01	
PMF								
MAV FS	0.9		0.8		0.95		0.01	
Payloads								
m_{Sample}	0.5	kg	0.5	kg	3.0	kg	0.1	kg
m_{EEC}	40	kg	20	kg	150	kg	10	kg
m_{Rover}	900	kg	500	kg	2,000	kg	100	kg

Table 5.5: Parameter variations for MOR-2S.

Parameter	Baseline		Lower Bound		Upper Bound		Increment Size	
$(V_{HE})_{arv}$	4.418	km/s	2.4	km/s	5.5	km/s	varies by launch date	
h_p	500	km	250	km	600	km	50	km
ΔV								
Descent	0.35	km/s	0.25	km/s	0.50	km/s	0.01	km/s
Ascent, FS	3.25	km/s	3.0	km/s	3.25	km/s	0.05	km/s
Ascent, US	3.25	km/s	3.0	km/s	3.25	km/s	0.05	km/s
TEI	1.5	km/s	1	km/s	2	km/s	0.1	km/s
I_{sp}								
ERV	320.1	s	313.6	s	446.3	s	varies by propellant	
MAV US	320.1	s	313.6	s	446.3	s	varies by propellant	
MAV FS	285	s	260	s	300	s	5	s
Lander	320.1	s	313.6	s	446.3	s	varies by propellant	
Orbiter	320.1	s	313.6	s	446.3	s	varies by propellant	
MGA	1.3		1.15		1.3		0.01	
PMF								
MAV FS	0.9		0.8		0.95		0.01	
Payloads								
m_{Sample}	0.5	kg	0.5	kg	3.0	kg	0.1	kg
m_{EEC}	40	kg	20	kg	150	kg	10	kg
m_{Rover}	900	kg	500	kg	2,000	kg	100	kg

5.2.1 Launch Opportunity

V_{HE} is defined as the hyperbolic excess velocity required for a spacecraft to escape a planet's orbit. V_{HE} is a function of launch opportunity, and there is a distinct V_{HE} for Earth departure as well as for Mars arrival. Tables 9 through 16 in George [40] list the V_{HE} values associated with Earth departure and Mars arrival for the various launch opportunities from 2009 to 2024. These values are summarized in Table 5.6.

Table 5.6: Earth-Mars and Earth Return Opportunity Data.

Mission Year	TMI Date	ΔV_{TMI} (km/s)	Outbound TOF (days)	Earth Dept. V_{HE} (km/s)	Earth Dept. C_3 (km^2/s^2)	Mars Arrival V_{HE} (km/s)	Mars Arrival C_3 (km^2/s^2)
2009	10/14/2009	3.737	327	3.2048	10.27	2.470	6.10
2011	11/8/2011	3.673	297	2.9911	8.95	2.751	7.57
2014	**12/31/2013**	**6.665**	**328**	**2.9630**	**8.78**	**4.418**	**19.52**
2016	3/21/2016	3.627	305	2.8270	7.99	5.368	28.82
2018	5/17/2018	3.615	236	2.7820	7.74	3.263	10.65
2020	7/18/2020	3.877	193	3.6300	13.18	2.857	8.16
2022	9/14/2022	3.906	383	3.7137	13.79	3.074	9.45
2024	10/5/2024	3.782	345	3.3452	11.19	2.541	6.46

$(V_{HE})_{arv}$, the V_{HE} required for Mars arrival, is used to find ΔV_{MOI}, the ΔV required for the orbiter to insert into Mars orbit from the TMI approach hyperbola. The baseline mission opportunity used in this study was the 2014 opportunity (TMI year 2014); this was based on several of the studies reviewed [21-23] which used the 2013 Earth launch opportunity. The corresponding $(V_{HE})_{arv}$ is 4.418 km/s. Note that the values in Table 5.6 vary by launch opportunity from 2.470 to 5.368 km/s. The upper and lower bounds used in the sensitivity study were 2.4 and 5.5 km/s; note that this range of variation was not divided into even increments, as this varies by launch date.

5.2.2 Periapsis

The periapsis altitude (h_p) is a required input for calculating ΔV_{MOI}, using the process defined in Section 4.4.3. Because the periapsis of an orbit, by definition, can never be greater than the apoapsis (h_a), h_a was not varied in this study. The apoapsis was instead assumed to be equal to the periapsis to eliminate formula errors in the ΔV_{MOI} calculation defined in Section 4.4.3. Because V_p and $V_p^{'}$ are based on h_p, errors would arise in the formulas if the lower bound for the apoapsis were less than the periapsis. The

baseline value used in the feasibility study for h_p was 500 km. The upper and lower bounds used in the sensitivity study were 250 and 600 km, based on the information presented in Section 2.2.3.4. The periapsis was varied in increments of 50 km.

5.2.3 Payloads

This section describes the ranges of variation for the payload masses in this study. The payloads which were varied included surface sample, Earth entry capsule, and rover. Note that, although the sample canister was considered an inert payload, it was not varied. The SC mass was instead treated as a function of sample mass, as described in Section 4.4.2.

5.2.3.1 Surface Sample

For each of the four architectures, the baseline value used in the feasibility study for the mass of the surface sample was 0.5 kg. For the sensitivity study, the sample mass was varied over a range from 0.5 kg to 3.0 kg in increments of 0.1 kg.

5.2.3.2 Earth Entry Capsule

The baseline value used in the feasibility study for the mass of the Earth entry capsule was 40 kg. For the sensitivity study, the EEC mass was varied over a range from 20 kg to 150 kg in increments of 10 kg.

5.2.3.3 Rover

The baseline value used in the feasibility study for the mass of the rover was 900 kg, the predicted mass of Mars Science Laboratory [50]. For the sensitivity study, the rover mass was varied over a range from 500 kg to 2,000 kg in increments of 100 kg. Note that the intent for this variation is that the rover mass not be compiled into one rover, but rather divided over multiple rovers. Utilizing more than one rover to collect surface samples would allow for observation of more of the planet's area.

5.2.4 Propellant Mass Fraction of MAV First Stage

For all chemical bipropellant systems, the PMF was determined using the PMER [62]. This value was thus an output for all chemical propulsion systems. In the architectures which implemented a two-stage MAV, however, the first stage was assumed to be a solid rocket motor. The PMF values were obtained from ATK [63], which lists the STAR designation and PMF for numerous SRMs. The mean value, lower bound, and upper bound were determined based on the data tabulated, and were found to be 0.907, 0.78, and 0.95, respectively. The baseline value for PMF used in the feasibility study was 0.9. For the sensitivity study, the PMF of the MAV first stage was varied over a range from 0.8 to 0.95 in increments of 0.01.

5.2.5 ΔV

This section describes the ranges of variation for the ΔV assigned to the major maneuvers utilized in this study. The maneuvers of interest include Mars orbit insertion, Mars descent, Mars ascent, and trans-Earth injection. Note that some of these maneuvers are split or combined, as described in the following sections.

5.2.5.1 Mars Orbit Insertion

The ΔV required for Mars orbit insertion was calculated based on previously defined variables (C_3 and h_p) and was thus an output of the models rather than an input. Using the Mars planetary constants (R_o and μ) and orbital parameters (C_3 and h_p) in the process defined in Section 4.4.3, ΔV_{MOI} was calculated as 3.127 km/s. Because the outbound strategy is the same in all four architectures, ΔV_{MOI} will be the same throughout.

5.2.5.2 Descent

The ΔV required for Mars descent was taken to be 350 m/s, per Zubrin [18]. This assumes propulsive descent from a Mars orbit of 500 km, as well as the use of parachutes as a non-propulsive means of braking. The baseline value for $\Delta V_{Descent}$ used in the feasibility study was 0.35 km/s. For the sensitivity study, $\Delta V_{Descent}$ was varied over a range from 0.25 to 0.5 km/s in increments of 0.01 km/s. Because the outbound strategy is the same in all four architectures, $\Delta V_{Descent}$ will be the same throughout.

5.2.5.3 Ascent—Direct

The ΔV required for the combined ascent-to-TEI maneuver was taken to be 6.5 km/s, per Donahue [28] and Whitehead [30]. This value assumes the equivalent of ascent to a 400 km orbit, which accounts for 5 km/s of ΔV; and trans-Earth injection, which accounts for 1.5 km/s of ΔV. For the single-stage MAV architectures, the baseline value used in the feasibility study for ΔV_{Ascent} was 6.5 km/s. For the sensitivity study, ΔV_{Ascent} was varied over a range from 6.0 to 6.5 km/s in increments of 0.1 km/s. For the two-stage MAV architectures, ΔV_{Ascent} was assumed to be split equally between the two stages, per Whitehead [30]. The baseline value used in the feasibility study for ΔV_{Ascent} was thus 3.25 km/s for each stage. For the sensitivity study, ΔV_{Ascent} was varied over a range from 3.0 to 3.25 km/s, in increments of 0.01 km/s, for each stage. Note that for direct ascent, no additional ΔV is required to account for trans-Earth injection.

5.2.5.4 Ascent to Orbit

The ΔV required for Mars ascent to orbit was taken to be 5 km/s, per Donahue [28]. This value assumes ascent to a Mars orbit of 400 km. Although rendezvous and docking would occur at 500 km rather than at 400 km, the difference in required ΔV is

neglected. For the single-stage architectures, the baseline value used in the feasibility study for ΔV_{Ascent} was 5.0 km/s. For the sensitivity study, ΔV_{Ascent} was varied over a range from 4.5 to 5.5 km/s in increments of 0.1 km/s. For the two-stage architectures, ΔV_{Ascent} was assumed to be split equally between the two stages, per Whitehead [30]. The baseline value used in the feasibility study for ΔV_{Ascent} was thus 2.5 km/s for each stage. For the sensitivity study, ΔV_{Ascent} was varied over a range from 2.25 to 2.75 km/s, in increments of 0.01 km/s, for each stage. Note that for Mars orbit rendezvous, ΔV_{Ascent} accounts only for ascent to orbit. Additional ΔV for trans-Earth injection is allotted to the ERV for Earth return.

5.2.5.5 Trans-Earth Injection

For the Mars orbit rendezvous architectures, the ΔV required for trans-Earth injection was taken to be 1.5 km/s, per Donahue [28] and George [40]. The baseline value used in the feasibility study for ΔV_{TEI} was 1.5 km/s. For the sensitivity study, ΔV_{TEI} was varied over a range from 1.0 to 2.0 km/s in increments of 0.1 km/s.

5.2.6 Mass Growth Allowance

The baseline value for mass growth allowance (MGA) used in the feasibility study was 1.3 for all components in each of the architectures. For the sensitivity study, the MGA was varied over a range from 1.15 to 1.3 in increments of 0.01.

5.2.7 Specific Impulse

Table 1-4 in Huzel [64] lists the theoretical specific impulse for numerous chemical bipropellant combinations. To obtain a more realistic value for I_{sp}, the theoretical values listed in Huzel were multiplied by a nozzle efficiency factor (η_{noz}) of

0.97 and a combustion efficiency factor (η_{c^*}) of 0.96. The resulting values were taken to be the derived I_{sp} values for the propellant combinations. For all chemical bipropellant systems, the baseline value used in the feasibility study for I_{sp} was 320.1 sec, corresponding to nitrogen tetroxide and hydrazine (NTO/N_2H_4). The lower bound used in the sensitivity study was 313.6 sec, corresponding to hydrogen peroxide and monomethyl hydrazine (H_2O_2/MMH). The upper bound used in the sensitivity study was 446.3 sec, corresponding to fluorine and hydrogen (F_2/H_2). Note that the I_{sp} was not modeled for each individual propellant combination; because Model Center ® does not model discrete data points, the values were simply swept from the lowest to the highest value as presented in Table 5.7.

Table 5.7: Specific impulse of various liquid bipropellant systems.

	Oxidizer	Fuel	$I_{sp,theory}$	I_{sp}
1	LOX	H_2	455.3	424.0
2		CH_4	368.9	343.5
3		RP-1	358.2	333.6
4	F_2	H_2	479.3	446.3
5		CH_4	415.8	387.2
6		MMH	415.4	386.8
7		N_2H_4	430.1	400.5
8	N_2O_4	MMH	341.5	318.0
9		N_2H_4	343.8	320.1
10	MON-25	MMH	342.9	319.3
11		N_2H_4	345.0	321.3
12	H_2O_2	MMH	336.8	313.6
13		N_2H_4	337.6	314.4

In the architectures which implemented a two-stage MAV, the MAV configuration mimics that of Willenberg [35], where the first stage was assumed to be a

solid rocket motor (SRM) and the second stage a liquid bipropellant. The I_{sp} values were obtained from ATK [63], which lists the STAR designation and I_{sp} for numerous SRMs. The mean value, lower bound, and upper bound were determined based on the data tabulated, and were found to be 284.9, 260.0, and 297.1 sec, respectively. The baseline value for I_{sp} used in the feasibility study was 285 sec. For the sensitivity study, the I_{sp} of the MAV first stage was varied over a range from 260 to 300 sec in increments of 5 sec.

5.3 Results

This section illustrates the results of the feasibility and sensitivity studies. Section 5.3.1 presents the feasibility of the selected DRM, and Section 5.3.2 presents the sensitivities associated with selected system parameters.

5.3.1 Feasibility

This section presents the results of the feasibility study performed. Table 5.8 lists the component and system masses for each architecture, along with their corresponding mass margins. The reader will note that, because direct ascent utilizes a separate component for Earth return, the DA architectures do not require an ERV. Figure 5.1 gives a comparison of the predicted system masses of all four architectures, broken into their respective component masses. Additionally, all masses have units of mT unless otherwise specified. Table 5.8 lists the component and system masses for each architecture, along with their corresponding mass margins. Figure 5.1 gives a comparison of the predicted system masses of all four architectures, broken into their respective component masses.

Table 5.8: Numerical results of the baseline feasibility study.

Architecture	**1**	**2**	**3**	**4**	
	DA-SS	**MOR-SS**	**DA-2S**	**MOR-2S**	
$m_{o,pre}$	83.1	30.0	69.3	23.6	mT
m_{ERV}	-----	0.5	-----	0.5	mT
m_{MAV}	23.2	4.9	18.3	3.0	mT
m_{Land}	4.9	1.8	4.1	1.4	mT
m_{Orb}	54.0	21.8	45.9	17.7	mT
Inert Payloads	0.9	0.9	0.9	0.9	mT
$\left(m_{o,given}\right)_{EDS}$	47.5	47.5	47.5	47.5	mT
$\left(m_{o,given}\right)_{Centaur}$	51.7	51.7	51.7	51.7	mT
MM_{EDS}	-74.7 %	36.8 %	-45.7 %	50.3 %	
$MM_{Centaur}$	-60.6 %	41.9 %	-34.0 %	54.3 %	

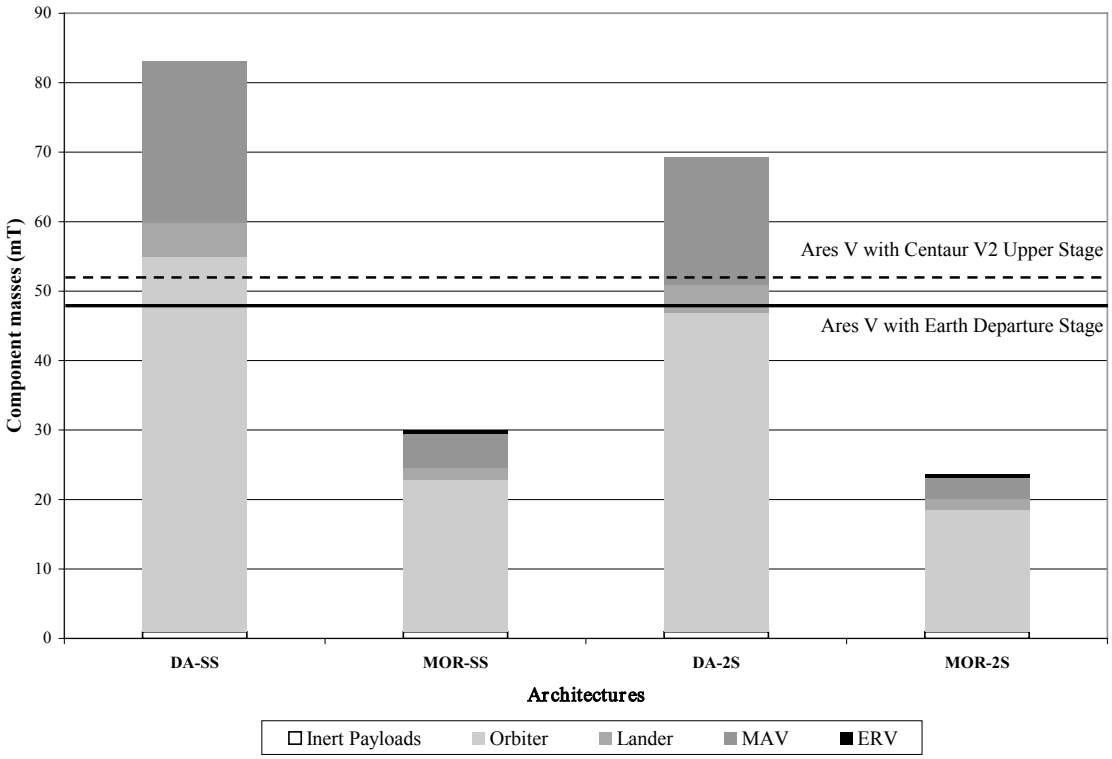

Figure 5.1: Baseline architecture component and system masses.

From Table 5.8 and Figure 5.1, the predicted system masses ($m_{o,pre}$) of the direct ascent architectures exceed the payload capability of both Ares V configurations for the selected DRM, as this can be seen from the negative mass margins. The Mars orbit rendezvous architectures, however, fall within the allowable payload capability of both Ares V configurations, as can be seen from the positive mass margins. Additionally, for the same return strategy, less mass is required for the two-stage MAV architectures than for the single-stage MAV architectures.

The mass of the inert payloads (surface sample, SC, EEC, and rover) was the same for all four architectures (0.946 mT). Additionally, the ERV mass was the same in both MOR architectures (0.544 mT).

5.3.2 Sensitivity

This section presents the results of the sensitivity study performed. Selected system parameters were varied over appropriate ranges, and the effects of these variations on overall system mass are presented in the following sections.

5.3.2.1 Earth Launch Opportunity

The effect of Earth launch opportunity on system mass was studied based on the process defined in Section 4.4.3. The TMI year (Mission Year), $(V_{HE})_{arv}$, and Earth departure C_3 for the various mission opportunities from 2009 to 2024 were taken from George [40] and listed in Table 5.6; the corresponding predicted system masses ($m_{o,pre}$) and Ares V allowable system masses ($m_{o,given}$) were calculated, and the graphical results of this section are presented in Figure 5.2.

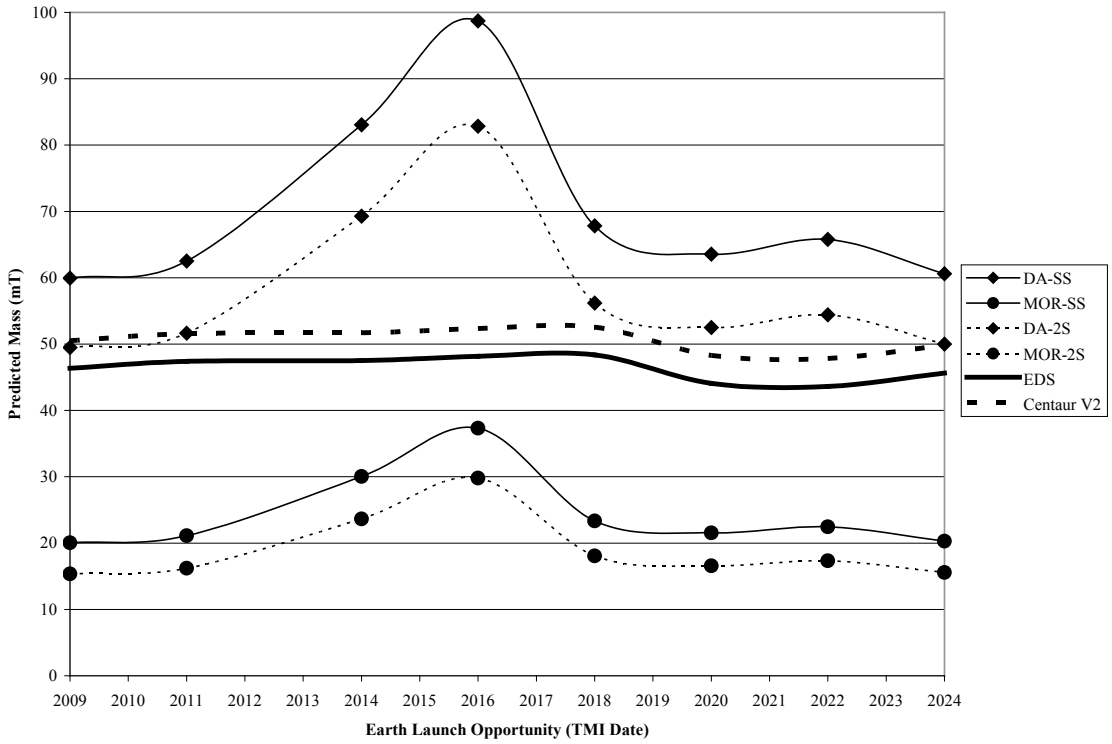

Figure 5.2: Launch opportunity effect on predicted launch mass.

Figure 5.2 shows that the MOR architectures are feasible on a single Ares V launch with either upper stage configuration for any of the mission opportunities considered. The DA-SS architecture, however, is not possible on a single Ares V launch for any of the mission opportunities, and the DA-2S architecture can not be performed with EDS.

5.3.2.2 Periapsis

The Mars periapsis altitude (h_p) was varied over a range from 250 to 600 km. The effect of h_p on system mass was tabulated, and the results are shown in Figure 5.3. It can be seen in the figure that, across the entire periapsis sweep, the MOR architectures

fall within the given Ares V allowance for both upper stage configurations, whereas neither of the DA architectures do. Additionally, it is evident that the system mass is nearly unaffected by the particular LMO altitude.

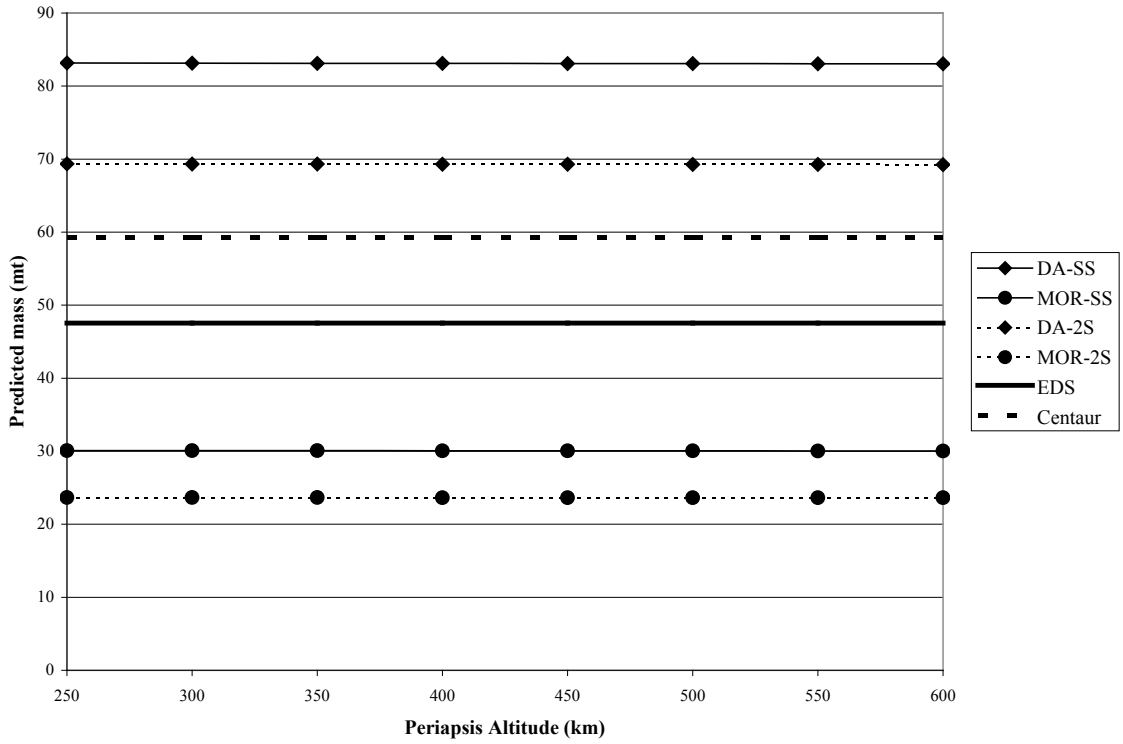

Figure 5.3: Predicted system mass vs. periapsis altitude.

5.3.2.3 Payloads

This section presents the effect of inert payload masses on system mass. The payloads studied include surface sample, EEC, and rover.

The surface sample mass (m_{Sample}) was varied over a range from 0.5 to 3.0 kg. The effect of m_{Sample} on system mass was tabulated, and the results are shown in

Figure 5.4. It can be seen in the figure that, across the entire m_{Sample} sweep, the MOR architectures fall within the given Ares V allowance for both upper stage configurations, whereas the DA architectures outweigh the given allowance. Additionally, it is evident that the sample mass has a very small effect on system mass.

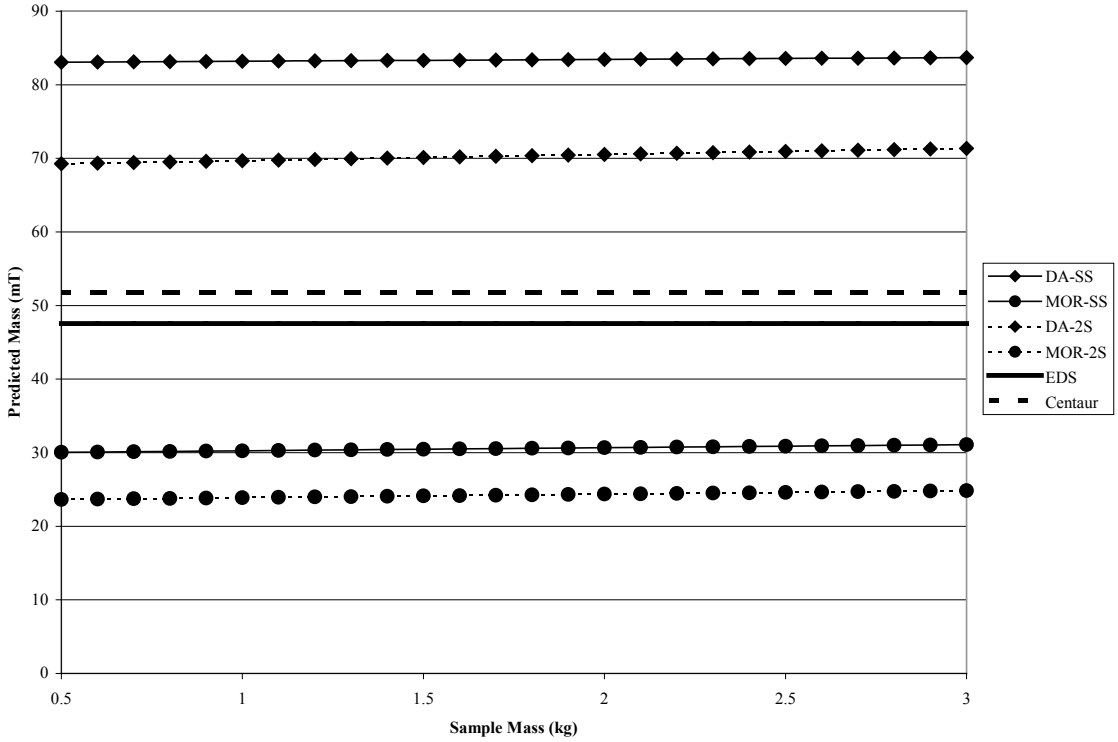

Figure 5.4: Predicted system mass vs. surface sample mass.

The Earth entry capsule mass (m_{EEC}) was varied over a range from 20 to 150 kg. The effect of m_{EEC} on system mass was tabulated, and the results are shown below in Figure 5.5. It can be seen in the figure that, across the entire m_{EEC} sweep, the MOR architectures fall within the given Ares V allowance for both upper stage configurations, whereas the DA architectures are more massive than the given allowance. Additionally,

it is evident that m_{EEC} has the greatest effect on the DA-2S architecture, as this architecture experiences roughly a 10 mT increase in system mass across the m_{EEC} sweep.

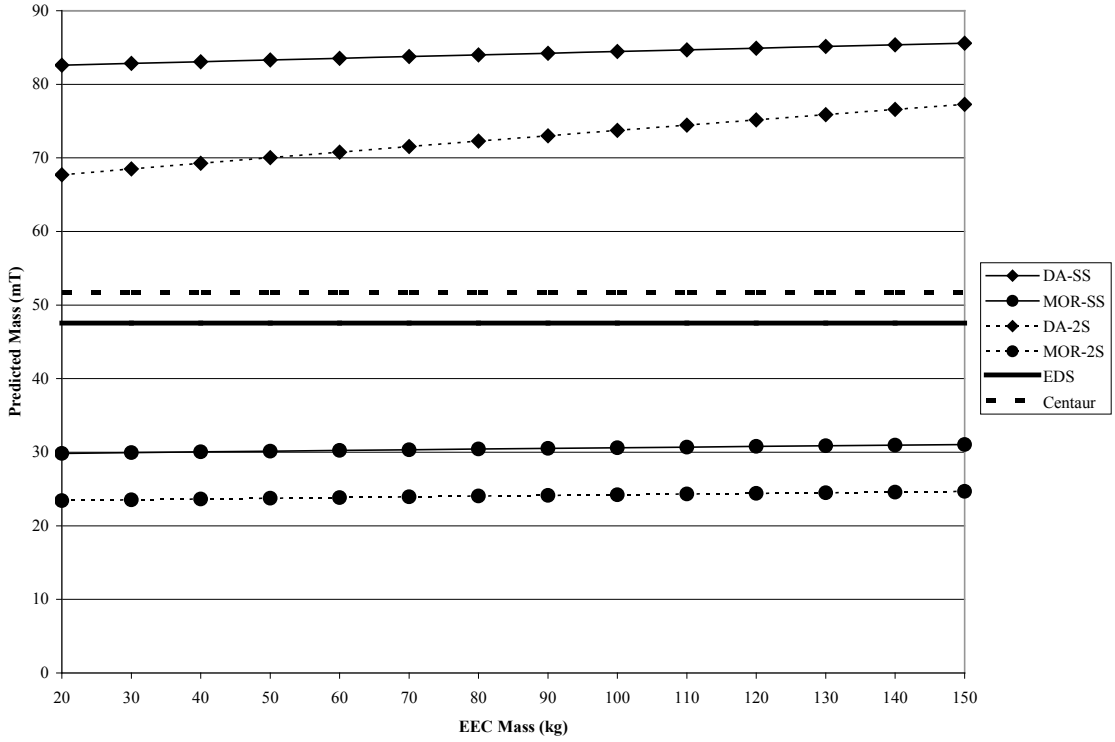

Figure 5.5: Predicted system mass vs. EEC mass.

The rover mass, m_{Rover}, was varied over a range from 500 to 2,000 kg. The effect of m_{Rover} on system mass was tabulated, and the results are shown in Figure 5.6. It can be seen in the figure that, across the entire m_{Rover} sweep, the MOR architectures fall within the given Ares V allowance for both upper stage configurations, whereas the DA architectures are more massive than the given allowance. Additionally, it is evident that

each of the architectures experiences an increase in system mass of roughly 4 to 6 mT from the m_{Rover} sweep.

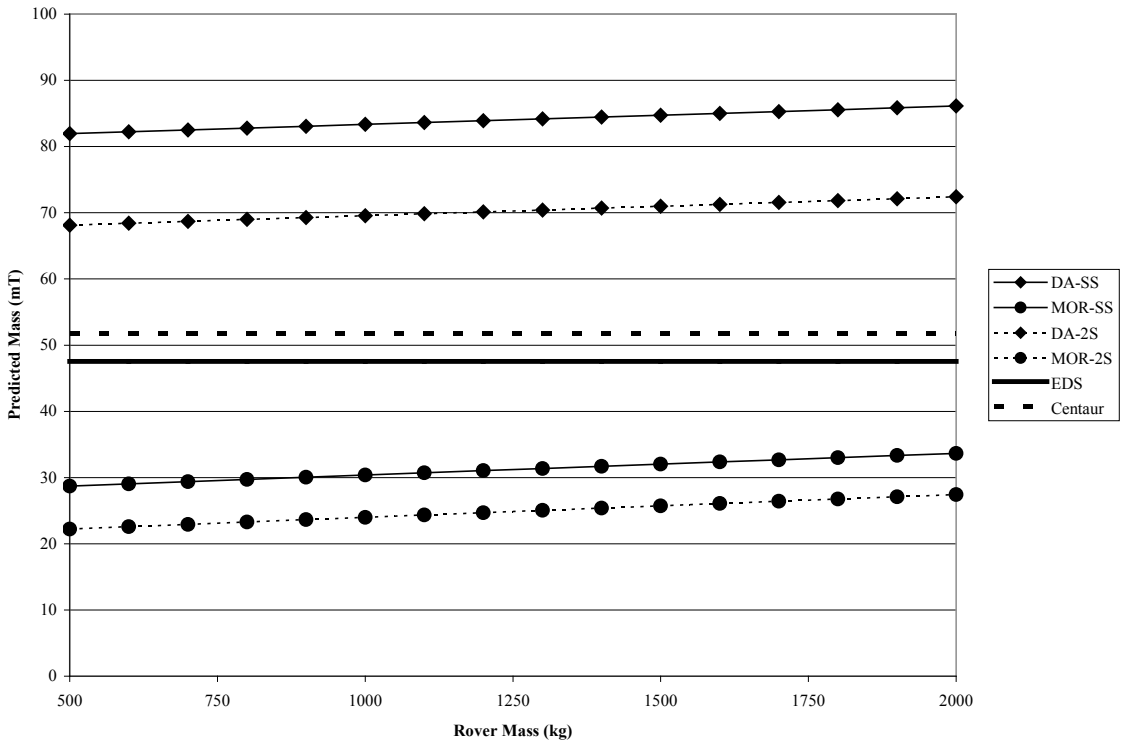

Figure 5.6: Predicted system mass vs. rover mass.

5.3.2.4 Propellant Mass Fraction of MAV First Stage

For the two-stage MAV architectures, the propellant mass fraction of the MAV first stage component was varied over a range from 0.8 to 0.95. The effect of PMF on system mass was tabulated, and the results are shown in Figure 5.7. It can be seen in the figure that, across the entire PMF sweep, the MOR architecture falls within the given Ares V allowance for both upper stage configurations. The DA architecture, however, is not feasible on a single Ares V launch with either upper stage configuration, even for the most optimal PMF. Additionally, it is evident that the direct ascent architecture

experiences a drastic drop in system mass (approximately 80 mT) when the MAV first stage PMF is increased. However, the MOR architecture experiences approximately 3 mT of decrease in system mass.

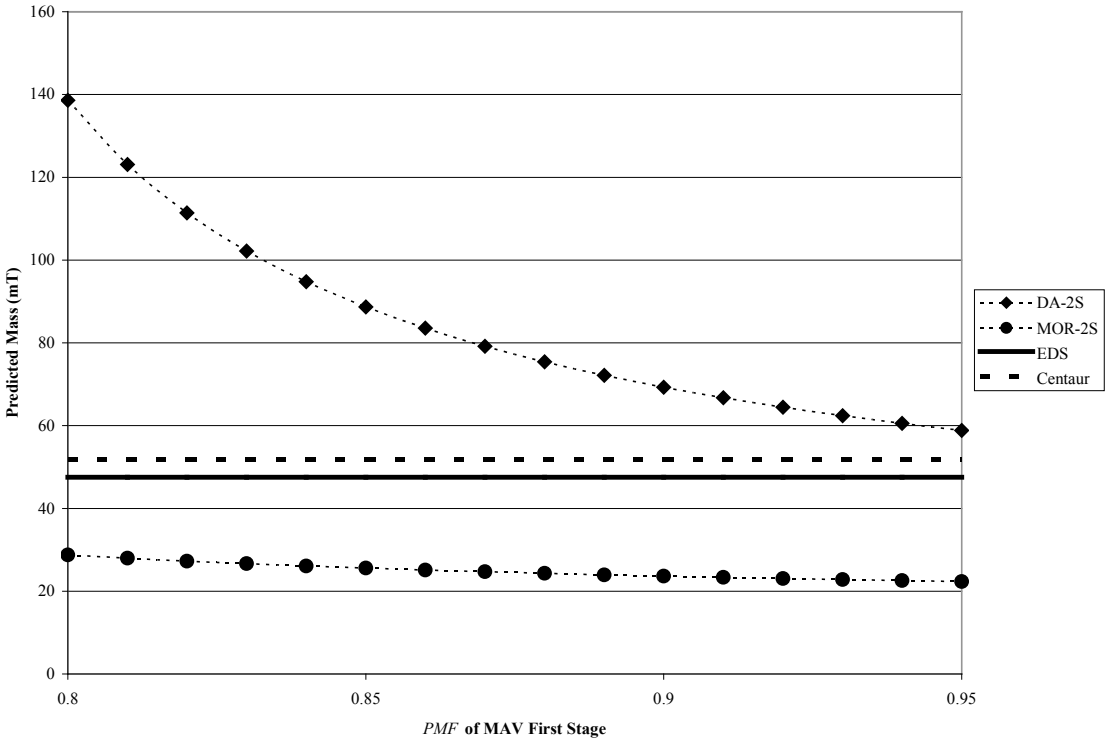

Figure 5.7: Predicted system mass vs. PMF of MAV first stage.

5.3.2.5 ΔV

This section presents the effect of ΔV on system mass. The ΔV was varied individually for the maneuvers of descent, ascent, and TEI. The descent ΔV ($\Delta V_{Descent}$) was varied over the same range for all four architectures. The ascent ΔV (ΔV_{Ascent}) was studied individually for all four architectures, as each of the architectures implemented a unique Mars ascent strategy. Finally, the TEI ΔV (ΔV_{TEI}) was studied only for the MOR

architectures, as the DA architectures combine the TEI maneuver and the ascent maneuver into one maneuver.

For all four architectures, the $\Delta V_{Descent}$ was varied over a range from 0.25 to 0.50 km/s. The effects on system mass were tabulated, and the results are shown in Figure 5.8. It can be seen in the figure that, across the entire $\Delta V_{Descent}$ sweep, the MOR architectures fall within the given Ares V allowance for both upper stage configurations, whereas the DA architectures outweigh the given allowance. Additionally, it is evident that the DA architectures experience a greater increase in system mass (approximately 8 mT each) than the MOR architectures (approximately 3 mT) when $\Delta V_{Descent}$ is increased.

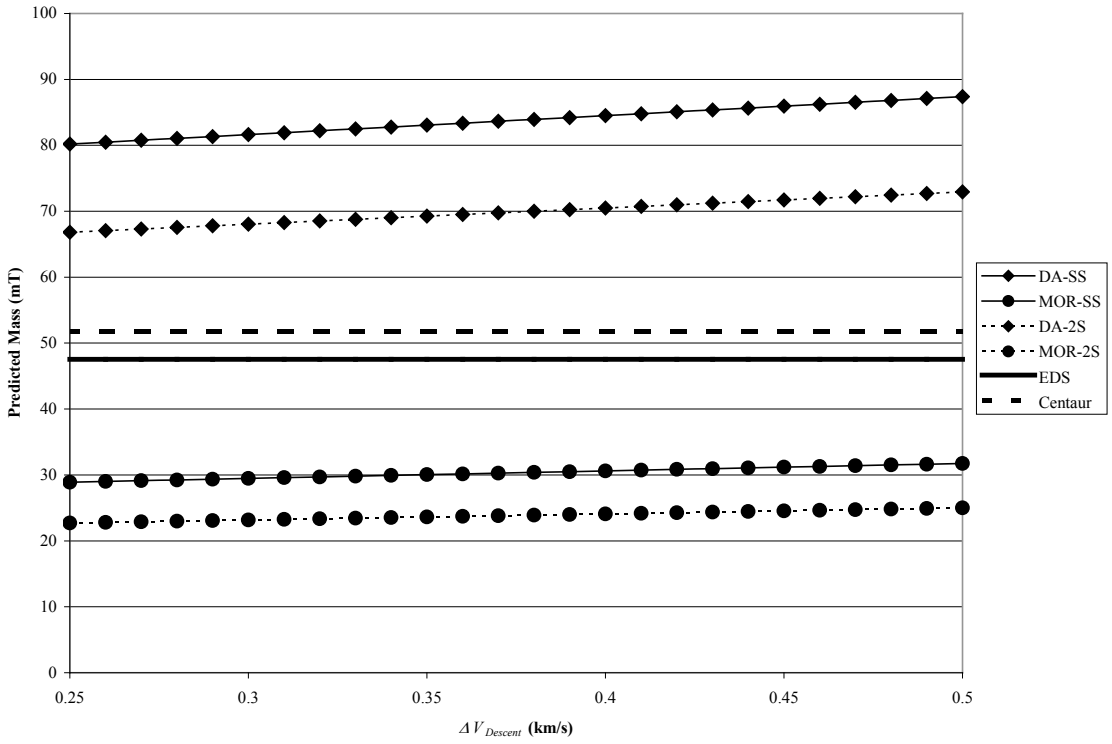

Figure 5.8: Predicted system mass vs. $\Delta V_{Descent}$.

The ascent ΔV (ΔV_{Ascent}) for the DA-SS architecture was varied over a range from 6.0 to 6.5 km/s. The effects on system mass were tabulated, and the results are shown in Figure 5.9. It can be seen in the figure that, across the entire ΔV_{Ascent} sweep, the DA-SS architecture outweighs the given Ares V allowance for both upper stage configurations. Additionally, it is evident that this architecture experiences approximately a 12 mT increase in system mass over the ΔV_{Ascent} sweep.

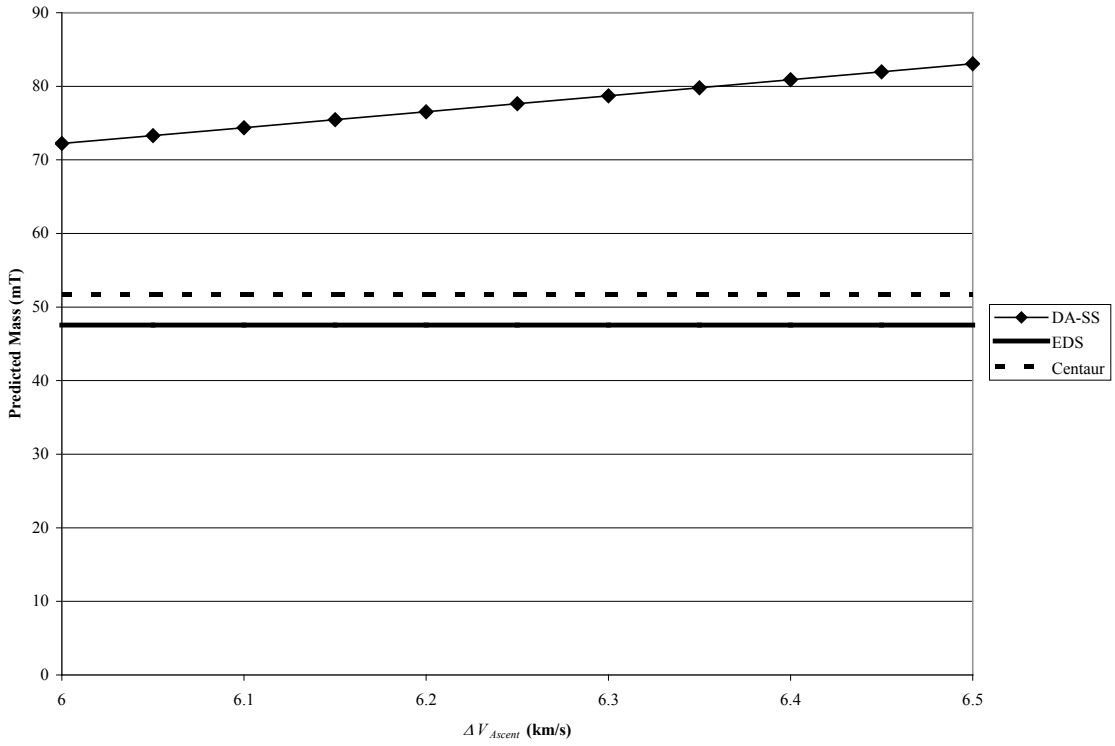

Figure 5.9: Predicted system mass vs. ΔV_{Ascent} (DA-SS).

The ΔV_{Ascent} for the MOR-SS architecture was varied over a range from 4.5 to 5.5 km/s. The effects on system mass were tabulated, and the results are shown in Figure

5.10. It can be seen in the figure that, across the entire ΔV_{Ascent} sweep, the MOR-SS architecture falls within the given Ares V allowance for both upper stage configurations. Additionally, it is evident that this architecture experiences approximately a 11 mT increase in system mass over the ΔV_{Ascent} sweep.

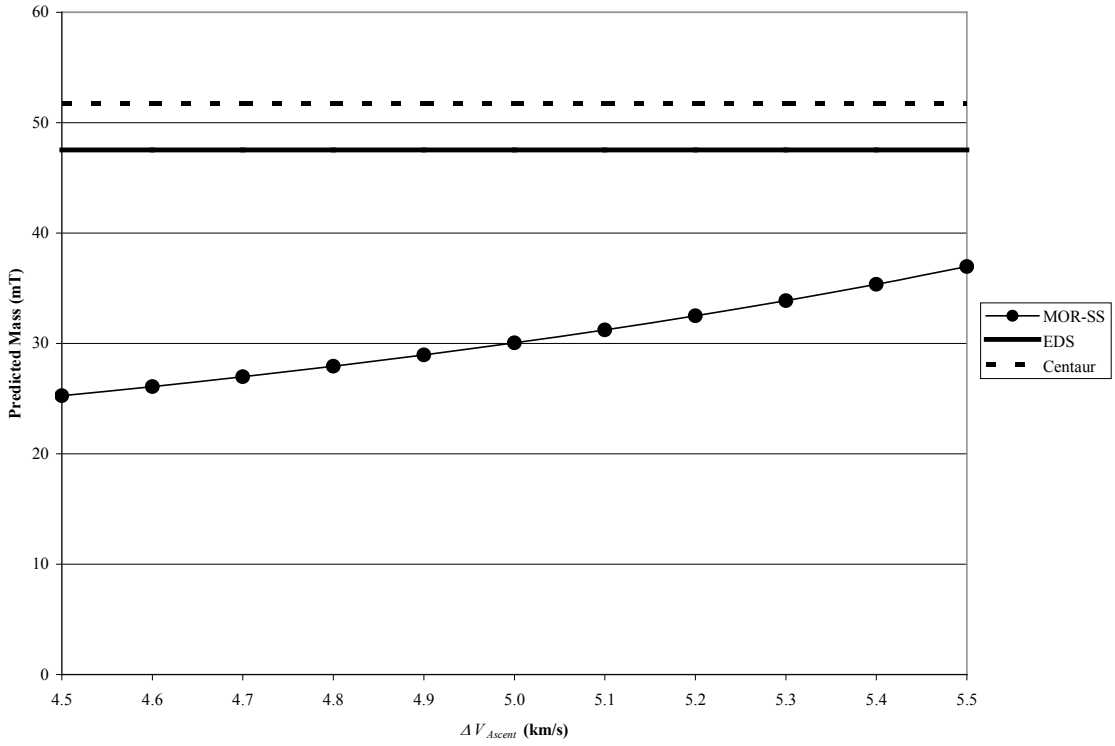

Figure 5.10: Predicted system mass vs. ΔV_{Ascent} (MOR-SS).

The ΔV_{Ascent} for the two-stage MAV architectures was divided equally between the two stages of the MAV; each ΔV was given the nomenclature $\Delta V_{Ascent,US}$ and $\Delta V_{Ascent,FS}$ to designate MAV upper stage and MAV first stage ascent, respectively.

Because the two-stage MAV architectures employ unique ascent strategies, the effects of ΔV_{Ascent} on system mass were studied separately for both stages.

The $\Delta V_{Ascent,US}$ for the DA-2S architecture was varied over a range from 3.0 to 3.25 km/s. The effects on system mass were tabulated, and the results are shown in Figure 5.11. It can be seen in the figure that, across the entire $\Delta V_{Ascent,US}$ sweep, the DA-2S architecture is more massive than the given Ares V allowance for the EDS configuration, and provides negligible mass margin at the most optimal $\Delta V_{Ascent,US}$ with the Centaur upper stage. Additionally, it is evident that the DA-2S architecture experiences a 10 mT increase in system mass over the $\Delta V_{Ascent,US}$ sweep.

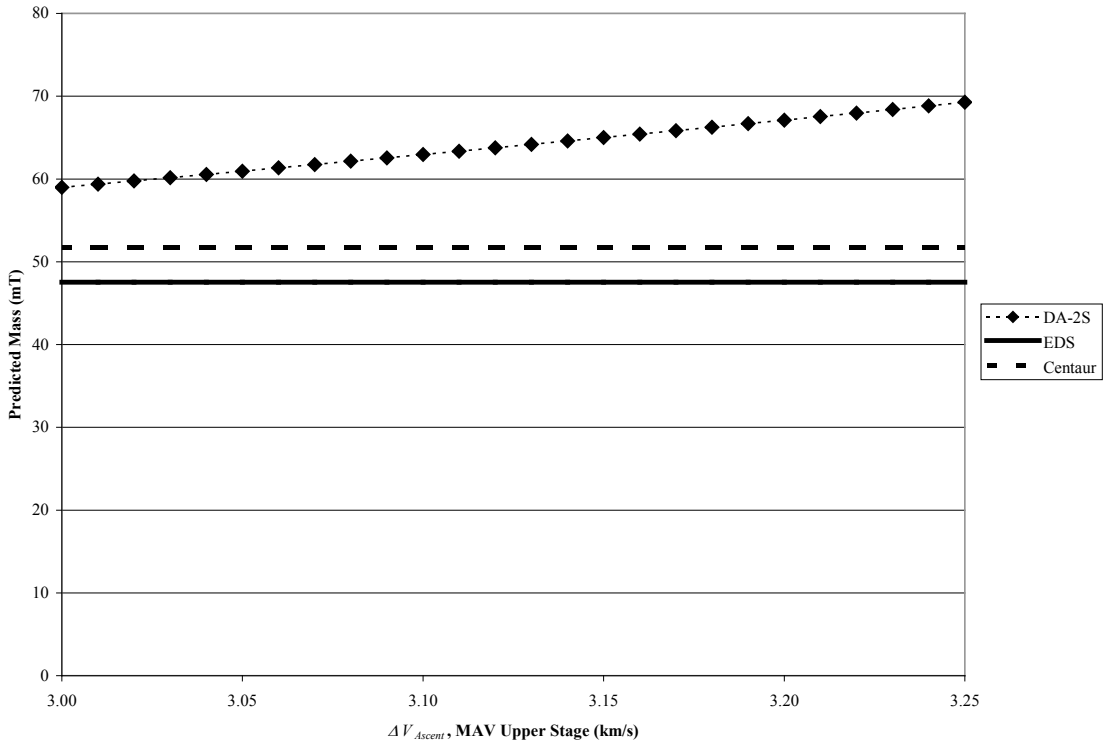

Figure 5.11: Predicted system mass vs. $\Delta V_{Ascent,US}$ (DA-2S).

As with the $\Delta V_{Ascent,US}$ sweep, the $\Delta V_{Ascent,FS}$ was varied from 3.0 to 3.25 km/s, and the effects on system mass were tabulated. It can be seen in Figure 5.12 that, across the entire $\Delta V_{Ascent,FS}$ sweep, the DA-2S architecture outweighs the given Ares V allowance for both upper stage configurations. Additionally, it is evident that this architecture experiences roughly an 8 mT increase in system mass over the $\Delta V_{Ascent,FS}$ sweep.

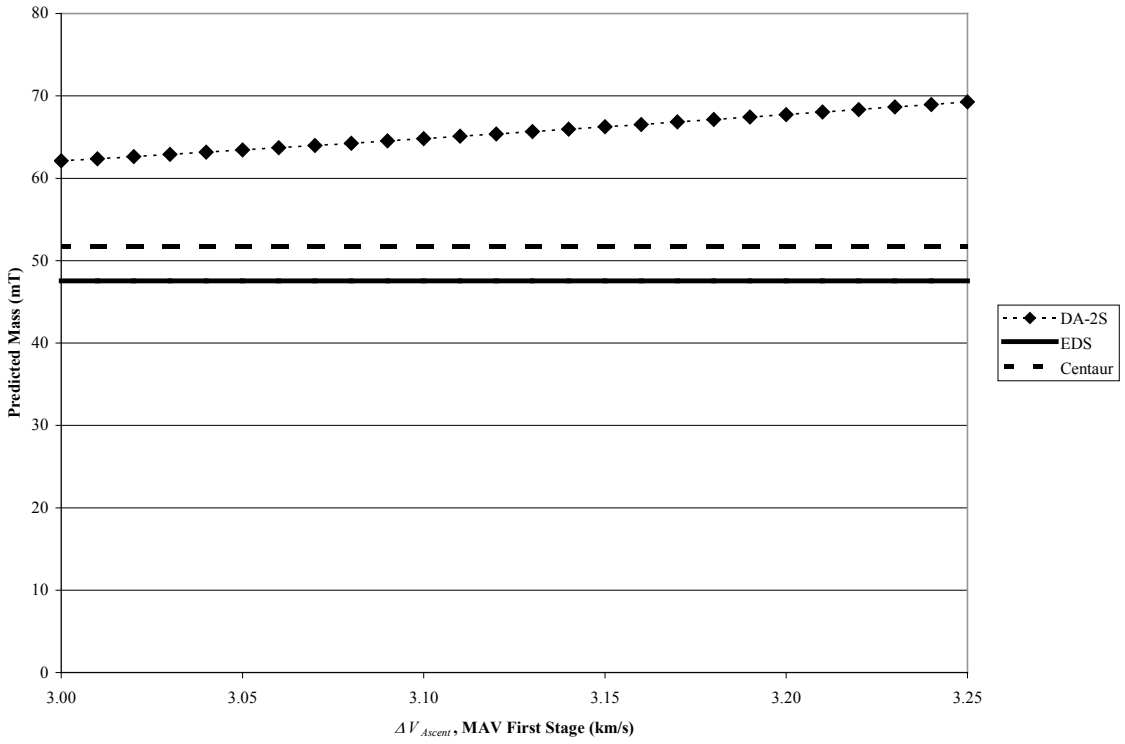

Figure 5.12: Predicted system mass vs. $\Delta V_{Ascent,FS}$ (DA-2S).

The $\Delta V_{Ascent,US}$ for the MOR-2S architecture was varied over a range from 2.25 to 2.75 km/s. The effects on system mass were tabulated, and the results are shown in

Figure 5.13. It can be seen in the figure that, across the entire $\Delta V_{Ascent,US}$ sweep, the MOR-2S architecture falls within the given Ares V allowance for both upper stage configurations. Additionally, it is evident that this architecture experiences roughly 4 mT increase in system mass over the $\Delta V_{Ascent,US}$ sweep.

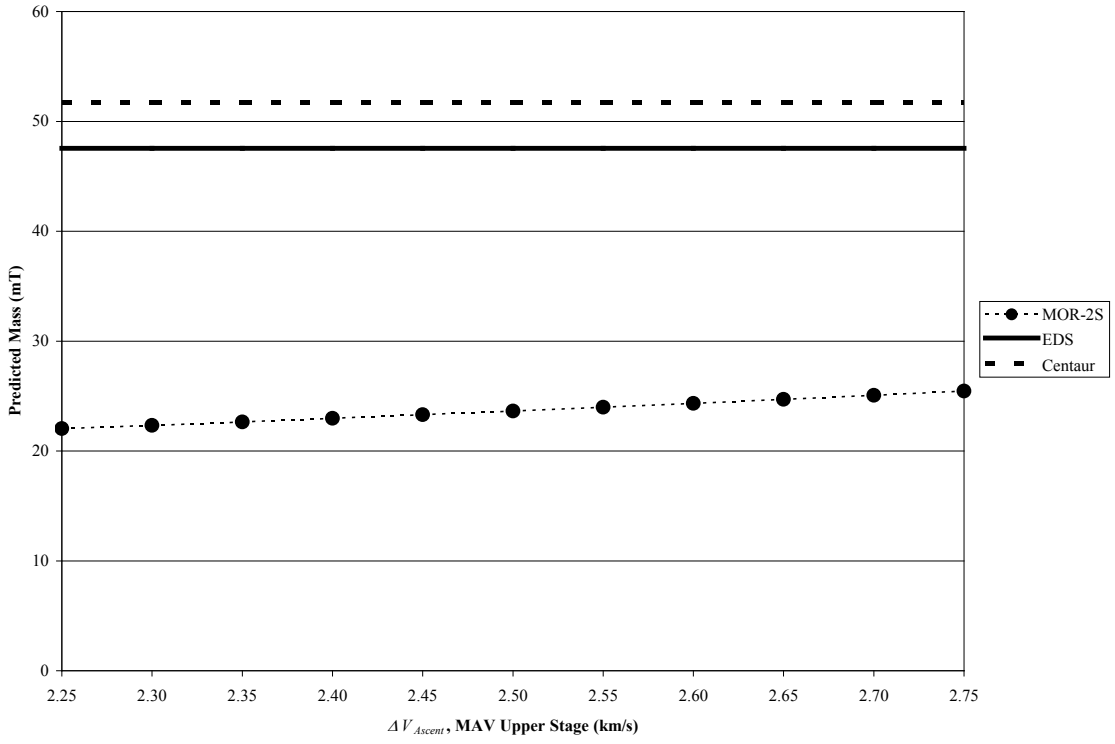

Figure 5.13: Predicted system mass vs. $\Delta V_{Ascent,US}$ (MOR-2S).

As with the $\Delta V_{Ascent,US}$ sweep, the $\Delta V_{Ascent,FS}$ was varied from 2.25 to 2.75 km/s, and the effects on system mass were tabulated. It can be seen in Figure 5.14 that, across the entire $\Delta V_{Ascent,FS}$ sweep, the MOR-2S architecture falls within the given Ares V

allowance for both upper stage configurations. Additionally, it is evident that this architecture experiences a 3 mT increase in system mass over the $\Delta V_{Ascent,FS}$ sweep.

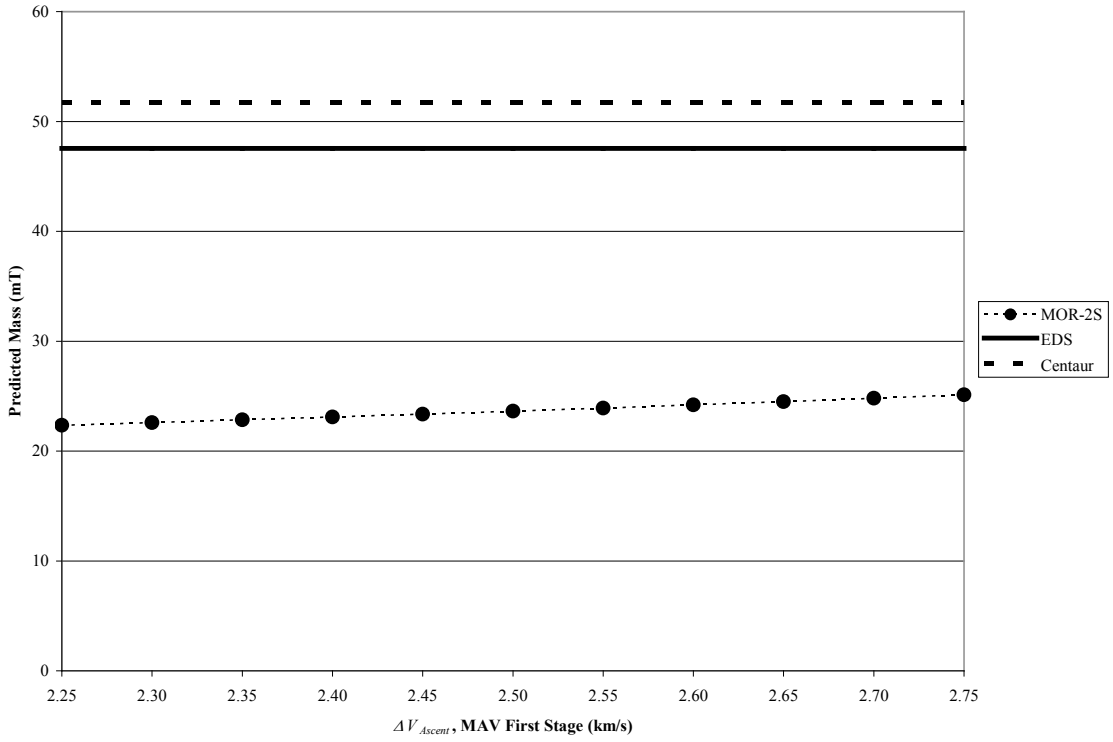

Figure 5.14: Predicted system mass vs. $\Delta V_{Ascent,FS}$ (MOR-2S).

In order to find the optimal ΔV split between the two MAV stages, the ΔV_{Ascent} was varied over the first stage and upper stage components such that the total ΔV_{Ascent} added up to 6.5 km/s for DA-2S and 5.0 km/s for MOR-2S. Note that the horizontal axes represent the portion of the ΔV_{Ascent} allotted to the upper stage, and the remainder is given to the first stage. For the DA-2S architecture, the predicted mass increases by 27 mT over the entire sweep, where the $\Delta V_{Ascent,US}$ ranges from 2.5 to 4.0 km/s, and the total

ΔV_{Ascent} remains constant at 6.5 km/s. Figure 5.15 shows that the DA-2S architecture was found to be more massive than the Ares V allowance for both upper stage configurations, even at the most optimal ΔV_{Ascent} split. It is evident in Figure 5.16, however, that the MOR-2S architecture falls within the Ares V allowance, providing sufficient mass margin for both upper stage configurations. The MOR-2S architecture experiences an increase in mass of 2.0 mT across the entire sweep.

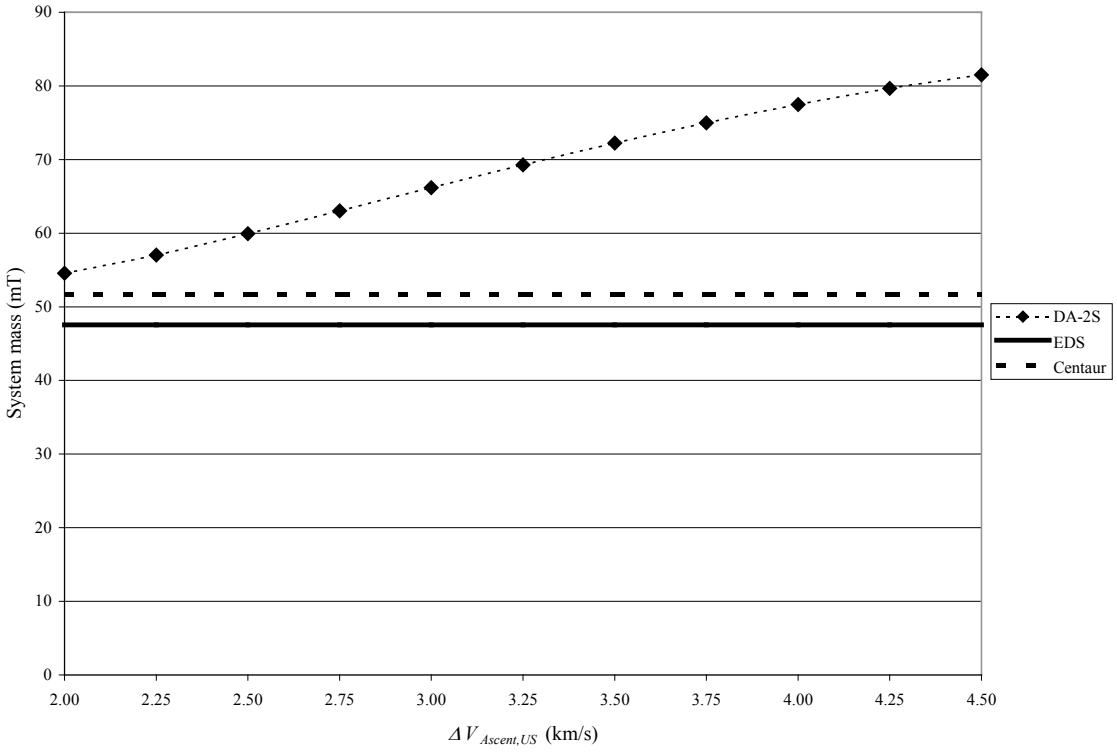

Figure 5.15: Predicted mass over ΔV_{Ascent} split (DA-2S).

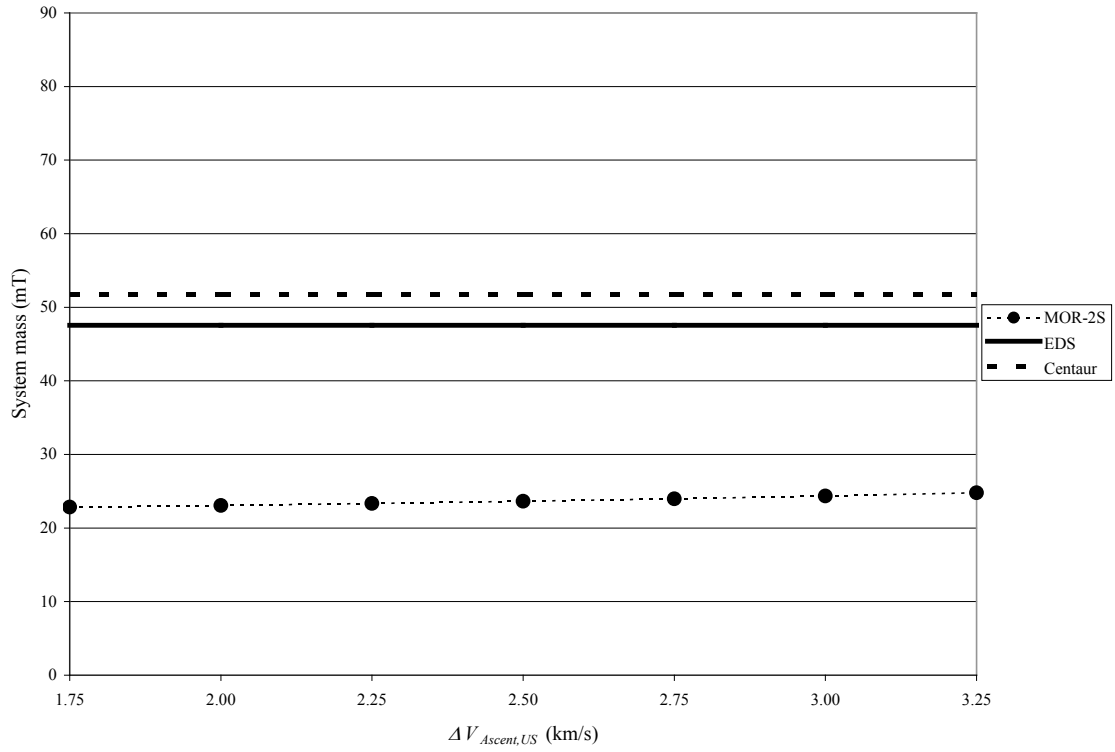

Figure 5.16: Predicted mass over ΔV_{Ascent} split (MOR-2S).

For the Mars orbit rendezvous architectures, the ΔV_{TEI} was varied over a range from 1.0 to 2.0 km/s. The effects on system mass were tabulated, and the results are shown in Figure 5.17. It can be seen in the figure that, across the entire ΔV_{TEI} sweep, both architectures fall within the given Ares V allowance for both upper stage configurations. Additionally, it is evident that both architectures increase 2 to 3 mT in system mass over the ΔV_{TEI} sweep.

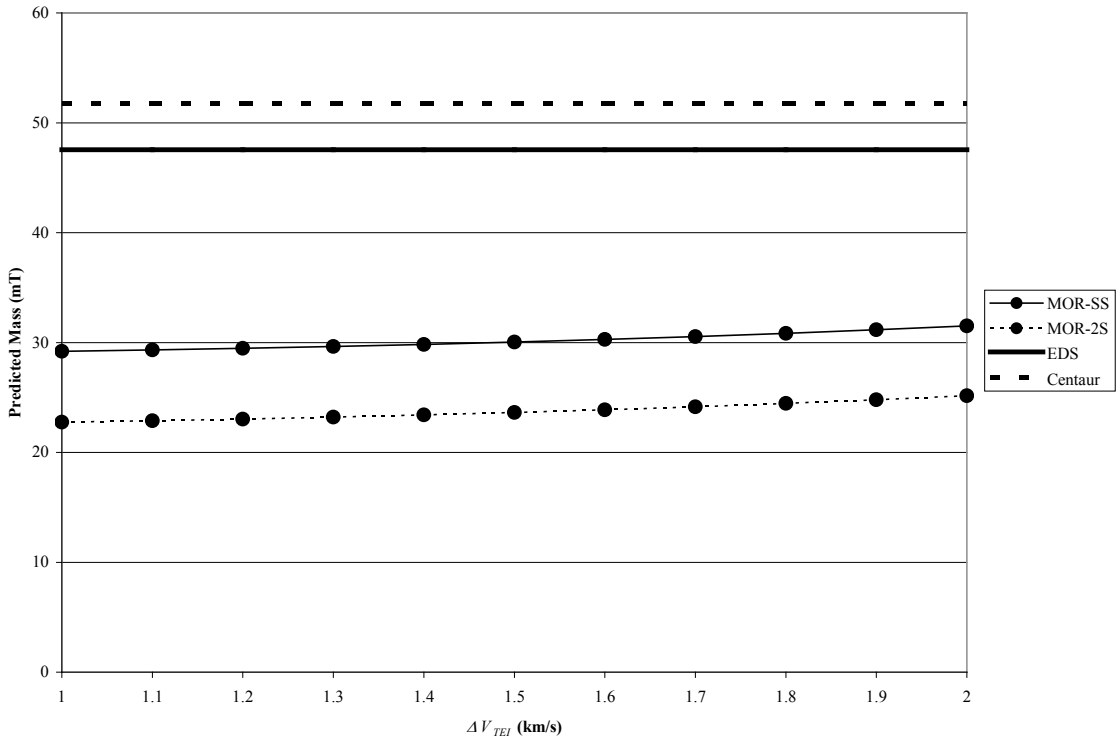

Figure 5.17: Predicted system mass vs. ΔV_{TEI} .

5.3.2.6 Mass Growth Allowance

This section presents the effects of mass growth allowance (*MGA*) on system mass. The *MGA* was varied over a range from 1.15 to 1.30 and was applied consistently to each component in all architectures. Figure 5.18 illustrates the effect of mass growth allowance on system mass. It can be seen in the figure that, across the entire *MGA* sweep, the MOR architectures fall within the given Ares V allowance for both upper stage configurations, whereas the DA architectures outweigh the given allowance. Additionally, it is evident that the DA-2S architecture, while less massive across the sweep than the DA-SS architecture, experiences a sharper increase in mass (15 mT) than

the DA-SS (9 mT). The reader will also note that the MOR-SS and MOR-2S architectures increase in mass by 5 and 3 mT respectively across the *MGA* sweep.

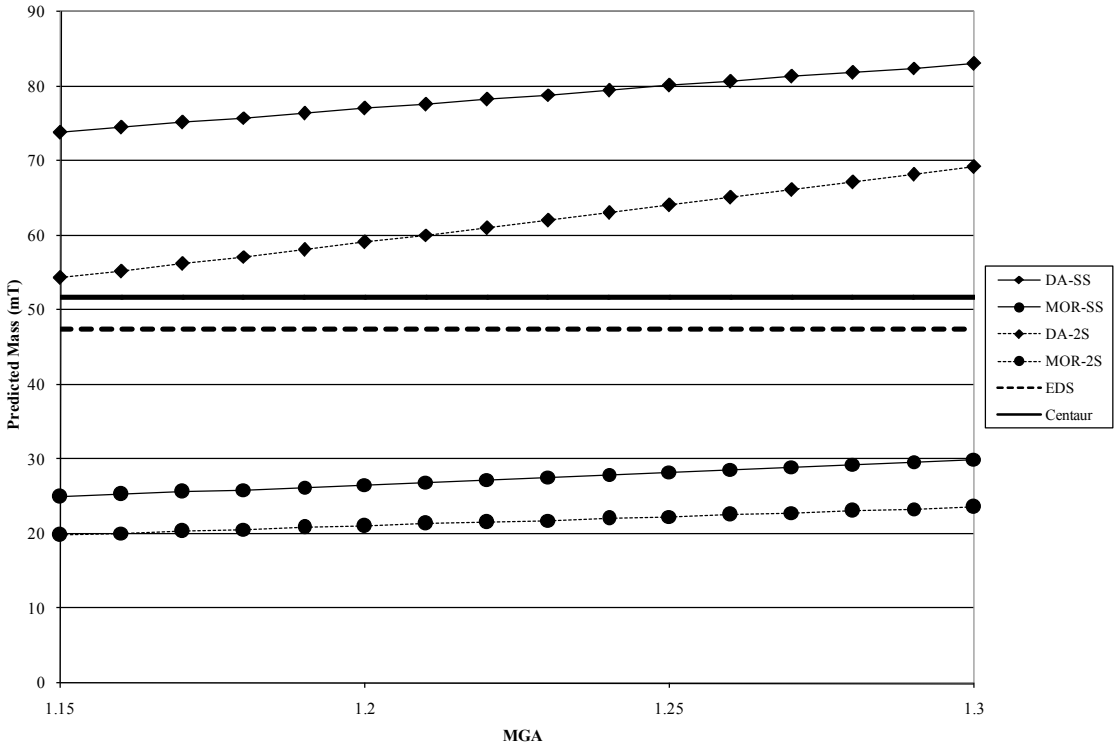

Figure 5.18: Predicted system mass vs. *MGA* .

5.3.2.7 Specific Impulse

This section presents the effects of specific impulse (I_{sp}) on system mass. The I_{sp} was varied consistently over a range from 313.6 to 446.3 sec (representing H_2O_2/MMH and F_2/H_2 respectively) for all bipropellant systems, and from 260 to 300 sec for all SRMs (applied only to MAV first stage components). The effect of I_{sp} on system mass was studied for each component, and the changes in system mass are illustrated in

Figures 19 – 24. Table 5.9 summarizes these figures, and the quantities listed are in units of mT.

Table 5.9: Effects of I_{sp} sweeps on system mass.

	DA-SS	**MOR-SS**	**DA-2S**	**MOR-2S**
Orbiter	-19.7	-8.6	-16.9	-7.2
Lander	-3.1	-1.2	-2.6	-1.0
MAV	-40.3	-11.6	-----	-----
MAV FS	-----	-----	-16.0	-2.1
MAV US	-----	-----	-34.9	-4.4
ERV	-----	-0.8	-----	-0.9

Figure 5.19 illustrates the effect of the orbiter's I_{sp} on system mass. It can be seen in the figure that, across the entire I_{sp} sweep, both of the MOR architectures fall within the given Ares V allowance for both upper stage configurations, whereas both DA architectures exceed the given allowance across the entire sweep. The DA-2S architecture could provide minimal mass margin with the Centaur upper stage for a lander I_{sp} of 450 sec or higher. Additionally, it is evident that the DA-SS and DA-2S architectures experience a sharper drop in system mass (17 and 20 mT, respectively) than the MOR-SS and MOR-2S architectures (9 and 7 mT, respectively).

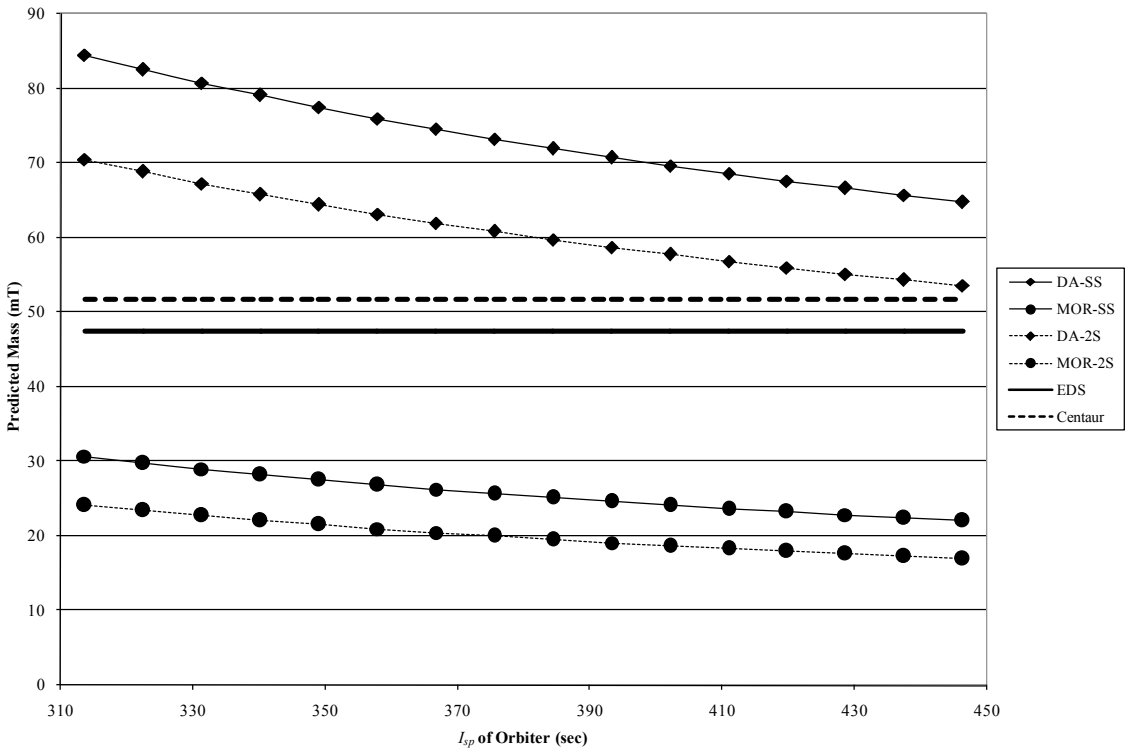

Figure 5.19: Predicted system mass vs. I_{sp} of orbiter.

Figure 5.20 illustrates the effect of the lander's I_{sp} on system mass. It can be seen in the figure that, across the entire I_{sp} sweep, both of the MOR architectures fall within the given Ares V allowance for both upper stage configurations, whereas the DA architectures outweigh the given allowance for all I_{sp} values. Additionally, it is evident that the direct ascent architectures experience a decrease in system mass of roughly 3 mT over the I_{sp} sweep, while the MOR architectures experience a decrease of 1 mT.

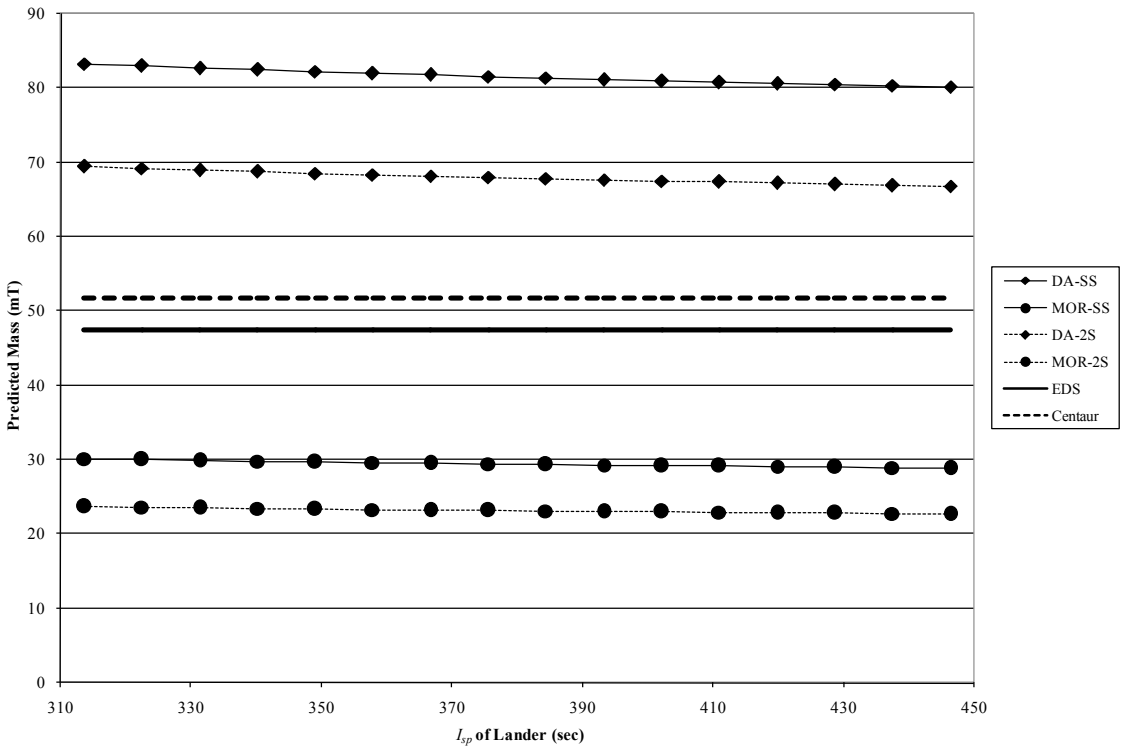

Figure 5.20: Predicted system mass vs. I_{sp} of lander.

Figure 5.21 illustrates the effect of the MAV's I_{sp} on system mass for the single-stage MAV architectures. It can be seen in the figure that, across the entire I_{sp} sweep, the MOR-SS architecture falls within the given Ares V allowance for both upper stage configurations. The DA-SS architecture, however, only provides a positive mass margin for I_{sp} values above 440 sec and 420 sec, respectively, for the EDS and Centaur configurations. Additionally, it is evident that the direct ascent architecture experiences a decrease in system mass of 40 mT over the I_{sp} sweep, while the Mars orbit rendezvous architecture experiences a decrease in system mass of approximately 12 mT.

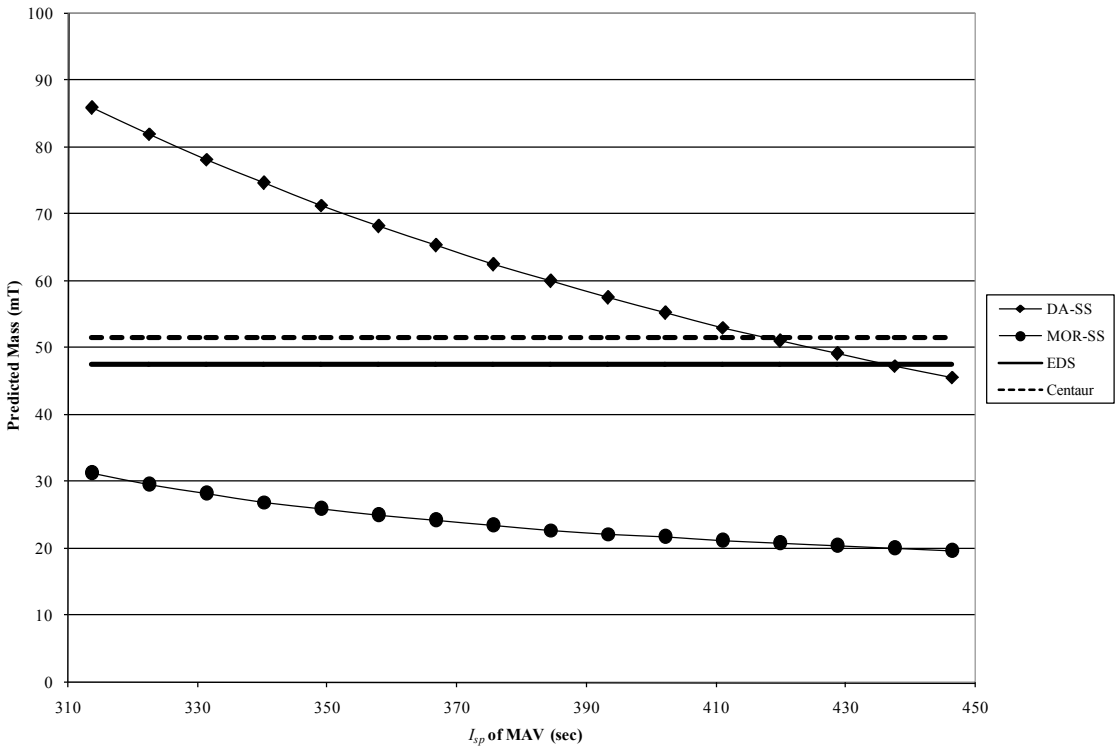

Figure 5.21: Predicted system mass vs. I_{sp} of MAV.

Figure 5.22 illustrates the effect of the MAV first stage component's I_{sp} on system mass for the two-stage MAV architectures. Unlike the chemical bipropellant systems, the MAV first stage was designated to be a SRM, and the I_{sp} was thus assigned a different range of variation (260 to 300 sec). It can be seen in the figure that, across the entire I_{sp} sweep, the MOR-2S architecture falls within the given Ares V allowance for both upper stage configurations, whereas the DA-2S architecture exceeds the given allowance. Additionally, it is evident that the DA architecture experiences a decrease in system mass of 16 mT over the I_{sp} sweep, while the MOR architecture decreases approximately 2 mT.

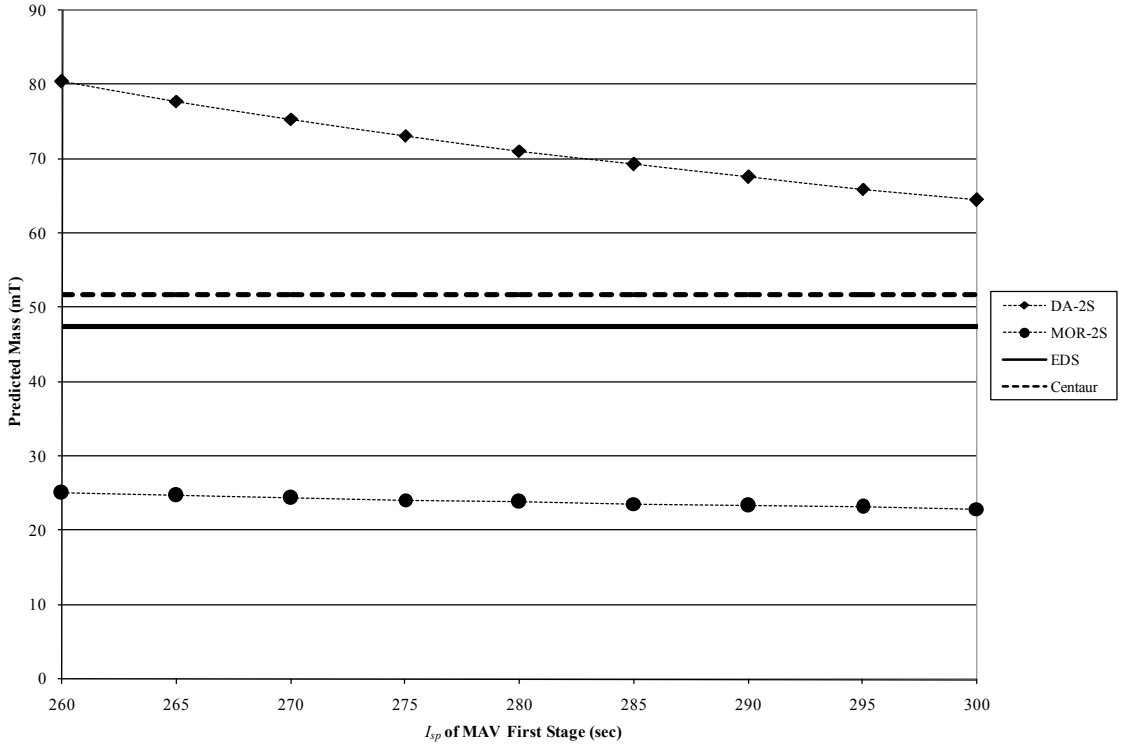

Figure 5.22: Predicted system mass vs. I_{sp} of MAV first stage.

Figure 5.23 illustrates the effect of the MAV upper stage component's I_{sp} on system mass for the two-stage MAV architectures. It can be seen in the figure that, across the entire I_{sp} sweep, the MOR-2S architecture falls within the given Ares V allowance. The DA-2S architecture, however, only provides a positive mass margin at I_{sp} values above 390 sec for the EDS upper stage, and above 370 sec for Centaur. Additionally, it is evident that the direct ascent architecture experiences a decrease in system mass of approximately 35 mT over the I_{sp} sweep, while the Mars orbit rendezvous architecture decreases approximately 4 mT.

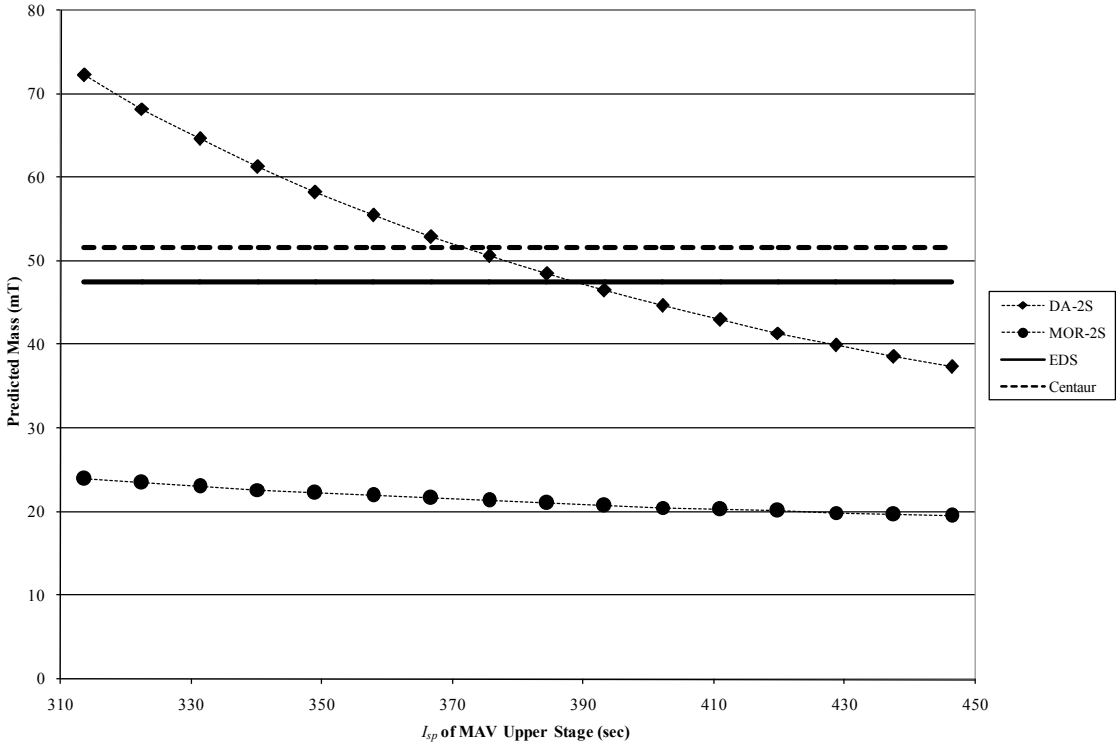

Figure 5.23: Predicted system mass vs. I_{sp} of MAV upper stage.

Figure 5.24 illustrates the effect of the ERV's I_{sp} on system mass for the Mars orbit rendezvous architectures. It can be seen in the figure that, across the entire I_{sp} sweep, both architectures fall within the given Ares V allowance. Additionally, it is evident that both architectures experience a decrease in system mass less than 1 mT over the I_{sp} sweep.

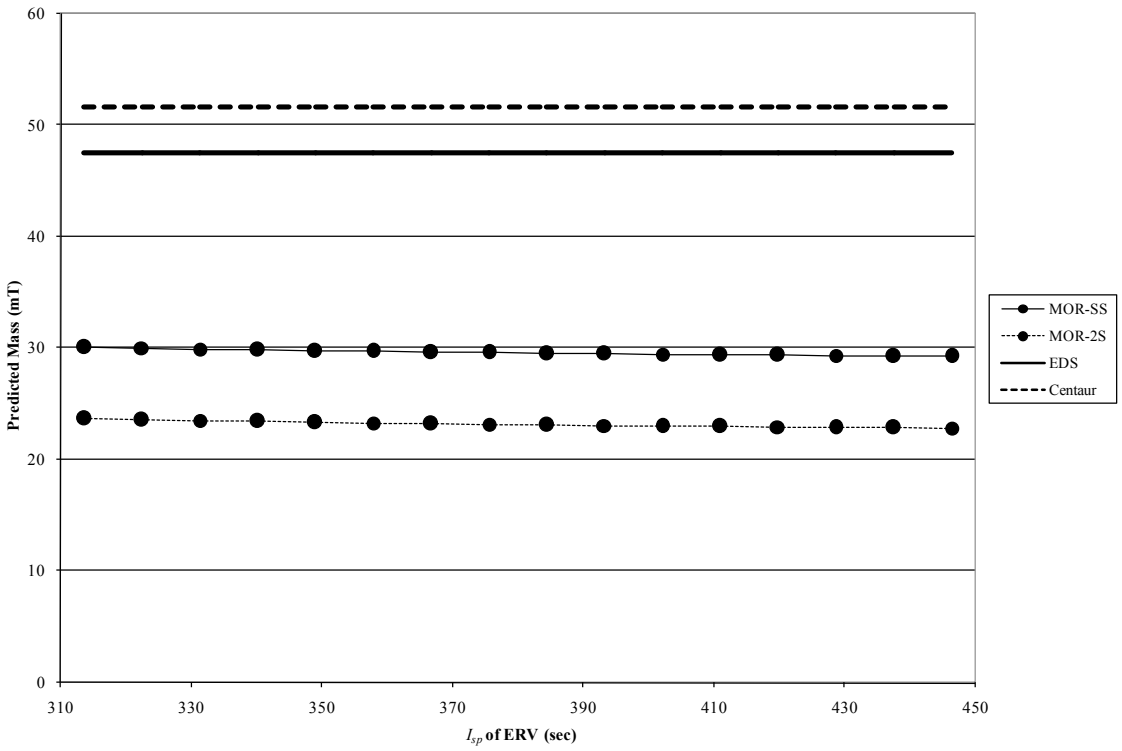

Figure 5.24: Predicted system mass vs. I_{sp} of ERV.

5.4 Summary

The results show that the design reference mission is feasible on a single Ares V launch, using either the EDS or Centaur V2 upper stage. The Mars orbit rendezvous architectures each yield a mass margin of greater than 30 percent for both upper stage configurations. The baseline direct ascent architectures, however, yield negative mass margins for both the EDS and Centaur V2 upper stages, and are thus not feasible on a single Ares V launch. Additionally, the sensitivity analysis shows that direct ascent provides significantly less (often negative) mass margin than Mars orbit rendezvous. There are few instances, however, in which direct ascent is feasible given the parameter

values used in the DRM. Given the information presented in this chapter, Table 5.10 summarizes these instances which allow for positive mass margin using direct ascent.

Table 5.10: Feasible instances for direct ascent.

Parameter Sweep	Data Point	Architecture	Ares V Configuration
Launch Opportunity	2009	DA-2S	Centaur V2
I_{sp} (MAV)	> 435 sec	DA-SS	EDS
	> 419 sec	DA-SS	Centaur V2
I_{sp} (MAV US)	> 380 sec	DA-2S	EDS
	> 370 sec	DA-2S	Centaur V2

The information presented in Section 5.3.2 shows that system mass is more sensitive to certain parameters than to others. Table 5.11 summarizes the changes in system mass (mT) for each of the specified parameter variations. Note that the launch opportunity sweep is not included in the table, as system mass (demonstrated in Figure 5.2) experiences cyclic changes with launch opportunity. The parameters which are shown to have the largest effect on system mass include MAV first stage PMF (two-stage MAV architectures), I_{sp} of MAV and MAV components, I_{sp} of orbiter, ΔV_{Ascent}, and MGA. Further conclusions about the findings of this study, as well as recommendations for future work, are discussed in Chapter 6.

Table 5.11: System mass sensitivities from parametric sweeps.

	DA-SS	**MOR-SS**	**DA-2S**	**MOR-2S**
Periapsis				
	-0.12	-0.05	-0.10	-0.04
Payloads				
m_{sample}	0.63	1.05	2.07	1.20
m_{EEC}	2.98	1.19	9.56	1.24
m_{Rover}	4.17	4.95	4.27	5.23
PMF of MAV FS				
	-----	-----	-79.76	-6.44
ΔV				
Descent	7.21	2.85	6.13	2.30
Ascent	10.83	11.70	-----	-----
Ascent, FS	-----	-----	7.16	2.78
Ascent, US	-----	-----	10.28	3.41
TEI	-----	-----	2.31	2.41
MGA				
	9.20	5.07	14.93	3.72
I_{sp}				
Orbiter	-19.66	-8.62	-16.90	-7.17
Lander	-3.06	-1.22	-2.61	-0.99
MAV	-40.31	-11.57	-----	-----
MAV FS	-----	-----	-15.98	-2.10
MAV US	-----	-----	-34.89	-4.42
ERV	-----	-0.82	-----	-0.86

CHAPTER 6

CONCLUSION

6.1 Overview

This chapter summarizes the overall results of the feasibility and sensitivity studies performed. Conclusions about the findings of these studies are presented in the following sections, and recommendations for further Mars sample return studies are given based on the results gathered in Chapter 5.

6.2 Feasibility

A feasibility study was performed based on a design reference mission. The results of this study are illustrated and described in Section 5.3.1. This section gives detailed explanation of the results of the feasibility study.

The numerical results of the feasibility study are presented in Table 5.8. The total predicted system masses for the four architectures were 83.07, 30.05, 69.27, and 23.63 mT, for DA-SS, MOR-SS, DA-2S, and MOR-2S, respectively. It can be seen in Figure 5.1 that the direct ascent architectures require significantly more mass than the MOR architectures, and therefore, do not allow any mass margin. Because the direct ascent strategy is a more energetic maneuver (i.e., it combines Mars ascent with trans-Earth injection) and is performed on a single component, the amount of propulsion

required for the ascent vehicle (i.e., MAV) is increased. In the case of MOR, the ERV remains onboard the orbiter, therefore reducing lift requirements by the lander and MAV. Because the MAV is considered a payload of the lander during the descent phase, the amount of propulsion required of the lander is increased, which in turn increases the overall mass of the lander. Similarly, because the lander is the payload of the orbiter, the orbiter's overall mass will be increased. The MOR architectures, however, were much lower, giving positive mass margins. Although utilizing two components for the ascent and TEI maneuvers (i.e., MAV and ERV, respectively) introduces more risk than with direct ascent, the MOR strategy reduces the amount of propulsion required for each component. A smaller MAV reduces the payload mass of the lander, thus reducing the lander's overall mass. The orbiter's mass is therefore decreased, thus yielding a less massive architecture than with direct ascent.

It can also be seen in Figure 5.1 that the two-stage MAV architectures have lower values for predicted system mass ($m_{o,pre}$) than their respective single-stage MAV architectures. In the case of a two-stage MAV, the first stage component only has to provide half the ΔV required to perform the ascent maneuver, and the upper stage component performs the other half. When the first stage is jettisoned, the remaining vehicle (upper stage component) has a lower dry mass, thus reducing the amount of propellant required to complete the ascent maneuver. Additionally, the two-stage MAV architectures use a SRM for the MAV first stage components, which has a higher PMF than a liquid bipropellant system.

The mass of the inert payloads (sample, SC, EEC, and rover) was equal (0.946 mT) in all four architectures. The ERV mass, m_{ERV}, was zero for the DA architectures,

as direct ascent assigns TEI to the MAV component. However, the MOR architectures yielded the same mass of 0.544 (mT); these components were equal in mass because the two architectures require the ERV to perform the TEI maneuver with the same system parameters.

For the baseline design reference mission, the payload capability given by Ares V $m_{o,given}$ was found to be 47.54 mT for EDS, and 51.71 mT for Centaur V2. The mass margins, the calculation procedure for which is defined in Section 4.4.8, for the DA-SS architecture were -74.73% and -60.64% for the EDS and Centaur upper stage configurations, respectively. The negative percentages imply that the architecture exceeds the given allowance for both configurations, as can be seen in Figure 5.1. Similarly, the DA-2S architecture exceeds the given allowance for both configurations, yielding mass margins of -45.71% and -33.96% for EDS and Centaur, respectively. While both of the DA architectures exceed the Ares V capability, the DA-2S is the more mass efficient of the two, as its mass margins were less negative. The mass margins for the MOR-SS architecture were 36.80% and 41.89% for the EDS and Centaur upper stage configurations, respectively. The positive percentages imply that the architecture is feasible on a single Ares V launch for both upper stage configurations. Similarly, the MOR-2S architecture yields mass margins of 50.29% and 54.29% for EDS and Centaur V2, respectively. Note that the mass margins calculated in the baseline design use a 30% mass growth allowance. While both MOR architectures are feasible on a single Ares V launch for both upper stage configurations, the MOR-2S architecture provides the greater mass margin. Based on the results given in Section 5.3.1, Mars orbit rendezvous is by far

the more mass efficient of the two outbound strategies analyzed in this study, and a two-stage MAV provides a greater mass margin than a single-stage MAV.

6.3 Sensitivity

A sensitivity study was performed to determine the effects of key system parameters on system mass and mass margin. The results of the sensitivity study are presented in Section 5.3.2, and this section gives detailed explanation of the results of the sensitivity study.

6.3.1 Launch Opportunity

Table 5.9 lists the $m_{o,pre}$ value for each architecture, as well as the corresponding values for $m_{o,given}$ associated with each launch opportunity. The results of the launch opportunity sweep are illustrated in Figure 5.2. The reader will note that the Ares V capability (i.e., $m_{o,given}$) for the two upper stages is not expressed linearly as it was in Figure 5.1. This is due to the fact that the launch opportunity was varied in the sensitivity study, whereas this parameter was held constant in the feasibility study. The Earth departure and Mars arrival variables therefore varied with launch opportunity. Figure 5.2 depicts the mass trend similarly for all architectures, as each exhibits a "hump" effect, reaching a maximum predicted mass for the 2016 launch opportunity. The given Ares V allowance does not exhibit the same trend, as $m_{o,given}$ is only a function of launch opportunity, per Figure 2.1. Increasing the Earth departure C_3 decreases $m_{o,given}$, which decreases mass margin. Similarly, increasing the Mars arrival V_{HE} increases $m_{o,pre}$, thus decreasing mass margin.

For all launch opportunities, both MOR architectures fall within the given Ares V allowance for both upper stage configurations. The DA-SS architecture, however, exceeds the given allowance for both Ares V configurations over the entire launch opportunity sweep. The DA-2S architecture exceeds the allowance given by EDS for all launch opportunities, and exceeds the allowance by Centaur V2 for all but the 2009 and 2011 opportunities. It can be concluded from Figure 5.2 that direct ascent does not provide adequate mass margin for a single Ares V launch. However, Mars orbit rendezvous, while requiring more components and thus introducing additional risk and complexity, provides positive mass margin at all launch opportunities.

6.3.2 Periapsis

Figure 5.3 illustrates the effect of periapsis altitude on system mass. It can be concluded from the figure that the particular Mars orbit has a very small effect on an architecture's predicted mass, and is therefore not a significant parameter when designing a mission.

6.3.3 Payloads

This section explains the logic behind the effects of payload mass on system mass. The parameters varied in this part of the sensitivity study were m_{sample}, m_{EEC}, and m_{rover}.

6.3.3.1 Sample Mass

Figure 5.4 illustrates the effect of m_{Sample} on system mass. Because the mass of the surface sample is orders of magnitude smaller than the predicted system mass, the sensitivity associated with m_{Sample} may appear negligible. The system mass, however, increases by approximately one mT in all architectures across the entire sweep.

Increasing m_{Sample}, even by only 1 to 2 kg, adds orders of magnitude of mass to the overall system. Although the sample mass may be orders of magnitude smaller than the system mass, the sample is a payload. Increases in the mass of a payload require more propulsion (and thus more component mass) to carry it. Increasing m_{Sample} thus increases m_{MAV}, which increases the mass of the component which carries the MAV (i.e., the lander); increases in lander mass require increase in the mass of the component which carries the lander (i.e., the orbiter). Additionally, in the MOR architectures, increasing the sample mass increases the amount of propulsion required to return the sample to Earth; the ERV mass is thus increased, which requires an increase in the mass of the component which carries the ERV (i.e., the orbiter). Additionally, one should take into consideration that increases in the size and mass of the surface sample and SC may require an increase in the size of the Earth entry capsule to allow for larger containment. Similarly, because the EEC is a dormant payload in any architecture, the system mass would increase to compensate for this increase in m_{EEC}.

6.3.3.2 Earth Entry Capsule Mass

Figure 5.5 illustrates the effect of m_{EEC} on system mass. The MOR architectures experience an increase in system mass of approximately 1 mT over the entire sweep. This is a result of the EEC being a payload of the ERV, whose only maneuver is TEI, which requires a smaller ΔV than other maneuvers. The propulsive mass required to carry the EEC back to Earth is therefore lower. The DA architectures experience a somewhat sharper increase across the sweep. This is a result of the EEC being a payload of the MAV, which performs both ascent and TEI. Although the DA-SS architecture requires the most mass across the entire sweep than any other architecture, the DA-2S

architecture experiences a sharper increase in system mass than the DA-SS architecture; this is to be expected because when the MAV first stage is jettisoned, the EEC now accounts for a higher percentage of the component mass. This decrease in mass fraction therefore increases the component mass and thus the overall system mass.

6.3.3.3 Rover Mass

Figure 5.6 illustrates the effect of m_{Rover} on system mass. It can be seen in the figure that all four architectures experience a similar increase of approximately mT in system mass. Because the rover is a payload of only the lander, increasing m_{Rover} increases the masses of only the lander and thus the orbiter. Any other components (i.e., MAV or ERV) would not be affected by an increase in m_{Rover}.

6.3.4 Propellant Mass Fraction of MAV First Stage

Figure 5.7 illustrates the effect of PMF of the MAV first stage on system mass for the two-stage MAV architectures. It can be seen in the figure that the DA architecture experiences a much more drastic decrease in mass (80 mT) over the sweep than the MOR architecture experiences (approximately 3 mT). This is the result of the difference in ascent ΔV between the two architectures. For Mars orbit rendezvous, the MAV must only provide enough ΔV to carry the SC to LMO; for direct ascent, however, the MAV must provide enough ΔV to carry the SC all the way back to Earth. Additionally, the MAV in the MOR architecture does not have to support the mass of the EEC. For MOR, the EEC is a payload of the ERV, which remains aboard the orbiter until sample transfer is complete; for direct ascent, however, the MAV supports the mass of the EEC throughout the combined ascent-to-TEI maneuver.

The system mass experiences a much sharper drop for the DA architecture because of the exponential function in the PMER (Equation 4.9). The higher payload mass of the MAV first stage in the DA-2S architecture increases the propellant mass, thus increasing the PMF. The PMF of the MAV first stage (for solid propellants) is therefore a critical design parameter which should be considered when selecting the outbound strategy.

6.3.5 ΔV

This section explains the logic behind the results of the effects of ΔV on system mass. The parameters varied in this study include $\Delta V_{Descent}$, ΔV_{Ascent}, $\Delta V_{Ascent,FS}$, $\Delta V_{Ascent,US}$, and ΔV_{TEI}.

6.3.5.1 Descent

Figure 5.8 illustrates the results of the effect of $\Delta V_{Descent}$ on system mass. From the figure, the reader will note that the DA architectures experience a sharper increase (8 mT) in system mass than the MOR architectures (approximately 2 mT). This is the result of the difference in payload masses. Because the MAV in the direct ascent architectures performs a more robust maneuver and supports a larger payload (i.e., EEC), the mass of the MAV is higher for direct ascent. Because the MAV is a payload of the lander, the lander's mass is increased. Similarly, the orbiter's mass is increased.

6.3.5.2 Ascent (Single-Stage MAV Architectures)

Figure 5.9 illustrates the effect of ΔV_{Ascent} on system mass for the DA-SS architecture. Over the entire ΔV_{Ascent} sweep, the DA-SS architecture experiences an increase in system mass of approximately 11 mT. Similarly, Figure 5.10 illustrates the effect of ΔV_{Ascent} on system mass for the MOR-SS architecture, which shows an increase

in system mass of approximately 12 mT. Although the architectures show similar increases in system mass, the range of variation for the MOR architecture (1.0 km/s) was twice the range of variation for the DA architecture (0.5 km/s). The system mass for direct ascent therefore increases more rapidly than for Mars orbit rendezvous, thus $m_{o,pre}$ is more sensitive to the combined ascent-to-TEI strategy than it is to the ascent-to-orbit strategy.

6.3.5.3 Ascent

Figure 5.11 illustrates the effect of $\Delta V_{Ascent,US}$ on system mass for the DA-2S architecture. Over the entire $\Delta V_{Ascent,US}$ sweep, the DA-2S architecture experiences an increase in system mass of approximately 10 mT and provides no mass margin for either Ares V configuration. Similarly, Figure 5.12 illustrates the effect of $\Delta V_{Ascent,FS}$ on system mass for the DA-2S architecture. Over the entire $\Delta V_{Ascent,FS}$ sweep, the DA-2S architecture experiences an increase in system mass of approximately 7 mT and provides no mass margin for either Ares V configuration. The reader will note from the figures that the DA-2S architecture produce the same $m_{o,pre}$ at the upper bound values for both ascent maneuvers; this is to be expected, as the upper bound value (3.25 km/s) was used as the baseline value in the DRM. It should also be noted that $m_{o,pre}$ at the lower bound was lower in the $\Delta V_{Ascent,US}$ sweep than in the $\Delta V_{Ascent,FS}$ sweep. This also is to be expected because even though the ΔV_{Ascent} was split equally between the two stages of the MAV, the first stage component carries a much greater payload mass than the upper stage component. The mass of the first stage is therefore increased to compensate for the higher propulsion requirement of first stage ascent. Increasing the mass of the MAV in

turn increases the mass of the lander, and thus the orbiter. The overall system mass at the lower bound is therefore higher in the $\Delta V_{Ascent,FS}$ sweep than in the $\Delta V_{Ascent,US}$.

Figure 5.13 illustrates the effect of $\Delta V_{Ascent,US}$ on system mass for the MOR-2S architecture. Over the entire $\Delta V_{Ascent,US}$ sweep, the MOR-2S architecture experiences an increase in system mass of approximately 3.5 mT and provides sufficient mass margin for both Ares V configurations. Similarly, Figure 5.14 illustrates the effect of $\Delta V_{Ascent,FS}$ on system mass for the MOR-2S architecture. Over the entire $\Delta V_{Ascent,FS}$ sweep, the MOR-2S architecture experiences an increase in system mass slightly less than 3 mT, also leaving plenty of mass margin. It should be noted that the value for $m_{o,pre}$ at the lower bound is higher in the $\Delta V_{Ascent,FS}$ sweep than in the $\Delta V_{Ascent,US}$ sweep. As with DA-2S, this is to be expected because, for an equal ΔV_{Ascent} split between the two stages, the first stage component carries higher payload mass (j.e., MAV upper stage) than the upper stage component.

In order to reduce system mass in the case of a two-stage MAV, it is necessary to find the optimal ΔV_{Ascent} split between the two stages. Figure 5.15 illustrates the effect of the variations in ΔV_{Ascent} (as described in Section 5.3.2.5) for the DA-2S architecture, and Figure 5.16 illustrates that of the MOR-2S architecture. The total ΔV_{Ascent} remains constant (6.5 and 5.0 km/s for DA-2S and MOR-2S respectively) over the entire sweep, but the allocations to the first and upper stage MAV components are varied. The DA-2S architecture experiences a much sharper increase in system mass (17 mT) than the MOR-2S architecture (2 mT). This difference in sensitivities between the architectures is the result of the differences in upper stage payload masses as well as propulsive

requirements. Because the upper stage component in the DA-2S architecture carries an additional payload (i.e. EEC), the amount of propellant required for that component is increased, which increases the overall component, and thus system, masses. Additionally, the DA-2S architecture has a higher ΔV_{Ascent} than the MOR-2S architecture; the required increase in propulsion associated with the combined ascent-to-TEI maneuver increases the overall system mass. It is evident from the results shown that reducing the amount of ΔV_{Ascent} applied to the MAV upper stage decreases the overall system mass.

6.3.5.4 Trans-Earth Injection (MOR Architectures)

Figure 5.17 illustrates the effect of ΔV_{TEI} on system mass. Over the entire ΔV_{TEI} sweep, both MOR architectures experience an increase in system mass of just under 2.5 mT and provide sufficient of mass margin for both Ares V configurations. It can be seen in the figure that the MOR-2S produces a consistently lower $m_{o,pre}$ over the sweep than the MOR-SS architecture. This is the result of the difference between the MAV component masses. While the TEI maneuver is unaffected by Mars ascent (only in the MOR architectures), the mass of the MAV proved to be lower in the staged architectures than in their respective single-stage architectures.

6.3.6 Mass Growth Allowance

Figure 5.18 illustrates the effect of MGA on system mass. It can be seen in the figure that, across the entire MGA sweep, the direct ascent architectures exceed the given Ares V allowance for both upper stage configurations, while the Mars orbit rendezvous architectures fall within the given allowance. The MOR-SS architecture experiences only a slightly larger mass increase (5 mT) than the MOR-2S architecture (4 mT). The DA-2S architecture, while less massive throughout the sweep than the DA-SS architecture,

experiences a sharper increase in mass. Note that the mass of the of the DA-2S architecture at an MGA of 1.15 is 20 mT less than that of the DA-SS architecture. While the single-stage and two-stage MAVs have the same total ΔV_{Ascent} requirement, the first stage component of the two-stage MAV only performs half the ascent maneuver, thus reducing propulsive mass. This reduction in propulsive mass reduces the overall mass of the MAV and thus the integrated vehicle.

6.3.7 Specific Impulse

This section explains the logic behind the results of the effects of I_{sp} on system mass. In all architectures, the I_{sp} of each component (excluding the MAV first stage component) was varied over a range from 313.6 sec to 446.3 sec. In the two-stage MAV architectures, the MAV first stage component was assigned a range of variation from 260 sec to 300 sec to represent a solid motor.

6.3.7.1 Orbiter

Figure 5.19 illustrates the effect of the orbiter's I_{sp} on system mass. It can be seen in the figure that, across the entire I_{sp} sweep, all four architectures experience an exponential decrease in system mass. The DA-SS and DA-2S architectures decrease in mass by 20 mT and 17 mT, respectively. The MOR-SS and MOR-2S architectures decrease in mass by approximately 9 mT and 7 mT, respectively. From Equation 4.16, increasing I_{sp} decreases m_{prop}, therefore decreasing $m_{o,pre}$. Additionally, from the PMER, the dry mass is a function of m_{prop}; an increase in the required propulsive mass thus increases the dry mass. It can be concluded from the figure that, for a larger system, $m_{o,pre}$ is more sensitive to variations in I_{sp} of the orbiter. Additionally, over the I_{sp}

sweep, the MOR architectures provide plenty of mass margin with both Ares V upper stage configurations. The DA architectures, however, provide no mass margin for either Ares V configuration.

6.3.7.2 Lander

Figure 5.20 illustrates the effect of the lander's I_{sp} on system mass. It can be seen in the figure that, across the entire I_{sp} sweep, the DA-SS and DA-2S architectures experience respective decreases in system mass of approximately 3.0 and 2.5 mT, while both MOR architectures decrease in mass by approximately1 mT. The system mass is conclusively less sensitive to its lander's I_{sp} than to that of its orbiter. This is a result of the difference in mass and propulsive requirements between the two components. The lander is the smaller of the two vehicles, and its ΔV requirement is an order of magnitude smaller than that of the orbiter. Additionally, over the I_{sp} sweep, the DA architectures provide no mass margin for either Ares V upper stage configuration, whereas the MOR architectures provide plenty of mass margin for both Ares V configurations.

6.3.7.3 MAV (Single-Stage MAV Architectures)

Figure 5.21 illustrates the effect of the MAV's I_{sp} on system mass for the single-stage MAV architectures. It can be seen in the figure that, across the entire I_{sp} sweep, the DA-SS architecture experiences a decrease in system mass of roughly 40 mT, and the MOR-SS architecture decreases in mass by approximately 11.5 mT. Because the MAV is a more energetic vehicle than the lander (i.e., higher mass and ΔV requirement), the system is conclusively far more sensitive to variations in the MAV's I_{sp} than in that of

the lander. Additionally, system mass is more sensitive to variations in the MAV's I_{sp} for the direct ascent architecture because it is a larger system. The DA-SS architecture provides mass margin for I_{sp} values above 420 sec with the Centaur configuration, and it provides only a slight mass margin for I_{sp} values above 440 sec for EDS. If it is determined that direct ascent is the desired return strategy, then the MAV propulsion system should be such that it provides the highest possible engine performance, i.e., the use of high-I_{sp} propellants such as cryogenic LOx/LH_2 or LF_2/LH_2. The MOR-SS architecture, however, provides sufficient mass margin over the entire sweep for both Ares V configurations.

6.3.7.4 MAV First Stage Component (Two-Stage MAV Architectures)

Figure 5.22 illustrates the effect of the MAV first stage component's I_{sp} on system mass for the two-stage MAV architectures. Note that for the two-stage MAV architectures, the MAV first stage was assumed to be a SRM, and was thus assigned a different range of variation (i.e., 260 to 300 sec). It can be seen in the figure that, across the entire I_{sp} sweep, the DA-2S and MOR-2S architectures experience respective decreases in system mass of 16 mT and 2 mT. The difference in mass decreases between the two architectures is a result of not only the difference in payload mass for the two architectures, but also the exponential function (i.e., Equation 4.16), which yields a significantly smaller m_{prop} for higher I_{sp}.

6.3.7.5 MAV Upper Stage Component (Two-Stage MAV Architectures)

Figure 5.23 illustrates the effect of the MAV upper stage component's I_{sp} on system mass for the two-stage MAV architectures. It can be seen in the figure that,

across the entire I_{sp} sweep, the DA-2S architecture experiences a decrease in system mass of 35 mT, while the MOR-2S architecture only decreases by 4.4 mT. As in the previous section, this difference in mass decrease between the two architectures is a result of both the difference in payload mass (i.e., MAV upper stage payload mass is higher for DA-2S than for MOR-2S) and the exponential function in Equation 4.16. Additionally, the MOR architecture provides plenty of mass margin over the entire sweep for both Ares V upper stage configurations. The DA architecture, however, provides mass margin for I_{sp} values above 390 sec and above 375 sec for the EDS and Centaur configurations, respectively. Should direct ascent be the chosen return strategy, it would be necessary to choose propellant combinations such as LOx/LH_2, or one that uses LF_2 as the oxidizer. The system mass is conclusively much more sensitive to variations in the MAV upper stage component's I_{sp} for more robust architectures (i.e., direct ascent).

6.3.7.6 ERV (MOR Architectures)

Figure 5.24 illustrates the effect of the ERV's I_{sp} on system mass for the Mars orbit rendezvous architectures. It can be seen in the figure that, across the entire I_{sp} sweep, both architectures experience a decrease in system mass of approximately 0.85 mT. This is a much smaller decrease in mass than in I_{sp} sweeps previously discussed because the ERV is a smaller component (carrying a payload mass of only 20 to 150 kg) and requires a lower ΔV (1 to 2 km/s) to perform its maneuver. Additionally, the exponential function in Equation 4.16 has shown to have far less effect on system mass for smaller architectures.

6.3.8 Conclusion

The parameters which are shown to have the greatest effect on system mass include launch opportunity, MAV first stage PMF (two-stage MAV architectures), ΔV_{Ascent}, MGA of MAV or MAV components, I_{sp} of orbiter, and I_{sp} of MAV or MAV components. The reader will note that most of these parameters are specific to the MAV. This suggests that the MAV should be the component of key interest when designing an MSR mission. Further conclusions about the findings of this study, as well as recommendations for future work, are discussed in the following section.

6.4 Final Discussion and Recommendations

This section discusses the general results of the feasibility and sensitivity studies performed for a Mars sample return mission with a single Ares V launch. A design reference mission was chosen based on information gathered from the studies discussed in the literature review, and the results of this mission were presented for two Ares V upper stage configurations, i.e., EDS and Centaur V2. Key system parameters were varied over appropriate ranges per Chapter 2, and these results were presented for each parameter that was varied.

6.4.1 Feasibility

This section discusses the recommendations drawn from the results of the feasibility study performed. Based on the information presented in Section 5.3.1, the Mars orbit rendezvous strategy is far more mass efficient than direct ascent. Although employing an additional component (i.e., ERV) to return the surface samples to Earth increases the risk, the rendezvous and docking technology (used since the Apollo era) associated with MOR exists [3], therefore compensating for some of this risk.

Additionally, while a two-stage MAV may increase risk of mission, it further reduces the system mass. This additional mass margin would not only allow for adjustments to key system parameters, but it would also allow for more payload mass to be taken to the surface. On a single mission, therefore, more science experiments could be performed, or more surface samples could be returned to Earth. Investing more into a single launch would not only reduce mission risk as previously discussed, but it would also be more cost efficient long-term by reducing the number of launches required to perform a series of MSR missions.

In the case that direct ascent is chosen over Mars orbit rendezvous, the Centaur V2 upper stage should be seriously considered, as this configuration provides significantly more mass margin than the Earth Departure Stage. Additionally, key system parameters should be adjusted such that the system mass falls within the given Ares V allowance. These parameters should be adjusted based on the information presented in Section 5.3.2, which is discussed in the next section.

6.4.2 Sensitivity

This section discusses the recommendations drawn from the results of the sensitivity study performed. Based on the information presented in Section 5.3.2, the parameters which have the largest effect on system mass are shown to be launch opportunity, MAV first stage PMF (two-stage MAV architectures), ΔV_{Ascent}, MGA of MAV or MAV components, I_{sp} of orbiter, and I_{sp} of MAV or MAV components. The recommended adjustments to these parameters are discussed in this section. Additionally, the direct ascent architectures experience sharper changes in mass than the

Mars orbit rendezvous architectures. This is the product of the difference in robustness of the return strategies presented in this study.

Based on Figure 5.2, the 2016 launch opportunity should be avoided if possible, as this gives the lowest mass margin for any architecture. In the case of a two-stage MAV architecture, the PMF of the MAV first stage can drastically reduce the system mass, especially for direct ascent. A solid rocket motor with a PMF of 0.9 or higher can provide significantly more mass margin. It should be noted that, from the ATK catalog of SRMs [63], 61.5% of the SRM specimens listed had propellant mass fractions equal to or greater than 0.9; this percentage implies that a PMF of 0.9 is relatively feasible. Finally, reducing the ΔV_{Ascent} also reduces system mass, as this would require less propellant for the ascent maneuver.

The sensitivity study has shown that the MAV is the component which has the most significance on system mass. The design of a mass efficient Mars ascent vehicle could produce an MSR architecture which yields a high enough mass margin so that more science payload can be landed on the surface. Increasing the number of science objectives that can be performed on a single MSR mission could decrease the number of MSR missions required before embracing on human Mars exploration.

6.4.3 Considerations for Future Analyses

The sensitivity study has shown that the component which has the most significance to system mass is the Mars ascent vehicle. Because $m_{o,pre}$ is exponentially affected by I_{sp} of the MAV, this component should perhaps utilize a cryogenic propellant system. If, however, a cryogenic system is not feasible on a robotic mission from Mars' surface with current technology, then an Earth storable or other chemical

propellant with a similar I_{sp} should be employed. As described in Section 6.3.5.3, a SRM with a propellant mass fraction greater than 0.9 should be used as the first stage of the ascent vehicle to optimize liftoff thrust and reduce overall system mass.

Trades to consider when choosing a MAV design would include ascent strategy (i.e., direct ascent, Mars orbit rendezvous, orbiting sample), number of stages, and propellant systems (i.e., chemical or SRM). If direct ascent is chosen over Mars orbit rendezvous, in-depth studies should be performed to determine how many stages the MAV should consist of, as well as stage propellant systems and the ΔV_{Ascent} split. Should MOR be the ascent strategy of choice, adding a third stage to the MAV may not be beneficial, as this would increase risk and complexity, while providing only little more (or possibly less) mass margin. Note that this study does not consider the concept of the orbiting sample, as this is very similar to the MOR architecture and introduces the additional risk associated with the on-orbit trajectory of the sample canister. An additional study to consider when choosing a MAV design would be to create a baseline design for two architectures: MOR and OS, keeping key system parameters (i.e., Earth launch opportunity, LMO altitude, ΔV_{Ascent}, propellant system, MGA, etc.) constant between the two architectures, and studying the sensitivities associated with the ΔV requirements for the less robust maneuvers in which the MAV is involved. These maneuvers would include rendezvous and docking (MOR), stage separation (MOR), and the on-orbit trajectory of the SC from the MAV to the orbiter or return vehicle. The ΔV_{Ascent} would be the same for both MOR and OS, but the aforementioned maneuvers would have their own respective ΔV requirements as well as risks.

The launch opportunity should be chosen such that Ares V gives the highest possible TMI capability and the C_3 for Mars arrival is as small as possible. Similarly, it is important to choose an Earth launch opportunity whose corresponding Mars departure C_3 (or V_{HE}) would reduce the ΔV_{TEI}.

As stated in Section 4.4.2, ΔV_{Ascent} is assumed to be unaffected by the LMO altitude. In a more detailed analysis, this would be taken into consideration, and the orbit could be lowered so as to reduce the ΔV_{Ascent} because the system mass is most sensitive to the MAV parameters. However, rather than simply lowering a circular orbit, it would be beneficial to study the effect of an elliptical orbit on not only ΔV_{Ascent}, but also on ΔV_{MOI}.

In the case that MOR is the return strategy chosen, the orbiter and ERV could be combined into a single component which performs both the MOI and TEI maneuvers. Although the orbiter would require additional propulsive mass to compensate for the return trip, this would reduce the number of components, thus reducing complexity.

Because the results presented in Chapter 5 showed that MGA has less effect on system mass than those associated with the MAV, it is recommended that a mass growth allowance of 1.3 be used on all components. To make a conservative design would reduce risking loss of mission, thus proving more cost efficient long-term.

Another important trade to consider would be to bring the surface sample to Earth orbit, rather than directly to Earth's surface. This would prevent potentially hazardous biochemical materials from being exposed on Earth. Additionally, the risks associated with the EEC surface landing (i.e., mixing of samples) would be nulled. Avoiding the surface landing would thus eliminate the need for the EEC, and this would allow for more mass to be allotted to returned samples. Earth orbit rendezvous (EOR), however,

increases mission risk by involving rendezvous and docking with the shuttle or ISS. In addition to risk, the ERV would require more propellant in order to compensate for the ΔV associated with Earth orbit insertion (EOI). Furthermore, a facility for sample handling and analysis would have to be designed and fabricated for onboard sample processing, and the iMARS working group has already decided that a sample handling and curation facility would be developed on Earth.

For an architecture which yields a high mass margin (greater than 30 percent), surface payload mass could be increased to optimize mission science. In other words, science payload could be increased while maintaining a reasonable mass margin. More rovers could be landed on the Martian surface to increase the area over which Mars is observed. More science instruments could be taken to Mars to increase the fidelity of the study of the surface and subsurface. A larger sample could also be returned to Earth; this could translate into multiple samples from a variety of locations.

6.5 Summary

This study shows that Mars orbit rendezvous can perform Mars sample return on a single Ares V launch, with a mass growth allowance of 1.3, and provide sufficient mass margin. The MAV has shown to be the most critical component when sizing an architecture. Staging the MAV proves to further reduce mass, especially in the case of a SRM first stage, and when reducing the ΔV_{Ascent} allotted to the upper stage. Additionally, while MOR introduces an additional component, thus increasing mission risk, the rendezvous and docking technology required for this strategy has been exercised for decades, and the margin provided by Ares V makes the MOR architectures developed in this study highly feasible. The next milestone in planetary exploration will be Mars

sample return. The upcoming Ares V launch vehicle will surpass the capability of any other launch vehicles to date, and will provide the payload mass capability to support the architectures developed and discussed in this study.

REFERENCES

[1] W. R. Swagerty and E. Mancke, "Exploration, Conquest, and Settlement, Era of European," vol. 2009, 2001 ed: Oxford University Press, 2001.

[2] "Lewis and Clark," vol. 2009: National Geographic.

[3] S. Garber and R. Launius, "A Brief History of NASA," vol. 2009.

[4] J. W. Dyer, R. O. Fimmel, L. Colin, P. Dyal, and J. P. Murphy, "The Continuing Missions of the Pioneer Spacecraft," in *AIAA 21st Aerospace Sciences Meeting*. Reno, Nevada: The American Institute of Aeronautics and Astronautics, Inc., 1983.

[5] J. M. Boyce, "Magellan Mission to Venus," in *AIAA Space Programs and Technologies Conference*. Huntsville, Alabama: The American Institute of Aeronautics and Astronautics, Inc., 1990.

[6] J. Brown, E. Wang, J. Hernandez, and A. Y. Lee, "Importance of Model Simulations in Cassini In-flight Mission Events," in *AIAA Guidance, Navigation, and Control Conference*. Chicago, Illinoise: The American Institute of Aeronautics and Astronautics, Inc., 2009.

[7] D. Beaty, M. Grady, D. J. Moura, M. Walter, C. Muller, F. Daerden, V. Hipkin, J.-P. Bibring, E. Flamini, G. G. Ori, M. Kato, T. Hode, P. Mani, J. Bridges, and F. Jordan, "Preliminary Planning for an International Mars Sample Return Mission," International Mars Architecture for the Return of Samples (iMARS) June 1, 2008 2008.

[8] J. R. Johnson, J. Amend, A. Steele, S. Bougher, S. Rafkin, P. Withers, J. Plescia, V. Hamilton, A. Tripathi, and J. Heldmann, "Mars Science Goals, Objectives,

Investigations, and Priorities: 2008," Mars Exploration Program Analysis Group, 2008.

[9] D. J. D. Marais, "Advancing Astrobiology Beyond Viking, Spirit, and Opportunity," in *Space 2006*. San Jose, California: The American Institute of Aeronautics and Astronautics, Inc., 2006.

[10] F. G. Lemoine, S. Bruinsma, D. S. Chinn, and J. M. Forbes, "Thermospheric Studies with Mars Global Surveyor," in *AIAA/AAS Astrodynamics Specialist Conference and Exhibit*. Keystone, Colorado: The American Institute of Aeronautics and Astronautics, Inc., 2006.

[11] G. Crowley and R. H. Tolson, "Mars Thermospheric Winds from Mars Global Surveyor and Mars Odyssey Accelerometers," *AIAA Journal of Spacecraft and Rockets*, vol. 44, pp. 1188 - 1194, 2007.

[12] B. M. Portock, G. Kruizinga, E. Bonfiglio, B. Raofi, and M. Ryne, "Navigation Challenges of the Mars Phoenix Lander Mission," in *AIAA/AAS Astrodynamics Specialist Conference and Exhibit*. Honolulu, Hawaii: The American Institute of Aeronautics and Astronautics, Inc., 2008.

[13] "The Vision for Space Exploration," vol. 2009. Washington, D.C., 2004.

[14] J. P. Sumrall, J. C. McArthur, and M. Lacey, "Foundation for Heavy Lift - Early Developments in the Ares V Cargo Launch Vehicle," in *43rd AIAA/ASME/SAE/ASEE Joint Propulsion Conference & Exhibit*. Cincinnati, Ohio, 2007.

[15] N. S. Dhanji, E. Dupuis, and M. Nahon, "Method for Evaluating Alternative Aerial Platforms for Mars Applications," in *SpaceOps 2006 Conference*: The American Institute of Aeronautics and Astronautics, Inc., 2006.

[16] P. N. Desai, R. D. Braun, W. C. Engelund, F. M. Cheatwood, and J. A. Kangas, "Mars Ascent Vehicle Flight Analysis," in *32nd AIAA Thermophysics Conference*. Albuquerque, New Mexico: The American Institute of Aeronautics and Astronautics, Inc., 1998.

[17] B. B. Donahue, S. E. Green, V. L. Coverstone, and B. Woo, "Chemical and Solar-Electric-Propulsion Systems Analyses for Mars Sample Return Missions," *AIAA Journal of Spacecraft and Rockets*, vol. 43, pp. 170 - 177, 2006.

[18] R. Zubrin, "A Comparison of Approaches for the Mars Sample Return Mission," presented at AIAA 34th Aerospace Sciences Meeting and Exhibit, Reno, Nevada, 1996.

[19] S. Matousek, M. Adler, and W. Lee, "A Few Good Rocks: The Mars Sample Return Mission Architecture." Reston, Virginia: The American Institute of Aeronautics and Astronautics, Inc., 1998.

[20] F. Jordan, "Mars Sample Return - Technical Challenges," NASA Jet Propulsion Laboratory, 2008.

[21] R. Mattingly, "Groundbreaking Mars Sample Return Earliest Possible "Pathways Compatible" Launch: November, 2013," Jet Propulsion Laboratory, California Institution of Technology, 2004, pp. 16.

[22] R. Mattingly, S. Matousek, and F. Jordan, "Continuing Evolution of Mars Sample Return," presented at 2004 IEEE Aerospace Conference, 2004.

[23] R. Mattingly, S. Hayati, and G. Udomkesmalee, "Technology Development Plans for the Mars Sample Return Mission," in *IEEE Aerospace Conference*: Institute of Electrical and Electronics Engineers, Inc., 2005.

[24] H. Price, K. D. Cramer, S. R. Doudrick, W. Lee, D. J. R. Matijevic, S. Weinstein, T. Lam-Trong, O. Marsal, and D. R. A. Mitcheltree, "Mars Sample Return Spacecraft Systems Architecture," 2000.

[25] R. Oberto, "Mars Sample Return, A Concept Point Design by Team-X (JPL's Advanced Project Design Team)," Institute of Electrical and Electronics Engineers, 2002.

[26] C. W. Smith and R. W. Maddock, "Intermediate Rendezvous: A Mars Sample Return Strategy," in *AAS/AIAA Astrodynamics Specialists Conference*. Tampa, Florida: American Astronautical Society, 2006.

[27] B. Sutter and M. McGee, "Mars Sample Return: The Design of Low Risk Architectures," Institute of Electrical and Electronics Engineers, Inc.

[28] B. B. Donahue, M. A. Farkas, N. T. Graham, R. M. Lajoie, and S. J. Weisberg, "Ares V Additional Mission Opportunities," in *AIAA SPACE 2008 Conference & Exposition*. San Diego, California: The American Institute of Aeronautics and Astronautics, Inc., 2008.

[29] S. A. Cook and T. Vanhooser, "Powering Exploration: The Ares I Crew Launch Vehicle and Ares V Cargo Launch Vehicle," in *44th AIAA/ASME/SAE/ASEE Joint Propulsion Conference & Exhibit*. Hartford, Connecticut: The American Institute of Aeronautics and Astronautics, Inc., 2008.

[30] J. C. Whitehead, "Mars Ascent Propulsion Options for Small Sample Return Vehicles," in *33rd AIAA/ASME/SAE/ASEE Joint Propulsion Conference & Exhibit*. Seattle, Washington: The American Institute of Aeronautics and Astronautics, Inc., 1997.

[31] C. D. Brown, *Elements of Spacecraft Design*, vol. 1, 1 ed. Reston, Virginia: The American Institute of Aeronautics and Astronautics, Inc., 2002.

[32] A. M. Baker, I. Coxhill, and P. Henshall, "Chemical Propulsion Systems for Low Cost Mars Sample Return," in *40th AIAA/ASME/SAE/ASEE Joint Propulsion Conference and Exhibit*. Fort Lauderdale, Florida: The American Institute of Aeronautics and Astronautics, Inc., 2004.

[33] R. A. Mitcheltree, S. J. Hughes, R. Dillman, and J. Teter, "Earth Entry Vehicle for Mars Sample Return."

[34] J. C. Whitehead, "Defining the Mars Ascent Problem for Sample Return," in *AIAA SPACE 2008 Conference & Exposition*. San Diego, California: The American Institute of Aeronautics and Astronautics, Inc., 2008.

[35] D. H. Willenberg, "Mars Ascent Vehicle Final Report," Gray Research, Inc., 2008.

[36] R. A. Mitcheltree and S. Kellas, "A Passive Earth-Entry Capsule for Mars Sample Return."

[37] D. Valentian, N. Cucco, M. Muszynski, and A. Souchier, "Green Propellants Perspectives for Future Missions," in *44th AIAA/ASME/SAE/ASEE Joint Propulsion Conference & Exhibit*. Hartford, Connecticut: The American Institute of Aeronautics and Astronautics, Inc., 2008.

[38] P. F. Wercinski, "Mars Sample Return: A Direct and Minimum-Risk Design," *AIAA Journal of Spacecraft and Rockets*, vol. 33, pp. 381-385, 1996.

[39] P. Sumrall, "Ares V Overview," in *Ares V Solar System Science Workshop*, 2008.

[40] L. E. George and L. D. Kos, "Interplanetary Mission Design Handbook:Earth-to-Mars Mission Opportunities and Mars-to-Earth Return Opportunities 2009 - 2024," N. A. a. S. A. (NASA), Ed., 1998.

[41] M. G. Benton Sr., "Crew and Cargo Landers for Human Exploration of Mars - Vehicle System Design," in *44th AIAA/ASME/SAE/ASEE Joint Propulsion Conference & Exhibit*. Hartford, Connecticut: The American Institute of Aeronautics and Astronautics, Inc., 2008.

[42] A. Cervone, E. Rapposelli, and L. d'Agostino, "A Simplified Model for the Evaluation of the Δv of Ascent Trajectories," in *41st AIAA/ASME/SAE/ASEE Joint Propulsion Conference & Exhibit*. Tucson, Arizona: The American Institute of Aeronautics and Astronautics, Inc., 2005.

[43] P. N. Desai and R. D. Braun, "Mars Parking Orbit Selection." Reston, Virginia: The American Institute of Aeronautics and Astronautics, Inc., 1990.

[44] G. Walberg, "How Shall We Go to Mars? A Review of Mission Scenarios," *AIAA Journal of Spacecraft and Rockets*, vol. 30, pp. 129-139, 1993.

[45] J. C. Whitehead, "Mars Ascent Propulsion Trades with Trajectory Analysis," in *AIAA/ASME/SAE/ASEE Joint Propulsion Conference and Exhibit*. Fort Lauderdale, Florida: The American Institute of Aeronautics and Astronautics, Inc., 2004.

[46] J. L. Prince, P. N. Desai, E. M. Queen, and M. R. Grover, "Entry, Descent, and Landing Operations Analysis for the Mars Phoenix Lander," in *AIAA/AAS Astrodynamics Specialist Conference and Exhibit*. Honolulu, Hawaii: The American Institute of Aeronautics and Astronautics, Inc., 2008.

[47] R. D. Braun, D. A. Spencer, P. H. Kallemeyn, and R. M. Vaughan, "Mars Pathfinder Atmospheric Entry Navigation Operations," *AIAA Journal of Spacecraft and Rockets*, vol. 36, pp. 348 - 356, 1999.

[48] D. W. Way, R. W. Powell, A. Chen, and A. D. Steltzner, "Asymptotic Parachute Performance Sensitivity," in *IEEE Aerospace Conference*.

[49] D. W. Way, R. W. Powell, A. Chen, A. D. Steltzner, A. M. San Martin, P. D. Burkhart, and G. F. Mendeck, "Mars Science Laboratory: Entry, Descent, and Landing System Performance," in *IEEE Aerospace Conference*, 2006.

[50] R. Prakash, P. D. Burkhart, A. Chen, K. A. Comeaux, C. S. Guernsey, D. M. Kipp, L. V. Lorenzoni, G. F. Mendeck, R. W. Powell, T. P. Rivellini, A. M. San Martin, S. W. Sell, A. D. Steltzner, and D. W. Way, "Mars Science Laboratory Entry, Descent, and Landing System Overview," in *IEEE Aerospace Conference*, 2008.

[51] G. Singh, A. M. SanMartin, and E. C. Wong, "Guidance and Control Design for Powered Descent and Landing on Mars," in *IEEE Aerospace Conference*: Institute of Electrical and Electronics Engineers, Inc., 2007.

[52] R. D. Braun and R. M. Manning, "Mars Exploration Entry, Descent, and Landing Challenges," in *IEEE Aerospace Conference*: Institute of Electrical and Electronics Engineers, Inc., 2006.

[53] A. Steltzner, D. Kipp, A. Chen, D. Burkhart, C. Guernsey, G. Mendeck, R. Mitcheltree, R. Powell, T. Rivellini, M. San Martin, and D. Way, "Mars Science Laboratory Entry, Descent, and Landing System," in *IEEE Aerospace Conference 2006*: Institute of Electrical and Electronics Engineers, Inc., 2006.

[54] G. P. Sutton and O. Biblarz, *Rocket Propulsion Elements*, vol. 1, 7 ed. New York, NY: John Wiley & Sons, 2001.

[55] M. E. P. A. G. (MEPAG), "Mars Science Goals, Objectives, Investigations, and Priorities: 2008," 2008.

[56] J. C. Whitehead, "Trajectory Analysis and Staging Trades for Smaller Mars Ascent Vehicles," *AIAA Journal of Spacecraft and Rockets*, vol. 42, pp. 1039 - 1046, 2005.

[57] P. Sumrall and S. Creech, "Refinements in the Design of the Ares V Cargo Launch Vehicle for NASA's Exploration Strategy," in *44th AIAA/ASME/SAE/ASEE Joint Propulsion Conference & Exhibit*. Hartford, Connecticut: The American Institute of Aeronautics and Astronautics, Inc., 2008.

[58] P. Sumrall, "Ares V Overview," 2008.

[59] H. N. Zeiner, C. E. French, and D. E. Howard, "Performance Optimization Technique for the 1975 Mars Viking Lander," *AIAA Journal of Spacecraft and Rockets*, vol. 9, pp. 364 - 369, 1972.

[60] A. Witkowski, "Mars Pathfinder Parachute System Performance." Reston, Virginia: The American Institute of Aeronautics and Astronautics, Inc., 1999.

[61] J. Matijevic and E. Dewell, "Anomaly Recovery and the Mars Exploration Rovers," in *SpaceOps 2006 Conference*: The American Institute of Aeronautics and Astronautics, Inc., 2006.

[62] D. Thomas, "Preliminary Mass Estimating Relationships," M. P. J. Benfield, Ph.D., Ed. Huntsville, Alabama, 2009, pp. Propellant Mass Fractions and curve-fit relations for various Mars vehicles.

[63] "ATK Space Propulsion Products Catalog," 2008.

[64] D. K. Huzel and D. H. Huang, *Modern Engineering for Design of Liquid-Propellant Rocket Engines*, vol. 147, 1 ed. Washington, D.C.: The American Institute of Aeronautics and Astronautics, Inc., 1992.